Université de Montréal

Nitric oxide signalling in astrocytes

par **Xuewei Wang**

Département de pharmacologie et physiologie

Faculté de médecine

Thèse présentée

en vue de l'obtention du grade de Doctorat (Ph. D.)

en pharmacologie

Juin, 2017

RÉSUMÉ

Dans le cerveau, les astrocytes sont les cellules gliales les plus abondantes et elles jouent divers rôles, y compris le maintien des synapses tripartites et la régulation du débit sanguin cérébral (DSC). Le monoxyde d'azote (NO) est une molécule de signal endogène qui a un impact sur la régulation de l'activité synaptique et du DSC. Des études antérieures ont démontré que le NO est produit dans les cellules endothéliales et les neurones par la synthase du monoxyde d'azote endothéliale (eNOS) et neuronale (nNOS), respectivement. Cependant, la source de production de NO dans les astrocytes reste incertaine. Par conséquent, nous proposons que la voie de signalisation NOS constitutive puisse coexister dans les astrocytes et puisse être activée par différents neurotransmetteurs. L'objectif de cette thèse est d'identifier les sources et les activateurs de la production de NO dans les astrocytes corticaux de la souris.

L'identification des isoformes constitutives de NOS effectuée au moyen de la microscopie électronique et d'immunohistochimie a révélé l'expression des eNOS et nNOS dans les astrocytes. Des préparations de culture d'astrocytes et de tranches de cerveau marquées avec du diacétate de 4-amino-5-méthylamino-2',7'-difluorescéine (DAF-FM), un indicateur de NO perméable aux cellules qui devient imperméable une fois à l'intérieur ont été réalisées. Cette fonctionnalité a été mise à profit pour évaluer la production de NO exclusivement dans les astrocytes en utilisant la microscopie confocale à uni- et multi-photons. De plus, des agonistes cholinergiques ou glutamatergiques qui ont la capacité d'augmenter la concentration de Ca^{2+} intracellulaire peuvent induire une production du NO in vitro et ex vivo dans les astrocytes, qui est supprimée en présence de l'inhibiteur de NOS non sélectif, L-N^G -Nitro-arginine. Fait intéressant, la réponse NO à l'acétylcholine était absente chez les souris $eNOS^{-/-}$, tandis que l'acide trans-1-aminocyclopentane-1,3-dicarboxylique (*t*-ACPD) a peu affecté la production de NO chez les souris $nNOS^{-/-}$. Ces résultats impliquent que les eNOS et nNOS astrocytaires peuvent être déclenchés par des cascades d'activation distinctes (cholinergique et glutamatergique métabotrope). En outre, les études sur la mobilisation cytosolique du Ca^{2+} indiquent l'importance du réticulum endoplasmique comme réservoir de Ca^{2+} pour la production de NO, et suggèrent aussi une voie de signalisation astrocytaire qui, une fois activée par le *t*-ACPD, provoque l'efflux de Ca^{2+} médié par le récepteur à la ryanodine, qui à son tour active les nNOS adjacents et conduit à la production de NO. Par ailleurs, la superfusion de préparations

in vitro et *ex vivo* avec du N-Méthyl-D-aspartate (NMDA) a provoqué une augmentation du NO tant dans les souris $eNOS^{-/-}$ que $nNOS^{-/-}$, ce qui indique l'implication des eNOS et nNOS astrocytaires. La production de NO a été atténuée par l'inhibition du complexe PSD-95 / nNOS ce qui suggère que le récepteur NMDA astrocytaire rend fonctionnelle la cassette de signalisation NR2B/PSD-95/nNOS.

En conclusion, nos résultats démontrent que : *i*) les astrocytes corticaux expriment à la fois eNOS et nNOS; *ii*) la nNOS cytosolique colocalise avec les récepteurs 2 et 3 de la ryanodine, alors que les nNOS membranaires colocalisent avec le récepteur NMDA contenant le NR2B; *iii*) la stimulation neuronale a la capacité d'induire la production de NO par les eNOS et nNOS astrocytaires par des voies de signalisation différentes; *iv*) l'activation des nNOS cytosoliques nécessite une activation des récepteurs à la ryanodine. Collectivement, ces données suggèrent une production de NO compartimentée et spécifique après une stimulation neuronale probablement dans le but de réguler finement et de façon polarisée les fonctions astrocytaires. Ce travail fournit un nouvel aperçu des conséquences physiologiques pour les fonctions neuronales et vasculaires et améliore notre compréhension de la fonction NO astrocytaire dans le cerveau.

Mots-clés : monoxide d’azote, synthase du monoxyde d’azote endothéliale, synthase du monoxyde d’azote neuronale, astrocyte, pieds astrocytaires, microdomains, cholinergique, glutamatergique, cortex somatosensoriel

SUMMARY

In the brain, astrocytes are the most abundant glial cells and play various roles including maintenance of tripartite synapses and regulation of CBF. An endogenous signal molecule that has a potential to have an effect on regulation of both synaptic activity and CBF is nitric oxide (NO). Previous studies have demonstrated that NO is produced in endothelial cells and neurons by endothelial nitric oxide synthase (eNOS) and neuronal nitric oxide synthase (nNOS), respectively. However, the source of NO production in astrocyte remains uncertain. Therefore, we propose that constitutive NOS signalling pathways may exist in astrocyte and can be activated by different neurotransmitters. The aim of this thesis is to identify the sources and activators of NO production in mouse cortical astrocytes.

Identification of constitutive NOS isoforms done by means of electron microscopy and immunohistochemistry revealed the expression of both eNOS and nNOS in astrocytes. All preparations were performed in astrocyte cultures and brain slice preparations labeled with 4-amino-5-methylamino-2',7'-difluorescein (DAF-FM) diacetate, a cell-permeant NO indicator that becomes cell-impermeable once inside cells. Therefore, I took advantage of this feature to evaluate NO production exclusively in astrocytes using single and multi-photon confocal microscopy. We then tested whether cholinergic and glutamatergic agonists that have the capacity to increase intracellular Ca^{2+} concentration can induce an increase in astrocytic NO. Both *in vitro* and *ex vivo*, NO production levels indicate that cholinergic and glutamatergic stimulations can induce astrocytic NO increases, which was abolished by the non-selective NOS inhibitor L- N^G -Nitro-arginine. Moreover, the NO response to ACh was absent in $eNOS^{-/-}$ mice, while trans-1-aminocyclopentane-1,3-dicarboxylic acid (*t*-ACPD) barely affected NO production in $nNOS^{-/-}$ mice. These results imply that astrocytic eNOS and nNOS can be triggered discretely by distinct activation cascades (cholinergic and metabotropic glutamatergic). Furthermore, studies on cytosolic Ca^{2+} mobilization point out the importance of the endoplasmic reticulum (ER) Ca^{2+} as key in the mechanism of NO production, and suggests a signalling pathway that *t*-ACPD causes IP_3Rs to elicit RyRs-mediated Ca^{2+} efflux, which in turn, activates adjacent nNOS and leads to NO production. Furthermore, superfusion of *in vitro* and *ex vivo* preparations with N-Methyl-D-aspartate (NMDA) evoked an increase in NO in $eNOS^{-/-}$ and $nNOS^{-/-}$ mice. The NO production was attenuated through removal of PSD-95/nNOS complex.

This result posits that astrocytic NMDA receptor may comprise the functional NR2B/PSD-95/nNOS signalling cassette.

In conclusion, our findings demonstrate that: *i*) cortical astrocytes express both eNOS and nNOS; *ii*) nNOS colocalizes with ryanodine receptor 2 and 3, whereas membrane nNOS colocalizes with NR2B-containing NMDA receptor; *iii*) neuronal stimulation has the capacity of inducing eNOS- and nNOS-produced NO in astrocytes via different activation signalling; *iv*) activation of cytosolic nNOS requires the activation of ryanodine receptors. Collectively, these data suggest a compartmentalized and specific NO production following neuronal stimulation probably for a fine and polarized regulation of astrocytic functions. This work provides new insight into physiological consequences for neuronal and vascular functions and ameliorates our understanding of astrocytic NO function in the brain.

Key words: nitric oxide, endothelial nitric oxide synthase, neuronal nitric oxide synthase, astrocyte, astrocytic endfoot, microdomains, cholinergic, glutamatergic, somatosensory cortex

TABLE OF CONTENTS

LIST OF FIGURES

LIST OF ABBREVIATIONS

AA	arachidonic acid
AC	adenylate cyclase
ACh	acetylcholine
aCSF	artificial cerebrospinal fluid
AD	Alzheimer's disease
ADP	adenosine diphosphate
AMPA	α-amino-3-hydroxy-5-methyl-4-isoxazolepropionic acid
AMPK	5' adenosine monophosphate- activated protein kinase
AQP4	aquaporin 4
ATP	adenosine triphosphate
BBB	blood-brain barrier
BDNF	brain-derived neurotrophic factor
BH4	tetrahydrobiopterin
BK channel	big-conductance potassium channel
CaM	calmodulin
CaMKII	calcium/calmodulin-dependent protein kinase II
cAMP	cyclic adenosine monophosphate
Cav	caveolin
CBF	cerebral blood flow
Cdk5	cyclin-dependent kinase 5
cGMP	cyclic guanosine monophosphate
ChAT	choline acetyltransferase
CNS	central nervous system
CO	carbon monoxide
COX-2	cyclooxygenase 2
CPA	cyclopiazonic acid
Cx	connexin
CYP	cytochrome P450 family
DAF-FM	4-Amino-5-methylamino-2′,7′-difluorescein

DAG	diacylglycerol
DHPG	RS-3,5-dihydroxyphenylglycine
Dlg	disc large tumor suppressor gene
DMSO	dimethyl sulfoxide
EAAT	excitatory amino acid transporter
EETs	epoxyeicosatrienoic acids
EFS	electric field stimulation
eNOS	endothelial nitric oxide synthase
ER	endoplasmic reticulum
ERK	extracellular signal-regulated kinase
FAD	flavin adenine dinucleotide
fMRI	functional magnetic resonance imaging
FMN	flavin mononucleotide
Fyn	proto-oncogene tyrosine-protein kinase
HIF	hypoxia inducible factor
HO-1	heme oxygenase-1
GABA	gamma-aminobutyric acid
GDP	guanosine diphosphate
GDNF	glial-derived neurotrophic factor
GFAP	glial fibrillary acidic protein
GFP	green fluorescent protein
GLT-1	glutamate transporter 1
GLUT	glucose transporter
G protein	GTP protein
GSK	glycogen synthase kinase
GTP	guanosine triphosphate
GSH	glutathione
IF	intermediate filament
IGF	insulin-like growth factor
iGluR	ionotropic glutamate receptor

IK	intermediate-conductance Ca^{2+}-activated K^+ channels
IL	interleukin
iNOS	inducible nitric oxide synthase
IP_3	inositol 1,4,5-trisphosphate
JNK	c-Jun N-terminal kinases
KA	kainate
kDa	kilodalton
K_2P channels	two-pore K^+ channels
L-NNA	$L\text{-}N^G$-Nitroarginine
LPS	lipopolysaccharide
mAChR	muscarinic acetylcholine receptor
MAPK	mitogen-activated protein kinase
MEK	MAPK kinase
mGluR	muscarinic glutamatergic receptor
min	minute
MLC_{20}	20-kDa myosin light chain
MLCP	MLC_{20} phosphatase
mM	millimolar
mV	millivolt
NAADP	nicotinic acid adenine dinucleotide phosphate
nAChR	nicotinic acetylcholine receptor
NADPH	nicotinamide adenine dinucleotide phosphate hydrogen
NDRGs	N-myc downstream-regulated genes
NEM	N-ethylmaleimide
NF-κB	nuclear factor - κB
nm	nanometer
NMDA	N-Methyl-D-aspartic acid
nNOS	neuronal nitric oxide synthase
NO	nitric oxide
NOS	nitric oxide synthase
Nrf2	nuclear factor-erythroid 2-released factor 2

NVC	neurovascular coupling
NVU	neurovascular unit
PBS	phosphate-buffered saline
PDZ	PSD-95/Dlg/ZO-1
PFA	paraformaldehyde
PGE_2	prostaglandin E_2
PI3K	phosphoinositide 3-kinase
PKA	protein kinase A
PKC	protein kinase C
PLA	phospholipase A
PLC	phospholipase C
PSD-95	postsynaptic density protein 95
ROS	reactive oxygen species
RNS	reactive nitrogen species
RyR	ryanodine receptor
SERCA	sarco/endoplasmic reticulum Ca^{2+}-ATPase
sGC	soluble guanylyl cyclase
SGK	Serum- and glucocorticoid-inducible kinase
SK	small-conductance Ca^{2+}-activated K^+ channels
SNP	sodium nitroprusside
SOCE	store-operated Ca^{2+} entry
SR	sarcoplasmic reticulum
SR 101	sulforhodamine 101
t-ACPD	1-aminocyclopentane-trans-1,3-dicarboxylic acid
TGF β	transforming growth factor β
TNFα	tumor necrosis factor α
tPA	tissue-type plasminogen activator
TrkB	tropomyosin receptor kinase B
VEGF	vascular endothelial growth factor
VSMC	vascular smooth muscle cell
ZO-1	zonula occludens-1

μm	micrometer
μM	micromolar
2-APB	2-aminoethoxydiphenyl borate
20-HETE	20-Hydroxy-5, 8, 11, 14-eicosatetraenoic acid

ACKNOWLEDGEMENTS

I would like to express the sincerest gratitude to my supervisor **Dr. Hélène Girouard** for giving me the opportunity to work in this amazing project and also for her insightful guidance, patience support and providing financial support to make my Ph.D. study productive. I am also grateful for her attitude, inspiration as well as enthusiasm for her research that encourage myself during both good and bad times in the study.

I would like to thank our collaborators **Dr. Adrée Lessard** and **Dr. Louis-Éric Trudeau** and **Marie-Josée Bourque** for the contributions and support. I would like to acknowledge the members of my pre-doctoral committees Dr. Eric Thorin, Dr. Guy Rousseau and Dr. Richard Robitaille for all their contributions of guidance, advice and time.

Many thanks to Dr. René Cardinal for your help and guidance in the development of my program of study in Département de pharmacologie et physiologie. I would like to thank Dr. Pierre-André Lavoie for his patience and help for my course.

I would like to extend my appreciation to the members of Dr. Girouard's lab past and present for their assistance and encouragement throughout the development of my project, especially to Mme. **Diane Vallerand** for her kind advice and help. I felt so lucky and had the great pleasure to work with Sonia, Nasr, Maryam, Gervais, Lin, Dima, **Sherri**, Florencia, who contributed valuable personal and professional ideas.

I am especially grateful to my parents for all their great love and supporting me to follow my dream.

Lastly, I would like to show my appreciations to China Scholarship Council (CSC) for giving me the opportunity to go abroad and funding my doctoral study at Université de Montréal for the first 4 years and to Faculté des études supérieures et postdoctorales for providing "Bourses de fin d'études doctorale" for year 5. My work was also funded by the Natural Sciences and Engineering Research Council of Canada (NSERC).

CHAPTER 1

INTRODUCTION AND LITERATURE REVIEW

1. Astrocytes in the brain: not only the supporting cells

In the brain, there are three main cell types: neurons, glia and vascular cells. Neurons, are the predominant signalling units in the nervous system. Glia was named by Dr. Rudolf Virchow according to the Greek word "γλια" (means glue in English) (Verkhratsky and Butt, 2007).

On the basis of glial development in the brain, glial cells are divided into two types by the origins: microglia derived from peripheral macrophages and macroglia derived from neurogenic ectoderm (Kandel et al., 2000). Furthermore, macroglia in the brain usually are usually subdivided into three main types (Figure 1-1): astrocytes (also called astroglia), oligodendrocytes and ependymal cells. With the evolution of the nervous system outnumbered glial cells were found in advanced animals, which were underestimated as basic supporting cells in the brain for a fairly long time. However, the novel prevailing view in the role of glia approves much closer but intricate interactions between glial cells and neurons as well as blood vessels. Therefore, the core subject of my study is astrocyte and I introduce detailed information on astrocytes in this chapter. Moreover, although there are many types of astrocytes found in the retina and different part of the central nervous system, this thesis will focus on the cortical ones.

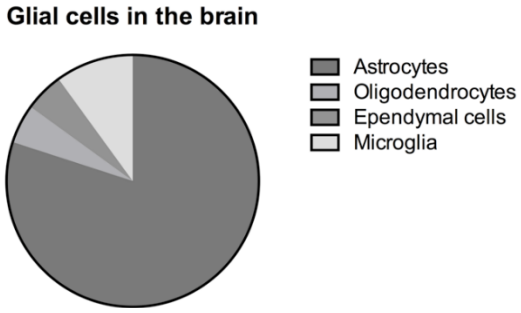

Figure 1-1 Percentages of different subtypes of glia in the human brain

By means of immunohistochemistry in the human brain, 80 % of glia are identified as astrocytes, the number of oligodendrocytes, ependymal cells and microglia is of approximately 5 %, 5 % and 10 %, respectively.

1.1 Definition and general distribution

In the central nervous system (CNS), about 80 % of glial cells are astrocytes (Verkhratsky and Butt, 2007), which leads to an extensive distribution throughout the whole brain from grey matter to white matter and the development of different functional properties of astrocytes in different brain regions.

The etymology of the word “astrocyte” comes from Greek words “astron” and “kyttaron”, indicating a kind of cell types with star-like appearance. Indeed, most astrocytes in grey matter present stellate (or protoplasmic) shape, with many thin and fine processes originating around the cell body, while the morphology in white matter is rather fibrous shape with thin but long processes (Redwine and Evans, 2002). Up to now there is no clear, consistent description to define subtypes of astrocyte yet, because of no exact specific marker. They are defined in functions of their morphology and distribution.

1.2 Astrocytes specific features

In light of the heterogenetic characteristics, astrocytes display several specific properties that distinguish them from other brain cells. In this section, I present two main astrocytic characteristics.

First, to support stellate and fibrous shape, astrocyte expresses a distinctive cytoskeleton protein to form intermediate filament (IF) - glial fibrillary acidic protein (GFAP) – which is deemed as a specific marker for immunostaining to distinguish from other cells such as microglia and neurons. Pathophysiologically, over expression of GFAP in astrocytes *in situ* is regarded as a hallmark of reactive astrocytosis and injury status of brain. Nevertheless, it is important to note that there are many limitations of GFAP as a marker of astrocyte, *i*) it is reported that only 20 % of astrocytes in the mature cortex and hippocampus *in vivo* are GFAP-positive, as the rest of astrocytes produce undetectable GFAP but glutamine synthetase and S100β (Norenberg, 1979; Feoli et al., 2008; Sofroniew and Vinters, 2010), which are not entirely exclusive to astrocytes; *ii*) GFAP immunostaining does not describe the whole territory of one astrocyte especially in those fine and remote processes, compared to other staining techniques like Golgi labeling, the expression of reporter proteins such as GFP or β-galactosidase or filling with fluorescent dyes (Bushong et al., 2002; Sofroniew and Vinters, 2010). However, the considerable investigations of GFAP in the CNS make applications of GFAP on immunohistochemistry and western blot more accessible for astrocyte labeling. To label living astrocytes, sulforhodamine 101 (SR101), a red fluorescent marker selectively traces astrocytes for imaging studies, which was used in our *ex vivo* studies.

The second but crucial feature of astrocytes is that they are not electrically excitable cells in terms of action potential such as in neurons. They rather convert external signals into

intracellular Ca^{2+} waves in response to neuronal stimulation. It is important to recognize that changes in intracellular Ca^{2+} levels enable astrocytes to establish astrocyte networks and tight intercellular communications both for synaptic transmissions and neurovascular coupling. Thus the mechanisms associated to Ca^{2+} waves in astrocytes seem to be central to understand how astrocytes respond to neuronal activity. Correspondingly, progressively emerging studies are unfolding the map of Ca^{2+} signalling in astrocytes. Detailed functions and mechanisms will be presented in section 3.

1.3 Classification and location

As mentioned, astrocytes are classified as stellate (or protoplasmic) astrocytes in grey matter and fibrous astrocytes in white matter by means of cellular morphology in the brain. Notably, there is a third subgroup of astrocytes existing the immature brain, termed radial glia, which are bipolar cells and extend two sets of processes arisen from the soma, one to pial surface and one terminated at the ventricular exterior. This subgroup is recognized as stem cells that give rise to neurons, astrocytes and oligodendrocytes during the developing CNS. Nonetheless, radial glia are also thought to exist in the mature brain in the form of tanycytes around the ventricles, Müller cells in the retina and Bergmann cells in the cerebellum (Lewis and Ebling, 2017).

During the development of the brain, astrocytes develop diverse morphologies once migrating out of the germinal zones (Redwine and Evans, 2002). Previous studies further identified three subtypes in the rodent cerebral cortex where astrocytes display distinctive morphologies and complex functions (Liu et al., 2013; Verkhratsky and Nedergaard, 2016; Vasile et al., 2017). *i*) Surface astrocytes (also called interlaminar astrocytes in the human brain) are located in cortical layer I. Their endfeet form continuous superficial glial limitans on the surface of pial vessels, but rarely contact neurons. *ii*) Protoplasmic astrocytes extending numerous fine processes are located in cortical layers II to IV and serve the most contacts with synapses as well as cerebral vasculature. *iii*) Few polarized astrocytes situate deeply in layer V and VI and stretch one or two very long processes upward till cortical layer III. These unipolar cells display rare contact with the vasculature and sparse coverage of neuropils. Moreover, there are another two subtypes of cortical astrocytes exclusively in the brains of human and higher-order primates (Figure 1-2). One is interlaminar astrocytes located in cortical layer I form pial

glia limitans and extend their longest processes to layer III or IV. They display similar features to surface astrocytes in the rodent brain. The second is varicose projection astrocytes located in layer V and VI. They extend few branches covering vessels and neuropils.

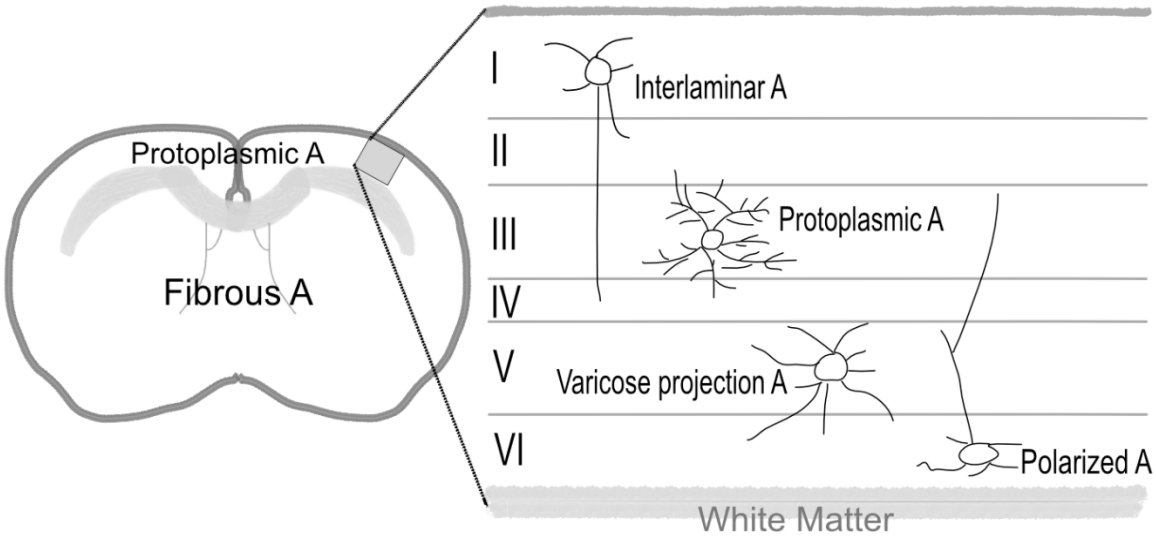

Figure 1-2 A schematic representation of astrocyte distribution in the human brain

On account of the difference in astrocyte (A) morphology, protoplasmic-like astrocytes are found in grey matter, and fibrous-like astrocytes are in white matter. To further understand astrocyte distribution from cortical layer I to layer VI, a piece of coronal section of the cerebral cortex is analyzed, showing interlaminar astrocytes, protoplasmic astrocytes, varicose projection astrocytes and polarized astrocytes, respectively.

In view of the contacts with cerebral vasculature and neuropils, we decide to choose the subjects of our *ex vivo* study - perivascular astrocytic endfeet from layers III to V of the mouse cerebral cortex, where it comprises most contacts with the vasculature walls and ensures the solely cellular source - protoplasmic astrocytes. This one of a kind architecture allows direct modulation of vascular tone by perivascular astrocytes-derived vasoactive factors. Considering the central position between neurons and blood vessels, perivascular astrocytes play vital roles in modulation of local blood flow in response to neuronal activity (MacVicar and Newman, 2015). Meanwhile, the area of astrocytic endfoot is fairly large, allowing imaging especially with two-photon confocal microscopy to identify and record changes in astrocytic endfeet *ex vivo* at morphological, spatial and temporal levels. Therefore, astrocytic endfoot was selected in

ex vivo studies to better understand responses of perivascular astrocytes

1.4 Functional roles of astrocytes in the brain

Far more than supporting cells, astrocytes play multiples roles in the brain. Key aspects of astrocyte function are described as follows:

1) During the early brain development, elongated radial glial cells are transformed from neuroepithelial cells. They have two main processes, one reaches the pial side and the other ends at the ventricular region. The pluripotent radial glia is regarded as precursor that has direct or indirect possibility to differentiate into neurons or macroglia. In the cortex, it is clear that radial glial cells form scaffold structure and give guidance for migration of neuronal precursors. Afterwards radial glia cells release multiple molecular factors to guide axon extension and assist with synapses formation and development (Sofroniew and Vinters, 2010). In addition, they also promote the formation and organization of the white matter and regulate vascularization in the cerebral cortex (Barry et al., 2014). In the mature brain, certain astrocytes in the hippocampus and in the subventricular zone have been identified as progenitor cells of neurons and astrocytes, though it is still under debate that in the adult brain tanycytes, Müller cells and Bergmann cells solely preserve the morphology of radial glia but not the stem cell capability.
2) Production of growth factors. Astrocytes secrete various growth factors upon neuronal damage or during synaptic ensembles. Throughout the embryonic and postnatal periods, astrocytes release synaptogenic molecules, such as cholesterol, thrombospondins and transforming growth factor (TGF) β1, which assist synaptic formation and remodelling (Diniz et al., 2012) and control synapse elimination by upregulating C1q expression and its complement cascade (Clarke and Barres, 2013). Production of astrocyte-derived growth factors in the mature brain is affected by aging, degeneration and injury. For instance, excess TGFβ production in astrocytes and neurons was triggered by obesity and aging, leading to inflammation and increased tissue degradation (Yan et al., 2014). When brain tissue suffers ischemia and hypoxia, astrocyte-produced erythropoietin, insulin-like growth factor (IGF) 1 as well as vascular endothelial growth factor (VEGF) are enhanced (Larpthaveesarp et al., 2015). Moreover, pathological astrocytes particularly form glial scars and reactive gliosis around lesions in the brain to prevent

inflammation and damage spread by secreting endothelin and VEGF (Burda and Sofroniew, 2014).

3) Interface between meninges and parenchyma. Surface astrocytes in the cerebral cortex and Begmann cells in the cerebellar cortex extend numerous endfeet toward the pial surface and form continuous superficial glia limitans. This unique structure, in part, isolates the brain parenchyma from the subarachnoid tissue. Under pathological conditions, incomplete glia limitans accompanied with neuronal loss was observed in Alzheimer's brain (Sofroniew and Vinters, 2010). Furthermore, surface astrocytes mediate the propagation of intra-cortical interactions, which are not only across the entire surface of glia limitans but go deep into the grey matter until cortical layer IV.
4) Contributions to the blood-brain barrier (BBB). All capillaries in the CNS are impermeable for big molecules, such as harmful substances and most medicines, owing to lack of fenestra. Generally, the principal BBB components comprise endothelial cells that form tight junctions, few vascular smooth muscle cells, pericytes and astrocytes (Daneman and Prat, 2015). Astrocytes are widely applied to induce formation of *in vitro* BBB. Paradoxically, *in vivo* evidence found that in the early brain development functional BBB appears before astrocyte generation and encirclement of blood vessels, suggesting that astrocyte does not take part in the initial formation of the BBB. However, astrocyte-secreted bioactive factors play crucial roles in maintenance and modulation of the BBB functions, for instance, astrocyte-secreted laminin was found to maintain the BBB integrity on the surface of blood vessels (Yao et al., 2014). Therefore, astrocyte is an important mediator, which assists endothelial cells to form tight junctions and maintains the BBB functions.
5) Contributions to brain energy. The energy utilization of neurons is very high, and nearly 80 % of brain energy goes to synaptic and action potentials, whereas the rest fuels glial cells-based activities such as glutamine synthesis which requires glutamate and ATP (Magistretti and Allaman, 2015). It is well established that glucose is the main source of brain energy and is imported from the blood supply through glucose transporters (GLUT) 1 in endothelial cells. After uptake by neurons via GLUT3, glucose is metabolized through active tricarboxylic acid (TCA) cycle and oxidative phosphorylation, which provide bulks of energy in the form of adenosine triphosphate (ATP). Alternatively, it

enters astrocyte through GLUT1 and is predominantly converted into lactate through the aerobic glycolysis pathway. Released lactates can be further uptaken by neurons and oxidized to yield ATP. Besides, astrocytes in the adult brain exclusively store glycogen which is a storage form of glucose. Hence, when glucose supply cannot meet energy requirements, glycogenolysis is stimulated in astrocytes to maintain axon activation, or in pathology, to prevent hypoglycemic neural injury (Brown and Ransom, 2007). It is also noteworthy that in the injured brain, reactive astrocytes downregulate glutamine synthase activity to decrease energy demands and save ATP, thereby further reducing adjacent synaptic currents (Burda and Sofroniew, 2014). Collectively, astrocyte acts as a warehouse of energy sources in the brain metabolism.

6) Astrocyte develops high-efficient uptake system of neurotransmitters, such as glutamate and gamma-aminobutyric acid (GABA). This function enhances signalling efficiency and accuracy during synaptic transmission, since the neurotransmitters removed into astrocytes have no effects on other cells and then are stored either for energy source or for neurotransmitter circulation. Astrocytes structurally extend perineuronal processes terminating to neuronal synapses, thus forming tripartite synapses, which comprise presynaptic terminal, postsynaptic terminal and the enclosed astrocytes. In addition, high levels of neurotransmitter transporters are clustered predominantly around perineuronal astrocytic membrane. In the modulation system of extracellular glutamate, slowly desensitizing metabotropic glutamate receptors (mGluR), a group of high-affinity glutamate transporters, are located at the areas close to synaptic cleft, while at the further distance astrocytic membrane enriches ionotropic glutamate receptors (iGluR), which are fast desensitizing but display low affinity for glutamate. In addition, a novel mechanism that was recently found in astrocytes to limit glutamate spillover from the cleft. Increased glutamate levels at synaptic cleft could recruit glutamate transporter 1 (GLT-1) membrane diffusion (Murphy-Royal et al., 2015) depending on the activity of astrocytes as well as neurons. Since glutamate is unable to penetrate into the BBB, all brain cells have to take the strategy to maximize utilization of glutamate. Therefore, a part of glutamates is converted into glutamine by glutamine synthase exclusively expressed in astrocytes. Released glutamine is taken up either by glutamatergic neurons or GABAergic neurons and further partakes to the synthesis of glutamate or GABA

(Schousboe et al., 2014).

7) To maintain extracellular ion and water homeostasis, astrocyte develops high-sensitive modulation system for ions such as potassium. Normally, extracellular K^+ concentration can be raised from 3 mM at the resting level to approximately 12 mM when nerve cells are firing. Those extra ions will be redistributed later by astrocytes through two means. One is local transportation, which is mediated mostly by individual astrocyte via Na^+/K^+ pumps and $Na^+/K^+/Cl^-$ transporters. Meanwhile, extracellular H_2O accompanied with K^+ movement also crosses into astrocytes and causes cell swelling, signifying a limitation of this mechanism. Hence, the second pathway termed spatial K^+ buffering allows loads of K^+ to be expelled to low-concentrated K^+ areas via astrocyte networks. This process recruits astrocytic gap junctions, the inward rectifying K^+ channels - K_{ir} 4.1 ensuring mildly inward and outward movement of K^+, as well as water channels aquaporin 4 (AQP4), which are enriched along perivascular astrocytes to regulate fluid volume. Notably, this spatial transportation not only contributes to maintenance of synaptic activity and protection of membrane potentials of neurons and astrocytes, but also removes both K^+ and H_2O into the blood. Besides, endfeet were found to be associated with the vascular outcome by releasing K^+ at perivascular side via big-conductance potassium (BK) channels (Girouard et al., 2010).
8) Bordering on the area of surface astrocytes in the grey matter, endfeet emanated from protoplasmic astrocytes are involved in regulation of cerebral blood flow (CBF) by contacting with blood vessels and releasing vasoactive factors. Prior studies have showed that in response to neuronal activity perivascular astrocytes produce and release diverse vasoactive factors derived from arachidonic acids (AA), which in turn modulate vascular tone. This real-time linkage is termed neurovascular coupling (NVC) and address brain activity and interpret neuroimaging data.

1.5 Ion channels, gap junctions and membrane receptors

In light of multiple tasks that astrocytes execute in the brain, a great variety of ion channels are expressed to regulate intra- and extracellular ion levels and maintain the high negative resting membrane potential in the range from -80 to -90 mV (Verkhratsky and Butt, 2007).

Furthermore, extensive intercellular interactions are established through gap junctions and membrane receptors. Those membrane structures contribute to the functional and informational integration of astrocytes within brain networks.

1.5.1 Ion channels

Unlike neurons, astrocytes have two distinctive features in ion distributions. One is the exclusive K^+ conductance that drives astrocytic resting membrane potential towards a very highly negative potential, approximately -90 mV. The other is the unusual high concentrations of chloride ions (~ 40 mM) in the astrocytic cytosol (Verkhratsky and Butt, 2007). In terms of these knowledges, the major ion channels in astrocytes are introduced as follows:

1.5.1.1 K^+ channels

Given the importance in the resting membrane potential, potassium channels have been well demonstrated as the most abundant channels in astrocytes. Biophysically, they are divided into four classes: inward rectifier K^+ channels (K_{ir}s), two-pore K^+ channels, outward rectifier K^+ channels and Ca^{2+}-dependent K^+ channels (K_{Ca}s).

1) K_{ir}s, are responsible for hyperpolarized resting membrane potentials via favoring large K^+ influx into the cell. It is observed that high density of K_{ir}s, the K_{ir} 4.1 subtype in particular, preferentially situated along the fine astrocytic processes facing neuronal synapses and at astrocytic endfeet enwrapping blood vessels (Verkhratsky and Steinhäuser, 2000). Astrocyte also expresses K_{ir} 2.0, K_{ir} 5.1 and ATP-dependent K_{ir}s (K_{ir} 6.1 and K_{ir} 6.2). (Olsen et al., 2015). In the early studies, the heterogeneous expression of K_{ir} channels in astrocytes was thought to serve the primary function in uptake and redistribution of extracellular K^+, termed spatial K^+ buffering. To date, investigations have demonstrated other facets of astrocytic K_{ir}s functions. In genetic models, K_{ir} 4.1 is associated with brain maturation and the prevention of epilepsy (Olsen et al., 2015). K_{ir} 5.1 forms heterometric channels with K_{ir} 4.1 and AQP4 in favor of regulating brain volume and chemoreception due to its sensitivity to alkaline conditions (Seifert et al., 2016). Upregulation of K_{ir} 6.2 was observed in reactive astrocytes in Alzheimer's disease (AD) (Griffith et al., 2016).

2) Astrocytic two-pore K^+ (K_2P) channels, consisting of TASK-1, TWIK-1and TREK-1/2

channels, function like K_{ir}s and have the capability of setting the resting membrane potential close to the K^+ equilibrium potential (E_K). Though K_2P channels are involved in ion/water homeostasis and gliotransmitter release (Seifert et al., 2016), their functional impact remains to be unraveled.

3) outward rectifier K^+ channels, include rapidly inactivating A-type channels (K_As) and delayed rectifier K^+ channels (K_{dr}s). Patch-clamp studies showed that those voltage-gated channels are predominants in immature astrocytes. In neurons, K_As and K_{dr}s are responsible for repolarizing the action potential via K^+ efflux, whereas in astrocytes, they play important roles in improvement of voltage control in astrocytic proliferation and regulation of astrocytic Ca^{2+} influx (Wu et al., 2015).

4) K_{Ca}s, are activated by an increase in intracellular Ca^{2+}, which in turn, leads to the K^+ influx. K_{Ca}s are classified into three subfamilies depending on the biophysical properties: small-conductance K^+ channels (SK), intermediate-conductance K^+ channels (IK) and BK channels. Both mRNA and protein expressions of IK channel are barely present in astrocytes in physiological conditions (Weaver et al., 2006). Despite slight subunit SK2 proteins were detected in astrocytes, the contribution of astrocytic SK channels to NVC remains a controversial issue at present (Weaver et al., 2006; Seifert et al., 2016). Unlike SK and IK channels which are voltage insensitive, BK channels are gated by both Ca^{2+} and the transmembrane voltage. High density of BK channels are resided in the cytoplasmic membrane of astrocytic endfeet facing blood vessels, presenting a non-uniformed distribution. Such properties underlie the implication of astrocytic endfeet BK channels in NVC. Once activated by neuronal activity via intracellular Ca^{2+} waves, astrocytic BK channels are functionally coupled with K^+ channels such as K_{ir}s in the membrane of vascular smooth muscle cell (VSMC) and modulate the membrane potential of VSMCs, thereby leading to vasodilation.

1.5.1.2 Ca^{2+} channels

Astrocytes have many channels and receptors that allow for increases in internal Ca^{2+} concentration. Astrocytes, especially immature astrocytes, possess L-type and T-type Ca^{2+} channels. The former is high-voltage activated, while the latter is low-voltage gated. Activation of astrocytic Ca^{2+} channels induces a large Ca^{2+} influx up to 1 μM. Nonetheless, those channels

are absent in some cerebellar astrocytes and Bergmann cells. Partially due to these anatomical findings, studies on L- and T-type channels in astrocytes are not as prevalent as other channels concerning Ca^{2+}. Though recent evidence reported that GABA activates astrocyte-like cells in subventricular zone by triggering Ca^{2+} influx through L-type and T-type Ca^{2+} channels (Young et al., 2010), L-type Ca^{2+} channels are prone to be involved in pathological response. For example, glial scars were found to overexpress L-type channels, which can be activated by the heme oxygenase-1 (HO-1) / carbon monoxide (CO) pathway after stroke (Verkhratsky and Steinhäuser, 2000; Choi et al., 2016).

The main sources of Ca^{2+} increases in astrocytes has been attributed to releases from internal stores. This signal occurs upon activation of Gq GPCRs and the phospholipase C (PLC). PLC breaks down PIP_2 into diacylglycerol (DAG) and inositol triphosphate (IP_3), which can activate the IP_3 receptor (IP_3R) on the endoplasmic reticulum (ER) to release Ca^{2+} (Hatton and Parpura, 2004). The other Ca^{2+} compartment in the ER is activated by the ryanodine receptor (RyR).

The phospholipase C pathway is also linked to transient receptor potential channels (TRPCs), which are non-selective Ca^{2+} channel. These channels can be activated by a second messenger induced by depletion of internal Ca^{2+} stores following activation of Gq GPCRs or by binding of IP_3 itself. The other product of the PLC pathway, DAG, also can open these channels. Blocking channels (TRPC1 in particular) in cultured astrocytes led to reduced Ca^{2+} signaling (Achour et al., 2010). TRPCs can also activate store operated Ca^{2+} entry in the absence of PLC activation (Achour et al., 2010).

1.5.1.3 Cl^- channels

Astrocyte is a natural Cl^- pool in the brain by largely transporting chloride ions via $Na^+/K^+/2Cl^-$ cotransporters. The intracellular concentration of chloride *in vitro* is in the range of 29 mM to 46 mM. Considering the roles that astrocytic K^+ channels play, cytosolic Cl^- levels potentially contribute to K^+ buffering and astrocytic volume (Verkhratsky and Steinhäuser, 2000). So far, three groups of chloride channels have been identified in astrocytes, including voltage-gated Cl^- channels, Ca^{2+}-activated Cl^- channels and volume-activated Cl^- channels. In addition to these three groups, increasing investigations imply that some astrocytic membrane proteins also function as Cl^- channels. For instance, excitatory amino acid transporter 1 (EAAT1)

was found to remove extracellular glutamate and mediate Cl^--selective conductance at the same time (Gonzalez-Suarez et al., 2017). It is likely that chloride not only participates in regulation of cell volume and K^+ redistribution but links to glutamatergic synaptic transmission.

1.5.2 Gap junctions

Gap-junctional couplings enable astrocytes to form extensive homocellular and heterocellular networks. Their spatial properties determine the strength and the spreading distance of astrocytic signal propagations. In addition, the strength correlates with the morphology alteration of local astrocytes as well as changes in temperature.

Between cytoplasmic membranes from two adjacent cells, two connexons align with each other forming one functional gap junction. Each connexon consists of 6 subunits, termed connexins (Cx), which form a pore allowing ions, water and several macromolecules (< ~ 1.2 kDa), such as second messengers ATP and ADP, to permeate and enter into homocellular or heterocellular cytosol (Giaume and Naus, 2013). Thus, gap junctions provide a direct pathway for cell-to-cell communication. By contrast, single connexon in the cytoplasmic membrane disconnecting with another connexon functions as a connexon hemichannel, which directly mediates exchanges of ions, metabolites and gliotransmitters with extracellular space. Recent research suggested that astrocytic connexon hemichannels are implicated in shaping excitatory synaptic transmission (Olsen et al., 2015).

Four-transmembrane connexin is named on the basis of the difference in molecular weight ranging from 26 to 62 kDa (Verkhratsky and Butt, 2007), for example, a 26-kDa connexin is called Cx26. Astrocytes, especially processes and endfeet encasing blood vessels, express the highest densities of Cx30 and Cx43. Their distributions are dynamic and non-uniformed. Indeed, gap junction coupling can be detected in the hippocampus right after the birth and reaches adult levels by the middle of the second postnatal week (Konietzko and Müller, 1994; Schools et al., 2006), whereas dynamic changes of astrocyte coupling could also occur after connexin phosphorylation (Márquez-Rosado et al., 2012). Astrocytic connexins selectively allow discrimination of signal spreads within disparate astrocyte networks, contributing to fine regulation of synaptic plasticity and energy supply. Additionally, Cx30/Cx43 facilitates BBB functions and has a tight interaction at the surface between astrocytic endfeet and cerebral

vasculature (Watanabe et al., 2016).

1.5.3 Membrane receptors

Astrocytes, alike neurons, are endowed with all major membrane receptors. Their expression differs during the development of the brain as well as under pathological conditions and exhibits spatial heterogeneities at subcellular and regional levels.

Astrocytic membrane receptors, due to their differences in structure and biophysical property, are classified into two species: ionotropic and metabotropic receptors. The former assembles ion-permeable channel directly allowing in and out movement of ions; while the latter forms several transmembrane domains and its intracellular part is coupled to various guanosine triphosphate (GTP) proteins, also termed G proteins, which in turn, induce second messengers entailing a much wider range of response. Furthermore, astrocytic membrane receptors are far more diverse than previously thought. They are further grouped on the basis of their ligand types, comprising amino acids (e.g. glutamate, glycine, histamine), peptides (e.g. vasoactive intestinal polypeptide), acetylcholine (ACh), purine nucleotides (e.g. adenosine, ATP), active factors (e.g. angiotensin, bradykinin, endothelin), hormones (e.g. adrenaline), cytokine, chemokine. Hence, in the present text, I describe several classic receptor types in astrocytes from the cerebral cortex where my study was instigated.

1.5.3.1 Glutamatergic receptors

Glutamate is the major excitatory amino acid in the brain. Astrocytes correspondingly express various glutamatergic receptors (Figure 1-3A) including iGluRs and mGluRs, which are similar to neurons.

iGluRs are ligand-activated ion channels. According to the discovery of selective agonists, iGluRs consist of three types of receptors: NMDA, AMPA and kainate (KA) receptors.

1) NMDA receptors, seven subunits of which are currently identified in the rodent and human astrocytes, including NR1, NR2A/B/C/D, NR3A/B (Lee et al., 2010). As a heterotetramer receptor, its activation requires two NR2-binding agonists (glutamate, NMDA or endogenous neurotoxin quinolinic acid) and two NR1-binding coagonists (glycine or D-serine), allowing K^+ efflux and Na^+/Ca^{2+} influx. Importantly, extracellular Mg^{2+} is a natural channel blocker of NMDA receptor inside its ion channel, and can be repelled when the receptor

is activated. Unlike neuronal NMDA receptor, many studies found that astrocytic NMDA receptor displayed a weak Mg^{2+} block, and therefore has the potential to be active at the resting membrane potential. Indeed, significant blockade of Ca^{2+} influx was monitored in brain slices only when the concentration of Mg^{2+} in buffer reached 10 mM (Maneshi et al., 2017). Those findings point out structural and pharmacological differences of astrocytic NMDA receptors compared to the neuronal ones (Palygin et al., 2011).

Compared to AMPA receptors and Kainate receptors, which have lower Ca^{2+} permeability and rapid desensitization, NMDA receptor is high permeable to Ca^{2+} and exhibits rare desensitization following intense inputs. The intracellular domain of NMDA receptor connects several enzymes, for instance, Ca^{2+}/calmodulin-dependent protein kinase II (CaMKII), PSD-95 (postsynaptic density protein 95) and proto-oncogene tyrosine-protein kinase (Fyn) via the NR2 subunit, and protein kinase A (PKA) and C (PKC) via the NR1 subunit. It should be noted that many psychoactive drugs such as anaesthetics are antagonists, which partially or fully impair NMDA receptor activity either by binding at the surface or situating inside the ion channel. For instance, pre-treatment of brain slice with the non-competitive antagonist of NMDA receptor MK-801, also known as dizocilpine, resulted in a full Ca^{2+} blockade of neuronal NMDA receptor (Brancaccio et al., 2017).

2) AMPA receptors, can be selectively activated by the artificial glutamate analog AMPA and induce a weak Ca^{2+} flow in astrocytes, leading to membrane depolarization. AMPA receptor possess four subunits: GluR1, GluR2, GluR3 and GluR4. These subunits form an ion channel permeable to Na^{+}, K^{+} and Ca^{2+}. The subunit GluR2 plays a key role in determination of Ca^{2+} permeability. Additionally, each subunit has a ligand binding site at the surface membrane, while in the intracellular space it links to kinases such as CaMKII and PKC via PDZ domains. AMPA receptors are widely distributed in the cerebral cells, particularly in protoplasmic astrocytes, but the expression of GluR2 and GluR3 is much lower compared to those in synapses of the CA1 region (Haglerød et al., 2017). It suggests a heterogeneity of subunits distribution. For instance, GluR4 subunit is enriched in the cerebral cortex. Also, either the presence or lack of GluR2 have been observed in astrocytes from the olfactory bulb (Droste et al., 2017). Notably, dysfunction of AMPA receptors underlies stroke, epilepsy and other neurodegenerative diseases (Chang et al., 2012).

3) KA receptors, can be fully activated by kainate and contain five subunits GluR5, GluR6,

GluR7, KA1 and KA2. It should be note that kainate is also a partial agonist of AMPA receptor, explaining the reason that AMPA/KA receptors are usually referred together. Even though few investigations reported functions of KA receptors in astrocytes, immunostaining confirmed that hippocampal astrocytes express subunit KA2 in the cytosol and the membrane (Matschke et al., 2015), and an upregulation of all KA receptors subunits was detected in reactive astrocytes (Vargas et al., 2013; Crepel and Mulle, 2015). Experimental studies demonstrated, that in a stressful state, activation of few KA2 in astrocytes may affect gene expression and turn down some metabolic action (Matschke et al., 2015).

The other large group of glutamatergic receptors is mGluRs, which consist of seven-transmembrane receptors coupled to G proteins at the intracellular surface. mGluRs in the brain are mainly responsible for modulatory action of glutamate. To date eight members of mGluRs have been identified, mGluR1~mGluR8, which are further categorized into three subgroups based on their intracellular signalling cascades.

1) Group I mGluRs, the only subgroup of mGluRs is coupled to phospholipase C (PLC) by G_q proteins and has the capacity to raise intracellular Ca^{2+}. It consists of mGluR1 and mGluR5. The distribution of the latter is very abundant in astrocytes, but the expression is influenced by age (Sun et al., 2013). Interestingly, emerging studies provided the information that astrocytic mGluR5 was upregulated in the early period following ischemia injury, peripheral nerve damage, and neuropathic pain (Dzamba et al., 2015; Kim et al., 2016; Kim et al., 2017). Those re-emerged mGluR5 may result in synaptic remodeling and modulation of circuit plasticity. Physiologically, cortical and hippocampal astrocytes express mGluR5, but the number of which is much less than that of mGluR3 (Sun et al., 2013; Kim et al., 2016).

2) Group II mGluRs, comprising mGluR2 and mGluR3. Group II is coupled to the inhibition of adenylate cyclase (AC) via G_0/G_{11} proteins. mGluR3 is the second prevalent mGluRs in astrocytes. Sun et al. specified that mGluR3 but not mGluR5 was exclusively expressed in adult cortical astrocytes of the mouse and human brain (Sun et al., 2013). Investigations on astrocytic mGluRs found that they can function by linking to other intracellular cascades than the PLC-inositol 1,4,5-trisphosphate (IP_3) signalling pathway.

3) Group III mGluRs, subtypes of mGluR4, mGluR6~mGluR8 belong to group III and share similar mode of action to group II, regulating intracellular cyclic adenosine monophosphate

(cAMP) levels. Up to now, there is no evidence with regard to the expression of group III in astrocytes in the brain.

1.5.3.2 Cholinergic receptors

ACh acts as a neurotransmitter for somatic and autonomic motor neurons. Most cholinergic neurons are located in the basal forebrain and the mid-brain and project upwards into the cerebral cortex, consequently leading to the enhancement of cortical responses to neuronal inputs. Cholinergic receptors (Figure 1-3B) are grouped into muscarinic cholinoreceptors (mAChRs) and nicotinic cholinoreceptors (nAChRs). Previous immunological studies have found that in the cerebral cortex protoplasmic astrocytes *in situ* especially express both mAChRs and nAChRs.

1) mAChRs, are metabotropic receptors coupled to G proteins and have five subtypes M1~M5. Experimental studies discovered that M1, M3 and M5 receptors are coupled to PLC and lead to an increase in intracellular Ca^{2+}, while M2 and M4 are coupled to ACs to suppress cAMP levels. Studies *in vivo* have showed that expression levels of mAChRs changes in response to neuronal activity and under pathological conditions, mostly resulting in the upregulation of mAChRs. It is likely a compensatory response, because activation of mAChRs is coupled to an increase in astrocytic Ca^{2+} levels, which further advances neuronal functions in attention, learning and memory (Hirase et al., 2014; Woehrling et al., 2015).

2) nAChRs, are ionotropic receptors permeable to Na^{+}, K^{+} and Ca^{2+}, and their binding sites show a high affinity for nicotine. Nine subunits of nAChRs are identified, α2~α7 and β2~β4. Subunit α7 expression is extensively distributed in the brain, such as in astrocytes, where it is involved in synaptic transmission. In brains from Alzheimer's patients, amyloid-β is associated to upregulation of nAChRs containing the α7 subunits in astrocytes, whereas, in an AD mouse model, an increase in astrocytic Ca^{2+} through α7-containing nAChRs (Pirttimaki et al., 2013; Dineley et al., 2015). Such abnormal expression of nAChRs subunits including α4, α7 and β2 in the cerebral cortex, are deemed as therapeutic targets for schizophrenia and autism.

1.5.3.3 Purinergic receptors

Although, not extensively studied in the present thesis, purinergic receptors are described here due to their importance in astrocytic Ca^{2+} regulation so that possible interactions with this

pathway has to be kept in mind. In the cerebrum, astrocytes are the main cellular source of purine. Purinergic receptors (Figure 1-3C) are classified into P1 and P2 receptors on the basis of the ligand types.

1) P1 receptors, G protein-linked receptors, are grouped into three subclasses A_1, A_2 and A_3 receptors. A_1 receptor has the capacity of reducing cAMP production, but activation of A_2 receptor increases cAMP production via activation of G_s protein. A_2 receptors can be further categorized into two subclasses A_{2A} and A_{2B}. It was found that astrocytic A_{2A} receptor is associated with glutamatergic function by regulation of GLT-1 activity (Matos et al., 2015). Activation of A_3 receptor increases PLC activity but reduces AC activity, resulting in attenuation of cAMP production. Low expression of A_3 mRNA was detected in the CNS, but it seems to play a neuroprotective role in mouse astrocytes (Borea et al., 2015). Additionally, A_3 receptor is the only subtype of P1 receptors recognized as a potential target for therapy due to the overexpression in inflammatory cells.

2) P2 receptors are further divided into P2X and P2Y receptors. P2X is an ATP-gated ionotropic receptor allowing K^+ efflux and Na^+/Ca^{2+} influx. It contains seven members, $P2X_1$~$P2X_7$. Each member displays different sensitivity to ATP, and both $P2X_1$ and $P2X_5$ receptors are the most sensitive P2X ones. Astrocytic functional $P2X_1$, $P2X_5$ and $P2X_7$ receptors were observed in astrocytes (Verkhratsky and Burnstock, 2014). Unlike $P2X_1$ and $P2X_5$ receptors, $P2X_7$ receptor is insensitive to ATP and requires millimolar concentrations of ATP for its activation. Importantly, astrocytic P2X receptor comprising $P2X_1$, $P2X_5$ and $P2X_7$ subunits has the capability of sensing ATP from nanomolar to millimolar concentrations and ensures the regulation of purinergic transmission in a wide-ranging but fine manner.

P2Y receptor is coupled to G proteins in the intracellular space and links to the PLC enzyme in particular. It has eight subtypes, including $P2Y_1$, $P2Y_2$, $P2Y_4$, $P2Y_6$, $P2Y_{11}$~$P2Y_{14}$. Once activated by extracellular nucleotides, $P2Y_{1/2/4/6/11}$ receptor coupled to G_q/G_{11} proteins can increase PLC activity and lead to IP_3-mediated Ca^{2+} waves, whereas $P2Y_{12/13/14}$ receptor is coupled to G_i protein which suppresses AC activity. Recent evidence of the cortex revealed a dynamic metabolism that neurons could ask astrocytes for supplies such as growth factors by releasing nucleotides instead of glutamate, which in turn, to stimulate adjacent astrocytic P2X and P2Y receptors (Vignoli and Canossa, 2017). Astrocytes can also participate to neuronal plasticity through a wide variety of signalling complexes.

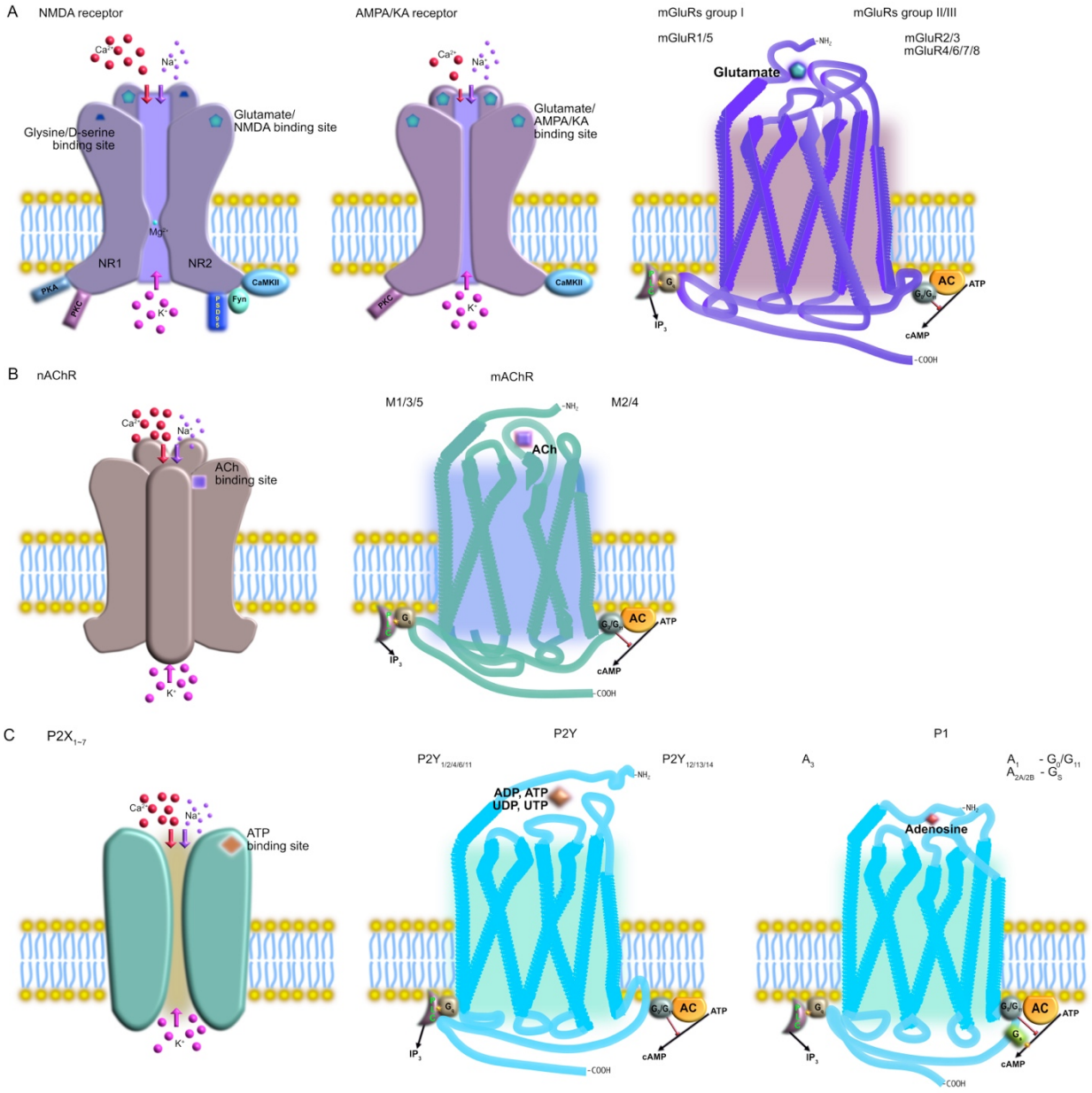

Figure 1-3 Schematic diagram of the structural complex of glutamate receptors, cholinergic receptors and purinergic receptors

Illustrations represent the architecture and biophysic properties of iGluRs (NMDA receptor and AMPA receptor) and mGluRs (A), nicotinic and muscarinic cholinergic receptors (B) and subgroups of purinergic receptors (i.e. P2X, P2Y, P1) (C).

2. Effects of major primary messengers on astrocytes

Neurotransmitters are the primary messengers of all the brain cells, controlling whole-brain communication. There is a great range of neurotransmitters in the body, comprising inhibitory transmitters such as GABA, and excitatory transmitters, e.g. glutamate, dopamine, norepinephrine, etc. They can be further grouped on the basis of their composition, i.e. amino acids, peptides, amines, purines, cholines, gasotransmitters, etc. For the purpose of this thesis, only effects of glutamate, acetylcholine, purine nucleotides will be discussed due to their shared capability of eliciting oscillatory increase in intracellular Ca^{2+}.

2.1 Glutamate

Glutamate is the most abundant excitatory neurotransmitter in the brain, acting on both ionotropic and metabotropic receptors. In the 1930s, high concentrations of glutamate were firstly found in the brain (Marmiroli and Cavaletti, 2012), with the highest concentration detected in the cerebral cortex. Since the BBB is impermeable to glutamate, all glutamates in the brain are produced by neurons and macroglia via TCA cycles (Schousboe et al., 2014). Apart from the glutamate snatched by neuronal receptors at the synaptic membrane, the rest is taken up by surrounding astrocytes via relative receptors and transporters. Here, the effects induced by activation of astrocytic glutamate receptors on astrocytes is presented.

2.1.1 Effects of iGluRs activation

In previous decades, the functional existence of iGluRs in astrocytes was a matter of debate, and then with the development of techniques, it is general believed that astrocytes do express functional iGluRs which shed light on a great variety of physiological and pathological processes (Hoft et al., 2014). Although the results on astrocytes are not fruitful, emerging investigations are unfolding the map of iGluRs signalling pathway.

2.1.1.1 NMDA receptor

Most findings in the field of iGluRs focus on neurons, particularly for the NMDA receptor. In adult human astrocytes, all subunits forming functional NMDA receptors was identified (Lee et al., 2010), but most astrocytic NMDA receptors in the mouse cortex comprise two NR1, one

NR2C/2D and one NR3, presenting a fairly low sensitivity to Mg^{2+} (Palygin et al., 2011). Furthermore, the classic co-agonists of NMDA receptor, glycine and D-serine, cannot potentiate the activation of NMDA receptors in cortical astrocytes (Palygin et al., 2011).

The primary function of astrocytic NMDA receptor is to achieve intracellular Ca^{2+} elevation, leading to the release of gliotransmitters such as glutamate and ATP. Once activated by high-doses of NMDA (100 μM), NMDA receptors induce significant Ca^{2+} efflux from astrocytic ER, but are suppressed later by the tyrosine kinases acting on subunits of NR1 and NR2A/2B subunits. Meanwhile, the uptake of free cytosolic Ca^{2+} by mitochondria causes a decrease of its membrane potential in cultured rat cortical astrocytes (Montes de Oca Balderas and Aguilera, 2015). In addition, subtle but persistent PLC-PKCδ-dependent NMDA signalling evoked release of Ca^{2+} from astrocytic ER in a Ca^{2+}-independent manner. The consequence of activation of NMDA receptors caused release of glutathione (GSH) precursors via activation of p35/cyclin-dependent kinase 5 (Cdk5)-mediated nuclear factor-erythroid 2-released factor 2 (Nrf2) phosphorylation (Jimenez-Blasco et al., 2015). This finding demonstrated an antioxidant role of NMDA receptor in astrocytes, since GSH precursors sustain neuronal survival. Furthermore, it supports the idea that activation of NMDA receptor also stimulates the corresponding kinases and phosphatases binding to its intracellular domains, termed metabotropic-like signalling, which subsequently trigger Ca^{2+} efflux from ER (Marmiroli and Cavaletti, 2012; Jimenez-Blasco et al., 2015; Montes de Oca Balderas and Aguilera, 2015). Indeed, MK-801 blocked the ion channel of NMDA receptor but activated its metabotropic signalling, when hippocampal astrocytes were repeatedly treated with MK-801. The signalling enhanced phosphorylation of the MAPK kinase (MEK)-MAPK pathway and the PI3K-Akt-glycogen synthase kinase (GSK)-3β pathway, leading to upregulation of BDNF and TrkB (Yu et al., 2015).

As a results of NMDA receptor activation in astrocytes, not only are the neuroprotective factors enhanced, but all subunits of NMDA receptor are upregulated in response to pathological insult. For instance, in the post-ischemic astrocytes, all subunits were upregulated, and specific upregulation of either NR2 or NR3A contributed to suppression of intracellular Ca^{2+} rises (Dzamba et al., 2015; Suhs et al., 2016). Interestingly, when astrocytes undergo excitotoxicity, activation of NMDA receptor may induce cell dysfunction and death. A prior study found that cortical astrocytes overexposed to glutamate both *in vitro* and *in vivo* caused excessive activation of astrocytic NMDA receptors, which suppressed $K_{ir}4.1$ expression and induced cell

dysfunction (Obara-Michlewska et al., 2015). In addition, endogenous excitotoxins such as microglia-produced quinolinic acid binding to NMDA receptor resulted in astrocyte death (Lee et al., 2010). Therefore, memantine, an antagonist possessing a much higher affinity for astrocytic NMDA receptor than neuronal NMDA receptor, is used to treat AD patients in clinics, partially weakening the glial pathology induced by quinolinic acid and decreasing astrocyte-secreted cytokines (Palygin et al., 2011; Suhs et al., 2016).

2.1.1.2 AMPA receptor

Previous studies have noted that the distribution of AMPA receptor is very much heterogeneous. AMPA receptors are localized abundantly in somatosensory cortical astrocytes and olfactory bulb astrocytes, partially in thalamic astrocytes, but undetectably in the CA1 region of the hippocampus (Hoft et al., 2014; Dzamba et al., 2015; Droste et al., 2017). Moreover, the heterogeneous distribution is presented at the subunit scale. For example, a recent study found that astrocytes in the olfactory bulb expressed AMPA receptors both containing and lacking GluR2, an AMPA receptor subunit responsible for Ca^{2+} permeability (Droste et al., 2017). These anatomical features are tightly linked to AMPA receptor functions such as modulation of energy supply and release of gliotransmitters, contributing to neuronal development.

Traditionally, Ca^{2+} permeability plays a key role in AMPA receptor-mediated neuron-glia interaction. Activation of astrocytic AMPA receptor causes an increase in intracellular Ca^{2+} arising from Ca^{2+} influx through AMPA receptor and ER Ca^{2+} efflux. This mechanism renders astrocytic AMPA receptor to be a sensor of axonal activity. Droste et al. (2017) found that Ca^{2+} transients in astrocytes evoked by activation of AMPA receptor depends principally on the concentration of extracellular Ca^{2+}, and then a weak Ca^{2+} efflux comes out of intracellular stores. Under pathological conditions, Ca^{2+} influx through astrocytic AMPA receptor is enhanced as well. For instance, cerebral artery occlusion upregulated all subunits of AMPA receptor in reactive astrocytes other than GluR2, the subunit limiting Ca^{2+} permeability (Dzamba et al., 2015). Collectively, astrocytic AMPA receptor requires higher Ca^{2+} permeability in response to pathologic insult.

2.1.1.3 KA receptor

KA receptor, located in the hippocampus, is considered to act as a sensor for excessive glutamate in the extracellular space. Since it is a nonselective cation channel partially permeable to Ca^{2+}, the modulatory mechanisms of KA receptor can be stimulated, *i*) through Ca^{2+} influx which could further potentiate release of gliotransmitters, such as glutamate and ATP, *ii*) via amplification of Na^{+} signals leading to activation of astrocytic Na^{+}/K^{+}/ATPase (Vargas et al., 2013). Nonetheless, under physiological conditions, hippocampal KA receptors were observed mainly in NG2 glial cells, a subgroup of glia specifically expressing chondroitin sulphate proteoglycan, in contrast to mature astrocytes (Vargas et al., 2013; Wang et al., 2016). After epilepsy or ischemia, however, KA receptor subunits, including KA1, KA2, GluR5 and GluR6, were all upregulated in hippocampal astrocytes (Vargas et al., 2013; Matschke et al., 2015). It is suggested that KA receptor is an active player in the pathologies of epilepsy and ischemia. However, Mastschke et al. deemed that dynamic expression of KA receptor in astrocytes contributes to neuroprotective mechanisms. This negative feedback mechanism is activated under pathologic conditions due to upregulation of N-myc downstream-regulated genes (NDRGs) proteins. Thus, serum- and glucocorticoid-inducible kinase (SGK) 1 phosphorylates overexpressed NDRGs at the site of Thr330, directly inhibiting KA2 expression in a dose-dependent manner and resulting in decreased number of functional KA receptors in astrocytes (Matschke et al., 2015). Therefore, KA receptor seems to play important roles in pathophysiological situations by way of dynamic expression.

2.1.2 Effects of mGluRs activation

mGluRs are a class of G protein-coupled receptors capable of evoking both metabolic and electrical cascades when activated in astrocytes. Considering the prevalent studies of astrocytes on mGluRs, only the effects of astrocytic mGluRs group I and group II on astrocytes will be presented.

2.1.2.1 mGluRs group I

Activation of group I receptors in astrocytes triggers numerous intracellular signalling pathways. Coupled to PLC_{β} via G_q/G_{11} proteins, astrocytic mGluRs group I receptors

predominantly promote the production of IP_3, which leads to Ca^{2+} spikes by binding to IP_3 receptor in endoplasmic reticulum (ER) membrane (Niswender and Conn, 2010). This signalling constitutes the underlying mechanism of the interaction between mGluRs group I and mAChRs in astrocytes, the activity of which depends on a novel effect in astrocytes, termed priming effect, which can be provoked by repetitive application of glutamate or trans-1-aminocyclopentane-1,3-dicarboxylic acid (*t*-ACPD), an agonist of group I/II receptors (Pasti et al., 1997; Dupont et al., 2011; Croft et al., 2015). The priming effect is elicited initially by a low frequency of Ca^{2+} oscillation arising from ER, and then Ca^{2+} oscillation is altered at a higher frequency by increasing either the intensity or the frequency of applied stimuli. The consequence of this effect potentiates astrocytic response to glutamate in a very long-lasting manner (for review in (Croft et al., 2015)).

The Ca^{2+} oscillation at a higher frequency, meanwhile, stimulates other Ca^{2+}-dependent signalling or Ca^{2+}-activated proteins. Indeed, studies investigating NVC showed that increased astrocytic Ca^{2+} in perivascular astrocytes evokes vasodilation of neighboring cerebral arterioles by secreting epoxyeicosatrienoic acids (EETs), an astrocyte-produced vasodilator. A recent study, however, unexpectedly detected mRNA and protein expressions of cytochrome P450 family (CYP) 4A ω-hydroxylase in rat brain astrocytes (Gebremedhin et al., 2016). This enzyme isoform catalyzes ω-hydroxylation of arachidonic acid to 20-Hydroxy-5, 8, 11, 14-eicosatetraenoic acid (20-HETE), a vasoconstrictor usually produced in VSMCs. Consequently, augmentation of 20-HETE secretion in rat astrocytes was uncovered following the application of an agonist of mGluRs group I, RS-3,5-dihydroxyphenylglycine (DHPG). Unlike EETs that are endogenous vasodilators and activate astrocytic K_{Ca} channel currents, 20-HETE causes vasoconstriction and inhibits K_{Ca} channel opening in astrocytes. Therefore, as a result of integrating intracellular Ca^{2+} events, astrocytes could modulate vascular tone by vasodilation or vasoconstriction. In addition to contributing to intracellular Ca^{2+} signals, group I receptors interact with other astrocytic membrane channels such as by activating K^+ channels via G_o or G_q protein, resulting in membrane depolarization or down-regulation of $K_{ir}4.1$ channels expression in retinal astrocytes (Hansson et al., 2000; Ji et al., 2012).

Though as yet no evidence of mGluR1 expression in astrocytes has been discovered, plenty of investigations have found that mGluR5 executes multiple tasks in astrocytes. Most importantly, with respect to group I receptors, neuroprotective roles in astrocytes are likely

played by mGluR5, significant upregulation of which was identified in reactive astrocytes after multiple sclerosis, post ischemia and neuropathic pain (Aronica et al., 2015; Dzamba et al., 2015; Kim et al., 2016). However, functional effects of upregulated mGluR5 vary according to physiologically or pathologically circumstances. On the other hand, activity of membrane-bound receptors can be modulated dynamically in different ways by intracellular kinases. In response to a long-lasting activation by DHPG, PKA and PKC phosphorylated astrocytic mGluR5, inducing the internalization of mGluR5 (Lee et al., 2008; Uematsu et al., 2015). Likewise, G-protein-coupled receptor protein kinase 2 also regulated the desensitization and endocytosis of mGluR5 via phosphorylation of Thr840 site on the C-terminus. The purpose of the two pathways is to modulate mGluR5 activity on the astrocytic membrane. However, mGluRs are the key sensors and modulators of extracellular glutamates for astrocytes under pathological conditions. Therefore, a novel pathway exists to rescue receptor activity. In addition, mGluR5 is temporarily inactivated by reversible phosphorylation of the C-terminus of mGluR5 at Ser839 by PKCε via astrocytic Ca^{2+} oscillation (Lee et al., 2008; Bradley and Challiss, 2011; Vergouts et al., 2017). This transient modulation avoids the desensitization of mGluR5 and conserves intracellular Ca^{2+} oscillation, contributing to the following neuroprotective actions of astrocytes.

Notably, recent investigations show that significant mGluR5s are expressed either in reactive astrocytes or immature astrocytes. Once activated, mGluR5 has the capacity to *i*) upregulate glutamate transporters to improve glutamate uptake; *ii*) enhance releases of gliotransmitters and neurotropic factors, i.e. ATP, D-serine and thrombospondin 1, to reconstruct synaptic wiring; *iii*) mediate astrocytic processes mobility in the form of filopodia; iv) regulate astrocyte proliferation; and *v*) take part to inflammatory responses (Lavialle et al., 2011; Aronica et al., 2015; Dzamba et al., 2015; Kim et al., 2016). Sun et al. reported that mGluR5 levels in astrocytes were undetectable in adult brain of mouse and human (Sun et al., 2013). Despite the possibility that upregulated astrocytic mGluR5 functions in pathophysiological conditions, it should be note that electronic microscopy detected few mGluR5 receptors on astrocytic membrane (Sun et al., 2013; Kim et al., 2016). Collectively, these reports suggest that the primary role of astrocytic mGluR5 is to maintain cellular stabilization and restoration.

2.1.2.2 mGluRs group II

Studies investigating mGluR group II receptors have discovered the intracellular coupling to ACs, as well as astrocytic group II receptors link to L-type voltage-dependent Ca^{2+} channels. Activation of group II receptors evoked a lasting depression on neurotransmitter-elicited Ca^{2+} rises such as serotonin and kainate, or induced by high K^+ concentration via blockage of L-type Ca^{2+} channels (Haak et al., 1997; Marmiroli and Cavaletti, 2012). In contrast to group I receptors, which induce elevated intracellular Ca^{2+}, group II receptors in astrocytes promote neuroprotective actions by suppressing Ca^{2+} rises, leading to: *i*) enhanced glutamate reuptake by upregulation glutamate transporters; *ii*) facilitated release of TGF-β via mitogen-activated protein kinase (MAPK)- phosphoinositide 3-kinase (PI3K) pathway, and *iii*) promotion of autocrine effects to resist against oxidative stress via, for example, promotion of cysteine uptake and suppression of inducible nitric oxide synthase (iNOS) expression (Aronica et al., 2000; Aronica et al., 2003; TANG and Kalivas, 2003; Yao et al., 2005; Durand et al., 2010; Aronica et al., 2015).

Interestingly, growth factors always upregulate astrocytic mGluRs but downregulate neuronal mGluRs. To date, it is found two new mechanisms were proposed to explain this dual effect. One is the desensitization of receptors that are phosphorylated by different kinases (Vergouts et al., 2017), where G-protein-coupled receptor protein kinase 2 and PKC act on astrocytic mGluR3 and neuronal mGluR4 respectively. The second mechanism relies on the kinase structure. For example, neurons express full length of tropomyosin receptor kinase B (TrkB), which down-regulates group II receptors in response to brain-derived neurotrophic factor (BDNF) stimulation. Nonetheless, this cascade is absent in astrocytes which expressed incomplete TrkB lacking the Shc-binding site (Suzuki et al., 2017).

mGluR group II receptors comprise two subtypes: mGluR2 and mGluR3, both of which perform distinct functional roles in astrocytes.

1) mGluR2: Though there is a lack of studies investigating astrocytic mGluR2, a recent study on the somatosensory ventrobasal thalamic nucleus has revealed a novel astrocyte-based mechanism underlying the tone of thalamic sensory transmission. Activation of astrocytic mGluR2 evoked a surge in intracellular Ca^{2+} exclusively in astrocytes, while the increase in Ca^{2+} cannot be detected in response to neuronal mGluR2 activation (Copeland et al., 2017). Consequently, these data suggest that mGluR2 has similar action to group I receptors.

2) mGluR3: Some characteristics of mGluR3 are reportedly similar to mGluR5. mGluR3 mediated glutamate-elicited movement of filopodia, can be desensitized by the same kinase G-protein-coupled receptor protein kinase 2, and was upregulated after epilepsy, cerebral injury, chronic inflammation and multiple sclerosis (Lavialle et al., 2011; Aronica et al., 2015; Vergouts et al., 2017). However, under physiological conditions, hippocampal astrocytes particularly express mGluRs instead of iGluRs, showing high levels of mGluR3 and few mGluR2 (Wang et al., 2016). Once stimulated, astrocytic mGluR3 initiates upregulation of TWIK-1 channels on the plasma membrane via the Rab-dependent endosome recycling pathway, resulting in enhanced glutamate-glutamine cycle. In reactive astrocytes, mGluR3 exhibited resistance to iNOS-produced NO toxicity through cAMP level reduction, PI3K/Akt pathway activation and stimulation of the communication between p65 and nuclear factor (NF)-κB (Aronica et al., 2000; Durand et al., 2010; Durand et al., 2011). In the presence of cytokine interleukin (IL)-1β, activation of mGluR3 was found to regulate astrocytic immune response by facilitating the release of IL-6 (Aronica et al., 2015).

2.2 Acetylcholine

The basal forebrain including the nucleus basalis and the nucleus of the diagonal band of Broca is the primary cholinergic input to cortex. Once stimulated, cholinergic neurons in the basal forebrain secret original source of ACh across distinct cortical layers towards specific targets, i.e. astrocytes, blood vessels, inhibitory interneurons and pyramidal neurons. To synthesize ACh, choline acetyltransferase (ChAT) in cholinergic neurons relocates an acetyl group from acetyl coenzyme A towards choline. Then the modulatory activity of ACh is mediated by nAChR and mAChR. Cholinergic neurons contribute to improve learning and memory processes in the hippocampus and forming cortical circuits. Consequently, most studies on cholinergic receptors are concentrating on relevant functional changes resulting from AD with respect to inflammation and cognition.

2.2.1 Effects of mAChRs activation

mAChRs are a class of G-protein coupled receptors highly located at layer II to VI of the cortex and hippocampus, implicated in learning and memory (Huang and Thathiah, 2015). The

basal forebrain-induced activation of astrocytes modulates cortical and hippocampal circuits exclusively through astrocytic mAChRs via IP_3R2–mediated Ca^{2+} release (Takata et al., 2011; Hassanpoor et al., 2014; Sugihara et al., 2016). A similar mechanism was also found in the hippocampus *ex vivo* by electrical stimulating alveus input (Perea and Araque, 2005). Subsequently, increased Ca^{2+} in astrocytes leads to gliotransmitter release, such as ATP and glutamate, resulting in synchronization of neuronal firing, as well as integration of astrocytic Ca^{2+} signals (Hassanpoor et al., 2014). Recent findings suggest that integrated Ca^{2+} response to mAChRs and mGluRs in single astrocyte could potentiate and propagate θ wave and eventually contribute to forming spatial memory (Hassanpoor et al., 2014; Croft et al., 2015). However, this complex integration of Ca^{2+} contributes to slow timescale of astrocytes to consolidate the phenomenon, whereas inhibitory neurons involved in learning encodes faster response (Butts et al., 2007; Chen et al., 2012).

Some other studies found that mAChRs also mediate cholinergic activation of astrocytes. Carbamylcholine, an agonist of M3 receptor, was found to activate cortical and hippocampal astrocytes (Guizzetti et al., 2011). The activation of M3 by carbamylcholine in retinal astrocyte cultures, raises IL-4 levels (Granja et al., 2015).

2.2.2 Effects of nAChRs activation

Accumulating evidence indicate that nAChR can modulate release of multiple neurotransmitters and modify long-term plasticity. A recent investigation presented that activation of astrocytic α7 nAChRs recruited neuronal AMPA receptors toward synaptic zone in hippocampus (Wang et al., 2013). It seems that recruited synaptic receptors were silent before, suggesting an enhancing synaptic plasticity induced by astrocytic nAChRs. Importantly, in response to the volume transmission of cholinergic signalling in the cortex and hippocampus, they found that astrocyte-mediated recruitment exclusively promoted the maturation of functional glutamatergic circuits containing PSD-95 synapses. α7 nAChRs are highly permeable to Ca^{2+} (Wang et al., 2013; Dineley et al., 2015). In AD brain, amyloid-β interacts with astrocytic α7 AChR resulting in activation of astrocytes, glutamate release and notable potentiation of Ca^{2+} in a much higher frequency compared to physiological astrocytes (Shen and Yakel, 2012). However, in contrast to the response of interneurons to the treatment of choline in CA1 region

ex vivo, α7 nAChR in astrocytes triggers smaller response amplitude of Ca^{2+} increases (Shen and Yakel, 2012).

Our current knowledge of astrocytic nAChRs focus on two subtypes, α4β2 nAChR and α7 nAChRs, which are both interlinked with inflammatory and immune pathology induced by AD and other neuropsychiatric disorders. Activation of both receptors in astrocytes leads to increased intracellular Ca^{2+} levels and upregulated glial-derived neurotrophic factor (GDNF) which further inhibits microglia activation (Takarada et al., 2012). However, α7 nAChRs are down-regulated in neurons but are significantly upregulated in astrocytes of the AD hippocampus, whereas expression of α4 nAChRs was found to be stable in AD patients (Chu et al., 2005; Yu et al., 2005; Kamynina et al., 2013). Thereby, it has been well demonstrated that activation of astrocytic α7 receptors alone is able to generate several anti-inflammatory responses as well. For instance, once activated, levels of astrocyte-released inflammatory factors, such as IL-6 and tumor necrosis factor α (TNF-α), were reduced in hippocampus *in vitro* (Zhu et al., 2016). Structural studies have shown that nAChR agonists like nicotine reduced, but α7 (179-190) epitope binding to part of the ACh binding site in astrocytic nAChR stimulated IL-6 production. It is indicated that α7 nAChR-mediated inflammation is modulated in an ion-independent manner (Kalashnyk et al., 2014). By contrast, another report working on human astrocyte cultures believed that α7 nAChRs stimulated prostaglandin E_2 (PGE_2) release inhibits astrocyte-released cytokines including IL-6 and TNF-α, in the presence of a high concentrations of nicotine (100 μM), via cyclooxygenase 2 (COX-2)-dependent signalling (Revathikumar et al., 2016).

2.3 Purinergic substances

The ligands of purinergic receptors include ATP, ADP and adenosine. ATP, with glutamate, is the most abundant excitatory neurotransmitters in the brain and can be further metabolized into ADP, AMP, etc. Mediation of intercellular communications occur via ATP released from astrocyte either through channels or by exocytosis. Once released, ATP binds to corresponding P2 receptors present in astrocytes, neurons, microglia and oligodendrocytes. Adenosine, a metabolite of ATP, functions as a neurotransmitter as well as a modulator in the CNS by activating P1 receptors.

2.3.1 Effects of P1 activation

2.3.1.1 A1 receptors

A1 receptors are highly expressed in the cortex, hippocampus and cerebellum. Increasing experimental evidence show that A1 receptors in astrocytes display neuroprotective effects. Activation of A1 receptors in normal astrocytes elicited a fast glutamate release and opened adjacent TREK-1 channels (Woo et al., 2012). However, *in vitro* activation of overexpressed A1 receptors under pathological conditions may promote glutamate uptake into astrocytes through inhibition of AC activity leading to reduced levels of extracellular glutamate and elevated mRNA expression of excitatory amino acid transporters (EAAT) 2 (Wu et al., 2011). In response to cell apoptosis induced by ischemic damage, A1 receptors regulate the phosphorylation activity of Bad, c-Jun N-terminal kinases (JNK) and p38 by PI3K/Akt signalling as well as extracellular signal-regulated kinases (ERK)/MAPK signalling, which contributed to enhancement of cell survival. (Ciccarelli et al., 2007).

2.3.1.2 A2 receptors

A2A receptors have a fairly low distribution in the cortex and the hippocampus but are found mainly in the striatum, while A2B receptors as well as A3 receptors are rare in the brain. Though lowly expressed, A2A receptors play key roles in cognition maintenance. Knockout astrocytic A2A receptors facilitated upregulation of GLT-1 in astrocytes as well as NR2B-containing NMDA receptors in neurons, impacting on glutamatergic circuits and reducing working memory (Matos et al., 2015). Importantly, these few A2A receptors in the cortex likely stimulate opposite modulations on cognition, because procognitive effects were observed by either depressing neuronal A2A receptors or deleting of astrocytic A2A receptors.

2.3.1.3 A3 receptors

In spite of rare studies on astrocytic A3 receptor, it is suggested to be functionally distinct from A1 and A2 receptors in this cell types. For example, in the presence of ATP-elicited Ca^{2+} signals in astrocytes *in vitro*, a previous study found that activation of astrocytic A1 receptors attenuated the Ca^{2+} responses and activation of A2B receptors potentiated the Ca^{2+} peak value;

however, no change was observed on the Ca^{2+} plateau when stimulating A3 receptors (Alloisio et al., 2004).

2.3.2 Effects of P2 activation

Astrocytes express both P2X and P2Y receptors, but the detailed subgroups of each are debatable. In general, activation of astrocytic P2 receptors has influence over three aspects. First, increased Ca^{2+} mobilization is triggered in single astrocyte or through the astrocytic networks; second, P2-induced release of gliotransmitter impacts neighbouring cells; third, astrocytes under pathological conditions turn to be hyperactive, accompanied by enhanced intracellular responses and activated microglia.

2.3.2.1 P2X7 receptors

Only high concentrations of ATP (mM) can activate astrocytic P2X7 receptors which are involved in neuron-glia interaction. For example, activation of P2X7 receptors was found to contribute to D-serine release through pannexin-1 of P2X7-pannexin-1 complex via Ca^{2+}-independent PKC signalling in rat astrocyte cultures (Pan et al., 2015). It may further bind to NMDA receptors located at the synaptic membrane and potentiate neuronal circuits. Unlike neuronal P2X7, cortical astrocytes are thought to express a different splice variant of the P2X7 receptor, which is constitutively activated *ex vivo* under the non-stimulated resting states (Kamatsuka et al., 2014). Likewise, in mild ischemia, hypoxia inducible factor (HIF)-1α levels display long-lasting upregulation in astrocytes in a hypoxia-independent but P2X7- receptor-dependent manner, whereas neurons demand pre-treatment with hypoxia (Hirayama and Koizumi, 2017). The two functional differences between neuronal and astrocytic P2X7 receptors contribute to the essential roles of astrocytic P2X7 receptors in the maintenance of brain homeostasis.

2.3.2.2 P2Y receptors

Recent findings show that P2Y receptors contribute to physiological activity of astrocytes. The activation of subtypes of P2Y receptors in astrocytes (i.e. P2Y1, P2Y2 and P2Y4) caused $GABA_B$ receptors activation by phosphorylation, via P2Y receptor-CaM kinase kinase-5'

adenosine monophosphate- activated protein kinase (AMPK) signalling pathway (Terunuma et al., 2015). Additionally, P2Y1 receptors were found to activate PLC signalling but suppress the conductance of K_{ir} channels, resulting in extension of astrocytic processes in hippocampal astrocyte cultures (Chisari et al., 2016). In the presence of pathological conditions such as oxidative stress, astrocytic P2Y receptors exhibit antioxidant defence by reducing reactive oxygen species (ROS) production, raising levels of glutathione and cAMP as well as inducing expression of antioxidant genes via PKA signalling (Förster and Reiser, 2016).

3. Intracellular modulation − second messenger Ca^{2+} signals

Whilst astrocytic membrane receptors are activated, channels in the plasma and organelle membranes are opened and locked, intracellular proteins are phosphorylated and dephosphorylated, second messengers are triggered and genes are transcribed. Unlike neurons, astrocytes do not generate action potentials but respond to neuronal signals in the form of Ca^{2+} waves in a complex spatiotemporal pattern. Therefore, Ca^{2+} is not only a ubiquitous second messenger in astrocytes, but also a pivotal transmitter mediating astrocyte process and response. Ca^{2+} signals restricted to distinct astrocyte compartments can be elicited by different stimuli, and the increased Ca^{2+} microdomains are evoked from either extracellular space or internal storage. Thus, the present section addresses the modulation of intracellular Ca^{2+} in astrocytes.

3.1 External Ca^{2+} source - extracellular space

Since Ca^{2+} microdomains in astrocytes are isolated functionally, Ca^{2+} increases in microdomains do not necessarily correlate with Ca^{2+} measured in the soma. Furthermore, several lines of evidence found that these microdomains mostly occurred beneath the plasma membrane (Shigetomi et al., 2010; Rungta et al., 2016; Agarwal et al., 2017). Thus, the source of Ca^{2+} microdomains may be mainly the extracellular space via membrane ionotropic receptors and ion channels.

Once activated, transmembrane proteins permeable to Ca^{2+} ions in the plasma membrane have the capacity of allowing external Ca^{2+} influx, including ion channels (e. g. iGluRs, nAChRs and P2Xs, as stated above), Ca^{2+} transporters (e.g. Ca^{2+}-ATPase, Na^{+}/Ca^{2+} exchangers), voltage-dependent Ca^{2+} channels, transient receptor potential channels (e.g. TRPA1, TRPV4) and store-

operated Ca^{2+} channels (e.g. Orai families). Real-time imaging in the somata of astrocytes displayed that Ca^{2+} influx from extracellular fluid increased intracellular Ca^{2+} concentration much more rapidly than Ca^{2+} efflux from intracellular stores (Srinivasan et al., 2015; Bazargani and Attwell, 2016). Thus, in spite of the undefined relationship between membrane receptor-mediated Ca^{2+} influx and internal Ca^{2+} signals, increasing experimental investigations on astrocytic Ca^{2+} signals are unveiling detailed molecular and functional mechanisms of their interplay.

3.2 Internal Ca^{2+} sources

Intracellular Ca^{2+} stores are key sources of Ca^{2+} for generating and prolonging Ca^{2+} signalling in astrocytes. Previous reports recognized that localized Ca^{2+} signals displayed distinctive properties in astrocytic compartments, specifically, the soma, thick processes, fine processes and endfeet (Shigetomi et al., 2013; Stobart et al., 2016). Then, a thorough analysis of Ca^{2+} transients in the astrocyte pointed out that mitochondria in astrocytes were responsible for intracellular Ca^{2+} transients singularly in fine processes (Agarwal et al., 2017). This data implies that intracellular Ca^{2+} signals can be compartmentalized by different internal sources including ER, mitochondria as well as other cellular organelles and are then encoded into spatial extent of astrocyte modulation.

3.2.1 Endoplasmic reticulum

ER is the main source of Ca^{2+} within astrocytes and contains the highest concentration (micromolar) of Ca^{2+}, compared to the cytosol as well as mitochondria (Shigetomi et al., 2016). ER Ca^{2+} is evoked through ryanodine (RyR) and IP_3 (IP_3R) receptors stimulation, while the uptake of Ca^{2+} by ER is performed by sarco/endoplasmic reticulum Ca^{2+}-ATPase (SERCA).

3.2.1.1 IP_3Rs

Activation of IP_3R evokes the release of Ca^{2+} from ER. This ionotropic receptor has three isoforms, i.e. type 1 IP_3R, type 2 IP_3R and type 3 IP_3R. The major isoform in neurons is IP_3R1, whereas astrocytes are rich in IP_3R2. A recent research found three isoforms that co-existed in hippocampal astrocytes and contribute to Ca^{2+} signalling, leading to regulation of

gliotransmission and synaptic plasticity (Sherwood et al., 2017). This study indicated that IP_3R2 induced the largest spatial propagation of Ca^{2+}, whereas much less IP_3R1 and IP_3R3 were expressed and generated relatively localized, mono-phasic Ca^{2+} events to regulate confined astrocytic responses. Numerous studies discovered that global Ca^{2+} propagation was triggered in multiple modes, *i*) via IP_3R-meidated Ca^{2+} efflux from intracellular Ca^{2+} stores, which was further enhanced by Ca^{2+}-induced Ca^{2+} release at neighbouring IP_3Rs (Stavermann et al., 2015); *ii*) via TRPV4 channels from extracellular Ca^{2+} source, which was boosted by IP_3R-induced Ca^{2+} signals (Dunn. K et al., 2013); *iii*) by coordination between IP_3R-mediated Ca^{2+} efflux from ER and Ca^{2+} influx through store-operated Ca^{2+} channels (Orai1 and Orai2) in the plasma membrane (Sakuragi et al., 2017). The determination of downstream functional consequences and impacts neuronal plasticity relies on the method of Ca^{2+} release.

Considering that IP_3 is the endogenous ligand of IP_3R, activation of G-protein coupled receptors such as metabotropic receptors could indirectly facilitate IP_3R activity by activating PLC, an enzyme producing IP_3 via G_q/G_{11}, resulting in increased IP_3 levels and Ca^{2+} levels in the cytosol. Nevertheless, in *ex vivo* studies on the hippocampus of $IP_3R2^{-/-}$ mice, Ca^{2+} oscillations occurred as usual and were not changed in both the soma and in astrocytic processes (Srinivasan et al., 2015; Rungta et al., 2016). Moreover, Ca^{2+} oscillations were enhanced in fine processes when G-protein coupled receptors were activated by endothelin, signifying that Ca^{2+} oscillations in astrocytic processes were IP_3R2-independent (Srinivasan et al., 2015). Further *in vivo* studies showed similar negative results as well. Full knockout IP_3R2 had no effect on astrocytic IP_3/Ca^{2+} signalling, astrocyte responses as a whole, or functional hyperemia response in visual cortex (Bonder and McCarthy, 2014; Stobart et al., 2016). In a novel animal model with IP_3R2s knockout in over 80 % astrocytes, McCarthy et al. revealed no detectable behavioral changes (Petravicz et al., 2014).

However, another study of a transgenic animal model demonstrating accelerated IP_3 metabolism in astrocytes resulting in attenuated cytosolic IP_3 levels exhibited increased REM sleep and enhanced θ wave (Foley et al., 2017). Meanwhile, Rungta et al. (2016) found that it was extracellular Ca^{2+} that induced Ca^{2+} fluctuations in fine astrocytic processes in the hippocampus of $IP_3R2^{-/-}$ mice. Taking these controversial data together, it brings us to question why the effect of IP_3R signalling in astrocytes of intact brain is attenuated and whether astrocytic IP_3R signalling plays a major role in neuronal networks.

Instead of the genetic approach, heparin was used as an antagonist of IP_3R in the earlier periods. Since it displays low affinity, lack of selectivity and impermeability to cell membrane, new highly selective antagonists have been developed to overcome all those deficits, including Xestospongin C and 2-aminoethoxydiphenyl borate (2-APB, 100 μM) (Gafni et al., 1997; Drumm et al., 2015).

3.2.1.2 RyRs

The importance of RyR is initially recognized in the excitation-contraction coupling of muscle cells, where L-type Ca^{2+} channels in the plasma membrane is stimulated and results in activation of surrounding RyRs (i.e. RyR2, RyR3), inciting a rapid release of Ca^{2+} from sarcoplasmic reticulum into the cytosol and causes contraction (Xu et al., 1998). Three isoforms of RyR mediating release of Ca^{2+} from ER stores are identified in vertebrates: RyR1, RyR2 and RyR3. Although RyR3 is the main isoform in the brain, studies showed that RyR1s were enriched in Purkinje cells of the cerebellum, while astrocytes were rich in RyR2s which are upregulated in response to hypoxic/reperfusion injury (Kesherwani and Agrawal, 2012; Márkus et al., 2016). Intriguingly, more than one RyR isoform can be expressed in one cell. Studies found that one interstitial cell of Cajal possessed RyR2 and 3, while one specialized optic nerve head astrocyte expressed all three isoforms of RyRs (Drumm et al., 2015; Kaja et al., 2015).

Based on the analysis of cloned sequences of RyRs and IP_3Rs, these two receptors share approximately 35 % identical sequence. Furthermore, the evolutionary analysis pointed out the possibility that N-terminal domain of IP_3Rs were evolved from a lower order RyRs. The size of the primary sequences of RyRs is twice as big as that of IP_3Rs (Amador et al., 2013) and it is hinted that the excess spaces may be reserved for binding small active molecules as regulators of RyRs. Indeed, a review from Kushnir et al. indicated ions (such as Mg^{2+}) and proteins (e.g. CaM, PKA, CaMKII) regulated activity of RyRs (Kushnir et al., 2010). However, despite a pivotal role in Ca^{2+} signalling mediated by IP_3Rs, much less is known about the expression and functional role of RyRs. Since RyRs were found to generate Ca^{2+} nanodomains in neurons (Johenning et al., 2015), the functional property of RyRs was deemed to initiate amplification of intracellular Ca^{2+} signals by Ca^{2+}-induced Ca^{2+} release in astrocytes (Earley et al., 2005; Drumm et al., 2015; Kaja et al., 2015). In contrast, other investigations displayed that RyRs in

astrocytes were associated with local physiological response other than contribution to global Ca^{2+} propagation, which was executed by IP_3Rs (Straub et al., 2006; Dunn. K et al., 2013; Drumm et al., 2015; Stavermann et al., 2015). For example, an *in vitro* study investigating pharmacological blockage or knockout of RyR3 reported that blockade of RyR3 activity significantly reduced astrocyte migration, thus implicating RyR3 in the control of astrocyte mobility (Matyash et al., 2001).

The pharmacological toolbox for studying RyRs are many small molecular compounds, such as heparin, caffeine and ryanodine. To date, it is widely accepted that ryanodine acts as an agonist of RyR below 10 μM and an antagonist of RyR at concentrations above 100 μM (Chiarella et al., 2004; Thomas and Williams, 2012).

3.2.1.3 Ca^{2+} crosstalk between RyR and IP_3R

Although RyR and IP_3R bind to different ligands, Ca^{2+} has the capability to activate both receptors due to an underlying mechanism termed Ca^{2+}-induced Ca^{2+} release. Indeed, it is found that activation of metabotropic-like NMDA receptor in astrocytes cause an increase in intracellular Ca^{2+} levels by activation of both IP_3Rs and RyRs (Montes de Oca Balderas and Aguilera, 2015). Nevertheless, it is disputable which receptor initiates the Ca^{2+}-induced Ca^{2+} release. For instance, localized Ca^{2+} transients were triggered by RyR-mediated Ca^{2+} efflux, which further activated ambient IP_3Rs, resulting in strong Ca^{2+} wave propagated along the cell (Drumm et al., 2015). In contrast, Kaja et al. (2015) found that RyR-mediated Ca^{2+} efflux contributed to amplification of Ca^{2+} signals generated by either extracellular Ca^{2+} influx or IP_3R-released Ca^{2+} sparks. Briefly, Ca^{2+} crosstalk between RyR and IP_3R fine-tunes modulation of cellular responses, adding to the complexity of intracellular Ca^{2+} signals regulation.

3.2.1.4 SERCAs

ER storage refilling of Ca^{2+} is dependent upon the uptake by SERCAs on the ER membrane. To be specific, SERCA consumes ATP and pumps Ca^{2+} against the gradient into ER, maintaining a quite low level of Ca^{2+} in the cytosol. Thus, blockade of SERCA either by cyclopiazonic acid (CPA) or by thapsigargin decreased Ca^{2+} levels within astrocytic ER and induced Ca^{2+} influx through store-operated Ca^{2+} channels in the plasma membrane (Kovacs et

al., 2005; Morita and Kudo, 2010). However, immediately following the traumatic brain injury, a drop of approximately 50 % in intracellular ATP levels occurred in astrocytes and inhibited SERCA activity leading to depletion of ER Ca^{2+} stores (Ahmed et al., 2000). Thereafter, endogenous growth factors (e.g. BDNF) promoted SERCA expression, SERCA-2b subtype in particular, resulting in increased Ca^{2+} oscillation in astrocytes (Morita and Kudo, 2010). Notably, this study also showed through western blot analysis that SERCA-2b was the only subtype expressed in astrocytes. Given that SERCA-2b displays highest affinity for Ca^{2+} but minimum capacity of Ca^{2+} transport, the highly sensitive SERCA-2b upregulates intracellular Ca^{2+} oscillation in astrocytes, contributing to the regulation of glutamate release in developing and pathologic brain.

3.2.2 Mitochondria

In addition to the metabolic functions, mitochondria are an underestimated large Ca^{2+} reservoir which store and release Ca^{2+} through the mitochondrial Ca^{2+} uniporter (MCU), the mitochondrial permeability transition pore (mPTP), the mitochondrial Na^{+}/Ca^{2+} (mNCX) and the H^{+}/Ca^{2+} (mHCX) exchangers.

1) MCU: It is a non-selective channel with high affinity for Ca^{2+}. Usually MCU is inactivated at rest, due to the Ca^{2+} concentration inside the mitochondria being high relative to the cytosol. Only when cytosolic Ca^{2+} is elevated, the mitochondrial membrane potential will drive the uptake of Ca^{2+} across the inner mitochondrial membrane through MCU.

2) mNCX: mNCX, is also known as NCLX, since it especially mediates Li^{+} flux instead of Na^{+} flux, differentiating it from the other NCXs in the plasma membrane. Astrocytic mitochondria are enriched with mNCX, which extrudes Ca^{2+} in a Na^{+}-dependent or Na^{+}-independent manner.

Synaptic mNCX is mainly responsible for regulating intracellular Ca^{2+} signals, leading to modulation of synaptic plasticity. Unlike neuronal mNCX, astrocytic mNCX has dual capacities of *i*) promoting mitochondrial Ca^{2+} shuttling, thus further enhancing production of ATP, resulting in regulation of astrocyte proliferation and migration; *ii*) facilitating the regulation of Ca^{2+} influx from extracellular space via store-operated Ca^{2+} entry (SOCE) in the vicinity of exocytosis areas (Parnis et al., 2013). Afterwards, Ca^{2+} transients enhanced by mNCX

participate in controlling slow cellular processes, e.g. release of glutamate and synaptic transmission. The findings suggest a strong mNCX-meditated crosstalk between mitochondria and the plasma membrane in astrocytes.

However, the mitochondria-ER interaction mediated by mNCX is relatively weak (Parnis et al., 2013). This could be explained by: *i*) the fact that mNCX in astrocytes neither was involved in SERCA-mediated refilling of ER Ca^{2+} storage nor partook in ER-dependent release of Ca^{2+}; *ii*) there was insignificant contribution of mNCX-dependent Ca^{2+} efflux to global Ca^{2+} propagation through astrocyte networks.

3) mHCX: Little is known about the properties of mHCX in astrocytes. In general, mHCX mediates Ca^{2+} efflux as same as mNCX. However, in rat myometrium, one study found that mitochondria accumulated Ca^{2+} through mHCX even though the mitochondrial membrane potential was depolarized (Babich et al., 2010).

4) mPTP: When both mNCX and mHCX operate at full capacity, mPTP facilitates the efflux of overloaded Ca^{2+} from the mitochondrion in high-conductance mode. This fast process protects mitochondria from toxic Ca^{2+} levels and maintains Ca^{2+} homeostasis. Its transient openings may be involved in many cellular processes and responses (Agarwal et al., 2017). For instance, mPTP was opening when high oxidative phosphorylation occurred, and the corresponding Ca^{2+} efflux was further enhanced by production of mitochondrial superoxide such as ROS (Agarwal et al., 2017). Meanwhile, neuronal activity could raise intracellular Ca^{2+} levels in astrocytes in a mitochondria-dependent manner via mPTP-mediated Ca^{2+} waves, rather than ER Ca^{2+} stores (Srinivasan et al., 2015; Agarwal et al., 2017). This mPTP-dependent Ca^{2+} signalling was found mostly in astrocytic processes. By contrast, the openings of mPTP is prolonged and implicated in osmotic swelling, apoptosis and necrosis.

Mitochondria are distributed everywhere in astrocytes, some are located in proximity to the plasma membrane, some are close to ER/SR, and some within astrocytic processes (Jackson and Robinson, 2015; Agarwal et al., 2017). Study indicated that periodical release of Ca^{2+} from mitochondria was independent, which was not interfered either by IP_3R2-mediated Ca^{2+} signals or by membrane receptors-mediated Ca^{2+} transients (Agarwal et al., 2017). This feature contributes to mitochondrial functional roles: producing ATP and shaping Ca^{2+} signals.

In neurons, distributions of mitochondria are partially regulated by protein Miro, while in astrocytes Miro dynamically carries mitochondrion along cytoskeleton toward areas of elevated

activity. Since activation of Miro requires Ca^{2+}, mitochondrial trafficking is coupled to basal intracellular Ca^{2+} levels. In other words, mitochondrial effect on Ca^{2+} dynamics relies on its subcellular location where contains enough Ca^{2+} ions to activate Miro activity (Jackson and Robinson, 2015). Thereafter, increased mitochondrial Ca^{2+} shuttling is tied to ATP production, which subsequently regulates correlated ATP-dependent cellular processes. For example, mitochondrial Ca^{2+} transients regulated glutamate uptake by providing energy to Na^+/K^+ ATPase coupled to GLT-1 in the plasma membrane (Harris et al., 2012). In addition, mitochondria-mediated Ca^{2+} release underlying the Ca^{2+}-machinery interplay with ER likely partakes in intracellular Ca^{2+} events by coupling with SERCA and Ca^{2+} ATPases in the membrane (from a review in (Takeuchi et al., 2015)). Jointly, these results hint the importance of mitochondrial Ca^{2+} shuttling through modulating distinct cellular functions.

3.2.3 Others

Intracellular Ca^{2+} are stored in the Golgi and acidic organelles. The uptake of Ca^{2+} in the Golgi is mainly by Ca^{2+}-ATPase, and the extrusion of Ca^{2+} is mediated by Na^+/Ca^{2+} exchanger. Nonetheless, little is known about the effect of Ca^{2+} signalling on Golgi.

The lysosome, one of the acidic organelles in the cell, serves as a Ca^{2+} storage in astrocytes. Indeed, since astrocytes synthesize several lipids including cholesterol in the brain, lipid homeostasis in astrocytes affected lysosomal Ca^{2+} storage either through increasing Ca^{2+} storage or through causing Ca^{2+} release (Vienken et al., 2017). In addition to intracellular lipid levels, a previous study found that glutamate-activated mGluRs enhanced nicotinic acid adenine dinucleotide phosphate (NAADP) levels, which bound to NAADP receptors on lysosomal membrane, thus resulting in release of lysosomal Ca^{2+} (Pandey et al., 2009).

4. Roles of nitric oxide: a second messenger and a neurotransmitter

The 1998 Nobel Prize in physiology or medicine has put NO under the spotlight and awarded to Robert F. Furchgott, Louis J. Ignarro and Ferid Murad for discovering vasodilatory role of NO in the cardiovascular system. In the following years, more and more functional properties of NO have been discovered, focusing mainly on three facets. First is the improvement on cardiovascular health. It has been revealed that in response to multiple stimuli

(e.g. ACh, nitroglycerine, shear stress) endothelial cells produced NO, which travels into vascular smooth muscle cells and induces vasodilation (Ignarro et al., 1987; Morales-Ruiz et al., 1996; Murohara et al., 1996). Second, NO acts in physiological conditions as an intercellular messenger inside brain cells, while pathological conditions cause NO to function as an endotoxin and an inflammatory mediator implicated in neurotoxicity. The third feature identified is the immunological function of NO. Macrophage-derived NO diffuses into adjacent cells, leading to events such as cell apoptosis or inhibition of cell proliferation. In the present section, I present reports regarding NO production and NO signalling as well as probable functions.

4.1 Intracellular sources of nitric oxide

In the body, gaseous NO is produced by NO synthase (NOS) which catalyzes the oxygen-dependent formation of NO in the reaction:

$$O_2 + 2\ NADPH + \textbf{L-arginine} \xrightarrow[NOS]{[BH4,\ Heme,\ FMN,\ FAD,\ CaM\ (Ca^{2+})]} \textbf{NO} + 2\ NAD^+ + \text{L-citrulline}$$

In order to ensure the efficiency of the reaction, activation of NOS demands four cofactors: tetrahydrobiopterin (BH4), heme, flavin mononucleotide (FMN) and flavin adenine dinucleotide (FAD), as well as one co-agonist, the Ca^{2+}-bound CaM. Initially, FAD located at the reductase domain transfers two electrons from two nicotinamide adenine dinucleotide phosphates (NADPH), and then FMN accepts one electron and turns into the input state to lock the electron. With the help of CaM binding to both heme and FMN, the input state FMN transforms into the output state and passes the electron to the oxidase domain of heme, which contains BH4 and enzymatic substrates, O_2 and L-arginine (Smith et al., 2013). It is important to note that: *i*) CaM-mediated electron transfer is a rate-limiting step during the reaction; *ii*) in the case of heme being dissociated, the final product would be nitrate rather than NO; *iii*) if either L-arginine is insufficient or BH4 is dissociated, the outcome would be superoxide anions leading to the production of peroxynitrite.

On the other hand, NO is a type of free radicals capable of directly interacting with HS-

group proteins by covalent modification of sulfhydryl residues forming S-nitrosothiols (ONS-group), termed S-nitrosylation. Since the protein S-nitrosylation occurs quickly and reversibly, S-nitrosylated proteins can be deemed as an intracellular storage of NO, releasing NO under certain conditions (Stamler et al., 1992).

4.2 Nitric oxide probes

NO is a gaseous chemical signal in the cell, allowing only real-time imaging as a direct approach of observing its distribution. It is noteworthy that NO has many characteristics making it difficult to be labeled as well as be traced. First, NO is short-lived, the half-life of which depends on the concentration. Though NO can sustain from seconds to tens of seconds, unexpectedly, the lower the concentration of NO is, the longer the NO effect lasts. Second, NO is not stable in the cell and functions in the form of NO-related species, such as $NO^{\bullet}$, NO^{+}, NO^{-}, NO_2^{-}, NO_3^{-}, N_2O_3 and $ONOO^{-}$. Notably, some of these species belong to ROS family, for example, $NO^{\bullet}$, NO^{+} and $ONOO^{-}$. Third, NO is a cell-permeable molecule, indicating that it can travel across many cell membranes including the plasma and organelle membranes rapidly. This feature leads to the difficulty of identifying the NO source.

In 1998, Kojima et al. developed a series of diaminofluorescein (DAF), making it feasible to label and trace NO. In particular, 4-amino-5-methylamino-2',7'-difluorofluorescein (DAF-FM) diacetate is an innovator of DAF family for the bio-imaging of NO and is widely applied for tracing and qualitatively assessing cellular NO production. However, these series of fluorescent probes have some notable defects need to be noticed. As indicated, DAFs react with NO^{+} equivalents other than NO itself (Kojima et al., 1999). Furthermore, intensity of the fluorescence remains when NO disappears (Namin et al., 2003). DAF-FM diacetate is a reliable NO indicator in living preparations due to three reasons: *i*) Cell-permeant DAF-FM diacetate is deacetylated rapidly into water-soluble but cell-impermeable DAF-FM by cytosolic esterases (Kojima et al., 1999), *ii*) Once reacting with NO derivatives, weakly fluorescent DAF-FM irreversibly transforms into a complex releasing constant fluorescence (Namin et al., 2003), *iii*) The lowest NO concentration that DAF-FM can detect is approximately 3 nM (Kojima et al., 1999), indicating the highest sensitization of NO. Overall, DAF-FM can provide a semi quantitative information about how much NO is produced when a single cell receives a stimulus.

4.3 Isoforms of NOS

The product of gene translation of NOS is an inactive monomer containing a reductase domain and an oxidase domain (Ratovitski et al., 1999). When two monomers interact, they construct one active homodimer named NOS. Three isoforms of NOS have been identified in mammals, including endothelial NOS (eNOS), neuronal NOS (nNOS) and inducible NOS (iNOS). Despite being named according to the tissue in which they were primarily recognized, all of three enzymes are distributed widely in other cell types.

4.3.1 Endothelial NOS

Organization of the enzymatic domain:

In each monomer, the oxidase domain is found close to the N-terminal and contains the BH4 domian, the heme domain and the CaM binding site, which links the oxidase and the reductase domains. At the C-terminal of monomer, the reductase domain contains the FMN domain, which directly connects with the CaM binding site, then the following sequences are the FAD and the NADPH domains (Smith et al., 2013).

For example, in one monomer:

N-[Heme domain] - [CaM binding site] - [FMN domain]-[FAD domain]-[NADPH domain]-C

Oxidative domain — Reductase domain

CaM effect on eNOS:

CaM structurally consists of two granular lobes, N- and C- lobes, which are joined by one α-helix (Babu et al., 1985). To activate eNOS, CaM reversibly binds with the CaM binding site of eNOS. Prior study indicated that activation of eNOS requires full lobes of CaM, whereas iNOS only needed the N-lobe CaM (Piazza et al., 2012). They also pointed out that phosphorylation of CaM at the site of Tyr99 specifically facilitated activity of eNOS. These features highlight the importance of CaM in activation of eNOS.

Potential cell type containing eNOS in the brain:

i) Endothelial cells; *ii*) astrocytes (Wiencken and Casagrande, 1999); *iii*) CA1 pyramidal neurons (O'dell et al., 1994).

eNOS compartmentalization:

Caveolae, a subtype of lipid rafts in the membrane, holds various concentrated signal molecules, i.e. lipids and proteins. Caveolin (Cav) -1, Cav-2 and Cav-3 are the main components of caveolae membrane fractions and mediate "scaffolded" domains. Immunostaining studies revealed that eNOS was colocalized with Cav-1 in endothelial cells, while eNOS-Cav-3 were identified in cardiomyocytes. Furthermore, subcellular localization of eNOS was found in the Golgi complex membrane in addition to the plasma membrane (Feron et al., 1996; García-Cardeña et al., 1996; Massion et al., 2004). Interestingly, not all eNOS are located in caveolae. Some studies found that eNOS was enriched in other rafts (e.g. PI(4, 5)P_2-containing rafts) during cell migration (Bulotta et al., 2006).

4.3.2 Neuronal NOS

Organization of the enzymatic domain:

The domain organization of nNOS is similar to that of eNOS; however, the molecular weight of nNOS is greater than that of eNOS, denoting the extra portion located in the N-terminal of nNOS. Another distinction is that, the heme binding to nNOS carries Fe(II), while in eNOS it contains ferric oxide (also called Fe(III)).

CaM effect on nNOS:

Full-length CaM (N- and C-lobes) reversibly binds to nNOS. Scientific evidence suggests that CaM may activate nNOS by two means. One is the destabilization of combination between FMN and electron, leading to transfer of one electron from FMN towards Heme. The second is stabilization of interplay between the FMN domain and the Heme domain (Smith et al., 2013).

Potential cell types containing nNOS in the brain:

i) neurons, such as interneurons in the hippocampus and the neocortex (Tricoire and Vitalis, 2012); *ii*) VSMCs in the brain have the potential to express nNOS due to the identification of nNOS in the VSMCs of neointima, media and adventitia (Talukder et al., 2004; Nakata et al., 2007). Furthermore, cortical arterial VSMCs are formed through the extension of media of artery and could be one of the cellular sources of NO in the brain. *iii*) astrocytes, an objective of this dissertation.

nNOS compartmentalization:

nNOS is colocalized with caveolin-1 and caveolin-3 in skeletal muscle cells (Venema et al., 1997) and located in the sarcolemma via PDZ domain (Kai Y. Xu, 1999). In cardiomyocytes, nNOS is co-immunoprecipitated with RyRs in the SR (Barouch et al., 2002). In neuronal post-synaptic dendrites, nNOS is coupled with PSD-93 and PSD-95 via PDZ domain. Moreover, PSD-95 is further linked to NMDA receptor, the activation of which causes nNOS-derived NO (Brenman et al., 1996b; Brenman et al., 1996a).

nNOS variants:

In 1993, a study of the nervous system initially discovered a different nNOS mRNA, named nNOS-2 (Ogura et al., 1993). In the following years, accumulating investigations identified novel nNOS variants in the body. nNOSμ expression was initially reported in skeletal and cardiac muscles (Silvagno et al., 1996), whereas nNOSγ was detected only in muscle cells and displayed a fairly weak activity compared to nNOS (Brenman et al., 1996b). Next, nNOSβ was found in the brain (Brenman et al., 1997). Particularly, nNOSα was expressed in a wide range of tissues, such as brain, heart, liver and kidney (Elfering et al., 2002). Catalytic activity (excluding nNOSγ) is similar across nNOS variants.

4.3.3 Inducible NOS

iNOS is not expressed in physiological cells, but it can be induced under the stimulation of cytokines or other factors. Once expressed, iNOS is activated constantly in a Ca^{2+}-independent manner. Interestingly, iNOS contains high concentrations of hydrophobic residues in relation to eNOS or nNOS, resulting in the strongly irreversible interaction between iNOS and the N-lobe of CaM (Piazza et al., 2012; Smith et al., 2013).

4.3.4 Other NOS isoforms

1) NOS in red blood cells is thought as an eNOS-like NOS (Kleinbongard et al., 2006).

2) Mitochondrial NOS is considered to have two classes, one is specific mitochondrial NOS and has extensive distribution, the other is a subtype of nNOSα and also distributed widely in tissues, such as liver, heart and brain (Elfering et al., 2002; Dedkova and Blatter, 2009).

4.4 Second messenger and neurotransmitter

NO is a double-edged sword, i.e. it plays protective roles in low levels but becomes an endogenous toxin produced by either overactivated eNOS and/or nNOS or iNOS. Following production, NO diffuses into adjacent cells and reacts as a free radical with multiple substances, including oxygen, transition metals, free superoxide anion and chemical groups in proteins, resulting in production of NO metabolites (e.g. NO^-, NO^+, $ONOO^-$). Hence, NO functions as a second messenger inside of cells and a neurotransmitter outside of cells.

4.4.1 Cellular metabolism of NO

Once produced in cells, NO immediately receives one electron from either oxygen or transient metals (e.g. iron in the heme, copper in the superoxide dismutase), and then becomes $NO^\bullet$, which acts as an endogenous second messenger in cells and reacts with oxygen or superoxide immediately. The consequence of these reactions generates nitrosothiols and series of reactive nitrogen species (RNS). The latter either function like ROS or interact with other chemical groups such as thiols and cysteine by S-nitrosylation in the form of $NO^\bullet$, regulating NO-mediated signalling cascades inside of cells.

S-nitrosylation: $NO^\bullet + HS- \longrightarrow \mathbf{ONS-}$

Production of RNS:

$NO^\bullet + O_2 \longrightarrow \mathbf{N_2O_3}$

$NO^\bullet + O_2^{\bullet-} \longrightarrow \mathbf{ONOO^-}$

$ONOO^- + H^+ \longrightarrow ONOOH$

$ONOOH \longrightarrow \mathbf{NO_3}$ or $ONOOH \longrightarrow {}^\bullet OH + {}^\bullet\mathbf{NO_2}$

4.4.2 Functional properties of NO

NO is a critical signalling molecule for various physiological processes in the body, contributing mainly to two aspects in the brain (Figure 1-4), regulation of contraction of muscle cells as well as involvement in the CNS, via S-nitrosylation and RNS reaction.

4.4.2.1 Regulation of cerebral blood flow

Cerebral blood flow (CBF) is one parameter to evaluate the regional blood volume flowing

through the brain within one unit of time. In the brain, local increased neuronal activity calls for an increase in neighboring CBF, thereby leading to a metabolic balance between supply and demand. Artery and arteriole consisting of endothelial cells (ECs) and vascular smooth muscle cells (VSMCs) are responsible for the supply of blood that has a high oxygen content. It has been well demonstrated that the endogenous vasodilator NO is able to regulate CBF (for a review (Toda et al., 2009)).

eNOS in ECs preferentially binds to caveolin-1 in microdomains of caveolae-associated membrane (Feron et al., 1996). Once activated by factors, such as ACh and sheer stress, NO can either goes into blood to inhibit platelet aggregation and adhesion (Radomski et al., 1987), or crosses into VSMCs causing vasodilation.

In VSMCs, activation of soluble guanylyl cyclase (sGC) by binding NO to the cofactor heme facilitated production of cyclic guanosine monophosphate (cGMP) (Brophy et al., 1997). Increased cGMPs further reduced contractile force via activation of MLC_{20} phosphatase (MLCP) which dephosphorylated the regulatory 20-kDa myosin light chain (MLC_{20}) (Lee et al., 1997). In addition to the cGMP-dependent pathway, cardiomyocyte-derived NO at the sarcolemma also regulated vascular constriction in a cGMP-independent manner. NO reversibly activates RyRs activity by poly S-nitrosylation to enhance the sensitivity of cardiac muscles to Ca^{2+} (Stoyanovsky et al., 1997; Xu et al., 1998). Furthermore, NO has capacity to inhibit the enzymatic activity of CYP 4A which is expressed in VSMCs and produce the vasoconstrictor 20-HETE (Sun et al., 1998; Oyekan et al., 1999). Collectively, NO regulates muscle vasocontraction by either cGMP-dependent or -independent pathways (Figure 1-4).

4.4.2.2 NO roles in the tripartite synapse

Under physiological conditions, NO functions via S-nitrosylation to regulate Ca^{2+}-independent synaptic vesicle release and levels of multiple neurotransmitters in the CNS (Meffert et al., 1994). A recent study identified all protein S-nitrosocysteine sites in mouse brain and found that NO modulates glutamate concentration through different ways. For instance, extracellular glutamate levels could be raised by inactivating EAAT2 via NO-mediated S-nitrosylation at Cys^{373} and Cys^{562}. Intracellular glutamate levels were affected by inhibition of glutamate dehydrogenase and activation of glutamine synthetase (Raju et al., 2016). Not only

levels of glutamate, NO also promotes production of catecholamines (e.g. dopamine). During the post-translational modification, evidence indicated that nitration and S-glutathionylation inactivated tyrosine hydroxylase, which is responsible for the rate-limiting reaction of catacholamines production. Contrarily, NO-mediated S-nitrosylation increased the activity, leading to an increase in catacholamines (Wang et al., 2017b).

Oxidative stress can be induced by metal interaction by way of iron and/or copper chelation. Indeed, one study induced abnormal metal reactions in the brain using magnetic fields at extremely low frequencies. These reactions resulted in increased RNS formation by transient metal-activated NOS and S-nitrosylated proteins, the structural and functional alternations of which were related to aging-like symptoms (Selaković et al., 2013). Furthermore, in early oxidative stress, RNS altered normal conformation of p53 into unfolded form which cannot bind DNA (Buizza et al., 2012). Neuronal NMDA receptor is functional coupled to PSD-95/nNOS complex in the plasma membrane. In response to ischemia, overactivated NMDA receptors stimulated PSD-95/nNOS complex, resulting in high levels of NO and the NMDA receptor-induced toxicity (Sattler et al., 1999; Aarts et al., 2002). However, instead of worsening oxidative stress, nitrite-released NO could directly alleviate hypoxia by inhibition of HIF-α (Burnley-Hall et al., 2017).

Under pathological situations, excessive NO via S-nitrosylation affects function of critical proteins in neurons. For instance, S-nitrosylated Cdk5 induced over-phosphorylation of tau protein in AD, while S-nitrosylation of ubiquitin C-terminal hydrolase-1 promotes amyloid and amorphous protein aggregates with regard to AD and Parkinson's disease (Kumar et al., 2017; Wang et al., 2017a). Indirectly, NO assists endothelin-1-mediated neuronal degeneration by increasing Akt tyrosine nitration (Antoni et al., 2017). Concurrently, neurons, astrocytes and endothelium may overexpress endothelin-1, which upregulated iNOS levels but down-regulated nNOS levels, resulting in an increased NO-induced toxicity. Collectively, NO-mediated signalling contributes to regulation of synaptic transmission and CBF in the CNS and may be involved in the pathophysiology of neurodegenerative diseases.

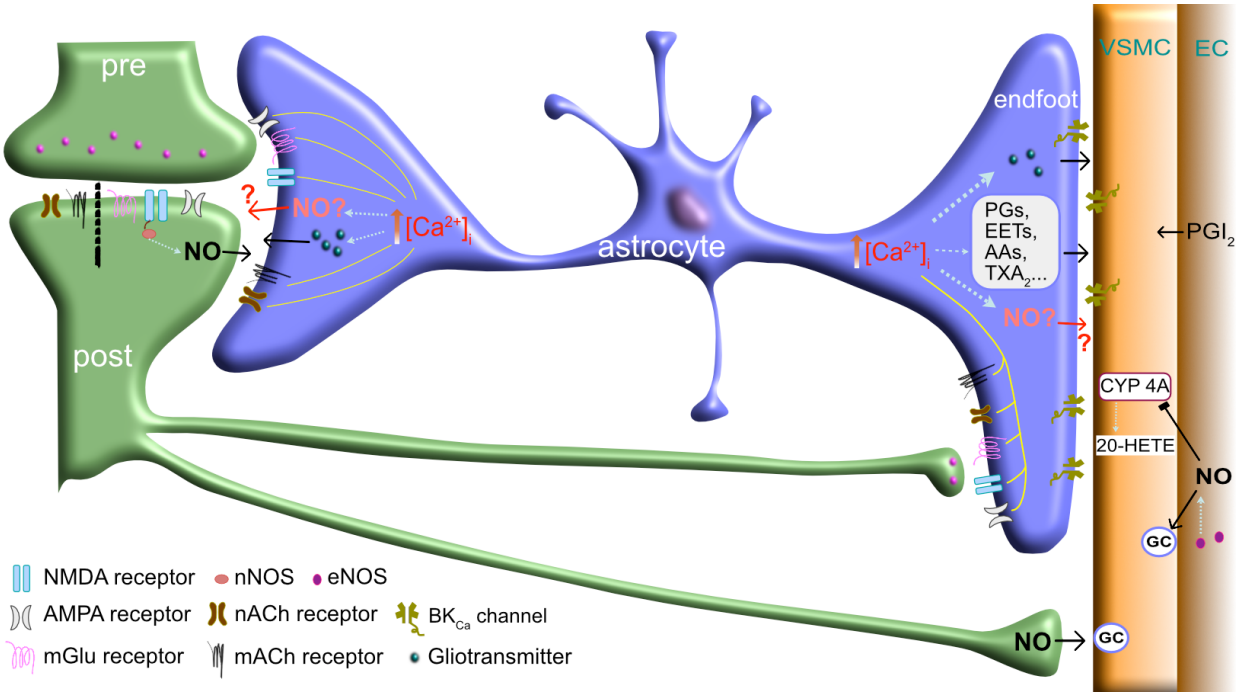

Figure 1-4 Potential roles of NO in astrocytic process and endfoot

5. Experimental hypotheses and objectives of the thesis

In the brain, astrocytes are no longer considered as supporting cells. They perform critical functions, including maintenance of synaptic plasticity and regulation of cerebrovascular coupling, under resting and active conditions. In response to neuronal signals, astrocytes generate a wide range of responses on the basis of intracellular Ca^{2+} events, which translate neuronal activity. It is clear that one main underlying mechanism by which astrocytes modulate local neuronal transmission and CBF is the release of gliotransmitters (e.g. glutamate, ATP). An importance potential gliotransmitter is NO which is a powerful vasodilator and a crucial neuromodulator. However, the mechanisms by which astrocyte can produce NO under physiological conditions is unclear.

We **hypothesize** that astrocytes can express functional constitutive eNOS and/or nNOS, which produces NO in response to neuronal activity.

The primary **objectives** of this thesis are: *i*) to identify the subtype of constitutive NOS in astrocytes, *ii*) to test whether isolated astrocytes can produce NO upon various cholinergic and glutamatergic pharmacological stimulations, *iii*) to determinate the polarity and microdomains of NO production in acute brain slices where astrocytes are polarized

CHAPTER 2

METHODOLOGY

Animals

All C57BL/6J mice, $eNOS^{-/-}$ mice and $nNOS^{-/-}$ mice were purchased from the Jackson Laboratory. All experimental protocols were approved by the animal ethics committees (CDEA) of the Université de Montréal. Mice were reproduced and bred with standard lab chow and water *ad libitum* in the Université de Montréal, which strictly conducted in accordance with the guidelines of the Canadian Council on Animal Care. Genotyping the offspring of KO nNOS mice was followed from the guidelines of the Jackson Laboratory. Only male homozygotes were used in the studies, and the wild-type (WT) controls were C57BL/6J mice.

Purified astrocyte culture

Dissociated cell cultures were obtained from cortical layers of postnatal day 0 to day 3 mouse pups. Primary astrocyte cultures were plated onto glass coverslips to form monolayer as described previously (Fasano et al., 2008). After 5 to 7 days, over 98 % GFAP+ astrocytes reached confluency and were identified by loading with sulforhodamine 101 (SR101, 100 μM; Sigma), a red fluorescent marker of astrocyte.

Acute brain slice preparation

Male mouse at 10-12 weeks was decapitated after anesthesia of overdosed isoflurane. Notably, mouse was decapitated immediately to alleviate effect of anesthetic on brain Ca^{2+} signalling (Stobart et al., 2016). Then brain was removed into iced aCSF (4 C°) as soon as possible, containing 125 mM NaCl, 3 mM KCl, 26 mM NaHCO3, 1.25 mM NaH2PO4, 2 mM $CaCl_2$, 1 mM $MgCl_2$, 4 mM glucose, and 400 μM L-ascorbic acid (Girouard et al., 2010). Coronal brain slices (180 μm) of mouse somatosensory cortex were prepared at the level between bregma 0.26 mm and bregma 1.18 mm using a vibratome (Leica VT1000S) (Paxinos and Franklin, 2004). After sectioning, brain slices were temporarily stored into aCSF at room temperature (RT), equilibrated with 5% CO_2 carbogen.

Dye loading

Astrocyte cultures were rinsed with HEPES buffer (pH 7.3), containing 118 mM NaCl, 4.69 mM KCl, 4.2 mM NaHCO3, 1.18 mM KH_2PO4, 1.29 mM $CaCl_2$, 1.18 mM $MgSO_4 \cdot 7H_2O$, 10 mM D-Glucose, 10 mM Hepes, and were loaded with a fluorescent nitric oxide indicator, 4-

Amino-5-methylamino-2′,7′-difluorofluorescein diacetate (DAF-FM diacetate, 10 μM; Invitrogen) and/or SR101 (100 μM; Sigma) for 45 min at RT. Brain slices were incubated with DAF-FM diacetate (10 μM) and/or SR101 (100 μM) for 60 min at 28 C°, well-shaking and equilibrated with 5% CO_2 carbogen. After loading the dye, subjects were rinsed and placed in HEPES buffer and aCSF respectively until used.

To avoid intereference from S-nitrosothiol-released NO, N- ethylmaleimide (NEM, 200 μM) was pre-incubated with brain slices for 10 min to deplete -SH groups (Chvanov M et al., 2006).

To study the responses of eNOS and nNOS to *t*-ACPD, L-NNA (L-N^G-Nitroarginine, 100 μM; Cayman) a non-selective competitive inhibitor of nitric oxide synthase (NOS) was pre-incubated with brain sections for 15 min; the selective inhibitor of nNOS, NPLA (N^{ω}-propyl-L-arginine, 10 μM; Tocris) and the inhibitor of eNOS, L-NIO (N^5-(1-iminoethyl)-L-ornithine, 10 μM; Tocris) were employed and pre-incubated with brain slices of WT, KO eNOS and KO nNOS mice for 25 min.

To assess the involvement of intracellular Ca^{2+} in astrocytic endfeet, BAPTA-AM, an intracellular calcium chelator (50 μM; Sigma) was pre-treated. CPA (cyclopiazonic acid, 30 μM; Millipore) was to deplete entire Ca^{2+} store in endfeet ER (endoplasmic reticulum), high-dose ryanodine (Ry, 100 μM; Tocris, abcam) was to block ryanodine receptor (RyR), Ry 2 μM was to active RyR, and 2-aminoethoxydiphenyl borate (2-APB, 100 μM; abcam) as well as xestospongin C (XeC, 20 μM; abcam) was to inhibit the activity of IP3 (inositol 1, 4, 5-triphosphate) receptor (Gafni et al., 1997). Except 2 μM Ry, the other four reagents were pretreated with subjects for 25 min.

To verify whether astrocytes has the functional structure of NMDAR-PSD-95- nNOS, we bath applied an inhibitor of NR2B subunit, Ro25-6981(3 μM, 20-30 min pre-treatment), or a peptide Tat-NR2Bct (YGRKKRRQRRRKLSSIESDV, 20 μM, 20 min pre-treatment), which is an inhibitor of PSD-95 domain and breaks the linkage between NMDA receptor and nNOS (control group was applied an inactive peptide S-Tat-NR2Bct-AA, YGRKKRRQRRRKLSSIEADA, 20 μM, pre-treatment for 20 min) (Girouard et al., 2009).

Imaging of electron microscopy

WT and knockout adult mice (3 months) were anesthetized deeply by an i.p. injection of 100 mg/kg sodium pentobarbital. Mice were perfused with 5-10 mL of heparin-saline, 40 mL of 3.75% acrolein in 2 % PFA (paraformaldehyde) solution in 0.1 M PBS (phosphate buffer solution, pH 7.4) followed by 200 mL of 2 % PFA in 0.1 M PBS. Coronal sections (40 μM) from the sensorimotor cortex were prepared using a vibratome (Leica Microsystems ®, Bannockburn, IL, USA), then were incubated in 1 % borohydride solution for 30 min, freeze-thawed and incubated in 0.1 % BSA (bovine serum albumin) solution in 0.1 M tris-saline (TS) buffer. Rabbit polyclonal antisera against eNOS (No. PA1-037) and nNOS (No. 61-7000) was purchased from Invitrogen (Camarillo, CA). The antiserum did not exhibit any cross-reactivity with the related eNOS/nNOS or iNOS proteins. Negative controls were previously performed on $nNOS^{-/-}$ and $eNOS^{-/-}$ brain slices with nNOS and eNOS antibody for specificity. Primary antisera 1:1000 was incubated with brain sections overnight at room temperature. Rinse several times in TS, then transferred into donkey anti-rabbit immunogold IgG, 1:50 for 2 hours. Incubation with 2 % gluataraldehyde in 0.01 M PBS for 10 min to fix the golden particles, then the antibody examination was detected by Ted Pella Silver IntensEM kit, 7 min at room temperature for intensification. Sections were postfixed in 2 % osmium tetroxide in 0.1 M PB, dehydrated and flat-embedded in EPON (EM Bed-812, Electron Microscopy Sciences, Fort Washington, PA, USA) between two pieces of Aclar plastic (Allied Signal, Pottsville, PA, USA).

Sections were examined using a H7000 Hitachi transmission electron microscope. An average of 2 samples per animal covering an area of at least 200 μm^2 per animal were examined, and each case generated about 50 images of magnifications ranging from 7,000X to 40,000X. A total area of 15,469 μm^2 was examined in 3 wild type and 3 knockout mice.

Imaging and identification of arteriole *ex vivo*

Astrocytic endfeet that enwrapped arterioles (regions of interest, ROIs) were selected and imaged for *ex vivo* studies. Parenchymal arterioles were identified in two ways, one is following the connections back to pial arteries, the other is verifying the thickness of vascular wall (around 5 μm) that encircled with a continuous smooth muscle layer. More detailed information on identification of arterioles have been demonstrated previously (Girouard et al., 2010).

Image acquisition

All *in vitro* and *ex vivo* living studies were performed on Olympus Fluoview FV1000 confocal microscope using a 40X water immersion objective (60X oil immersion objective was used for immunohistrochemistry study). Individual coverslip of astrocyte cultures was transferred into a chamber perfusing continuous HEPES buffer at RT, on the stage of confocal microscopy (Olympus BX61WI). DAF-FM (Figure 2-1a) and SR101 were excited by 488 nm laser and 543 nm laser of single photon, respectively. Individual brain slice was placed into another perfusion chamber, and was superfused with carbogenated aCSF continuously maintained at 32-35 ℃. *Ex vivo* data was collected by two-photon microscopy. The regions of interest are cortical layers III to V at S1 and S2 of primary somatosensory cortex, where cortical astrocyte Ca^{2+} signalling occurs in response to sensory stimulation (Paxinos and Franklin, 2004; Kim et al., 2016; Stobart et al., 2016). DAF-FM was excited at 765 nm wavelength, and astrocytic endfeet loaded with SR101 were identified at 820 nm wavelength.

ROIs were scanned by Z-stack images. XY time series *in vitro* were recorded for 10 minutes. 0 min was defined when the first Z-stack images were recorded before stimulation. Then the rest ten Z-stack images were taken right after every minute until 10-minute perfusion with freshly prepared stimulus (acetylcholine, 10 μM, Sigma; or t-ACPD, 100 μM, Tocris; or NMDA, 40 μM, Biomol; or AMPA 40 μM, Tocris; or ATP, 100 μM, Sigma). The same definition was applied on *ex vivo* scanning, five time points of Z-stack images were recorded at every 2.5 minutes and until 10-min stimulation. All images were taken based on the frame size of 512 × 512 pixels, at 20 or 40 μs/pixel.

Verification of the NO marker DAF-FM

To test the efficiency of DAF-FM diacetate to detect NO in our preparations, astrocytes cultures were incubated in the presence of a NO donor, sodium nitroprusside (SNP), which releases NO inside living cells (Figure 2-1b). The increased fluorescence was observed immediately following application of 100 μM SNP (Figure 2-1c). Hence, the data provided that DAF-FM worked very well in our experimental conditions and can detect concentrations as low as 3 nM (Kojima et al., 1999).

ATP is an important gliotransmitter partaking in Ca^{2+} signalling in astrocytes. Notably, a recent study found that ATP has the capacity of increasing intracellular Ca^{2+} in astrocytes and increasing intracellular DAF-FM intensity (Li NZ et al., 2003). After application of ATP in our experimental setting, fluorescent intensity of DAF-FM increased significantly in astrocyte cultures (Figure 2-2), whereas the increase was prevented by pretreatment with L-NNA (100 μM, 15 min), a non-selective NOS inhibitor. The data implied that i) our experimental condition was able to detect DAF-FM fluorescence and its changes upon positive (ATP) and negative (L-NNA) stimulation; ii) astrocytes *in vitro* express functional NOS which produce NO for approximately 21.8 % in response to stimulation of ATP (100 μM).

Immunohistochemistry

Immunohistochemistry (IHC) staining was performed on frozen sections from male mice at age 9-14 weeks (C56BL/6J mice and ChAT(BAC)-eGFP mice; Jackson Laboratory), anesthetized by sodium pentobarbital (100 mg/kg, i.p.) and intracardiac perfused with saline (pre-cooled at 4 C°). The brain was rapidly removed on aluminium foil upon dry ice for 20 min, and stored at -80 C° until used. Sections (30 μm) were cut in the cryostat (Leica CM1850 UV) at -22 C°, then mounted onto Superfrost Plus microscope slides (Fisher Science) and placed into a slide warmer pre-warmed at 60 C° for 10 min, stored at -20 C° until used (available within 2-3 month). Slides were dried for 20 min at RT and fixed with 95 % ethanol (pre-cooled at -20 C°) for 10 min at 4 C°, then rinsed three times with PBS, 5 min each and blocked with 5 % normal goat serum in PBS (pH 7.4) for 60 min, at RT.

Slides were incubated with primary antibody, *i*) eNOS (1:100; BD Bioscience) or nNOS (1:400, BD Bioscience); *ii*) caveolin-1 or -3 (Cav-1 or Cav-3) (1:1000; Thermo Fisher); *iii*) polyclonal anti-RyR antibody, RyR2 or RyR3, (1:1000, Millipore); *iv*) polyclonal anti-NR2B antibody (1: 500; Thermo Fisher)) overnight, at 4 C°. After rinse with tris-buffered saline (TBST, contained 0.2 % Triton X-100, 0.025 % Tween 20) three times, 5 min per rinse, second antibody of Alexa 488, Alexa 546 and Alexa 647 (1:500; Invitrogen) were applied for 60 min at RT. Rinse another three times with TBST, 5 min per rinse. In the end, GFAP (conjugated with Cy3, 1:800; Millipore) was incubated separately overnight at 4 C°. Last, slides were rinsed with TBST

three times and immersed into sudan black B solution (0.3 % in 70 % ethanol; Bioshop) to reduce autofluorescence for 15 min at RT. Slides were rinsed three times in TBST and two times in PBS. Then they were dried and coverslipped with Fluoromount-G (SouthernBiotech). Negative controls were performed with no antibody, primary antibody only and secondary antibody only, respectively.

Images were acquired under the single photon with 488 nm, 543 nm and 633 nm lasers, equipped with 60X oil immersion objective. ii) Cholinergic colocalization: Slides were dried for 20 min at RT and fixed with 4 % paraformaldehyde (PFA) (pH 7.4, pre-cooled at 4 C°) for 8 min at 4 C°, and rinsed with PBS three times, 5 min each and blocked with 5 % normal goat serum in PBS for 60 min at RT. Primary antibody of eNOS (1:100) was applied onto sections for 24 h, at 4 C°. Rinse three times with TBST, 5 min each. Alexa 647 secondary antibody (1:500; Invitrogen) was incubated for 1 h, at RT, and rinse with TBST three times. Slides then incubated with GFAP (1:800) overnight at 4 C°. Rinse three times with TBST, 5 min per time. Dry slides at RT for 20 min and added Fluoromount-G. Negative controls were performed with no antibody, primary antibody only and secondary antibody only, respectively. Images were acquired under the single photon with 488 nm, 543 nm and 633 nm lasers, equipped with 60X oil immersion objective.

Analysis of hot spots of nitric oxide *ex vivo*

Fluorescent intensity of NO is analyzed by using background-subtracted $\Delta F/F_0 = (F_n-F_0)/F_0$, where Fn is the fluorescence intensity at frame n and F_0 is the baseline of DAF-FM fluorescence calculated from the average of several frames right before stimulation (Li et al., 2003). ROIs are selected randomly (Ito et al., 2010) and covered the whole cell (Li et al., 2003). However, in *ex vivo* potency assay, the approach that assessed the intensity of whole astrocytic endfoot was not effective and accurate enough to evaluate the capacity of NO production. Because NO in astrocytes acts as a gaseous neurotransmitter and diffuses radially into low concentration areas, and may effuse through NO permeable openings such as Connexin 43-formed hemichannel (Figueroa et al., 2013) and aquaporin-1 water channel (Herrera et al., 2006) into neighboring cells. Theoretically, release of NO release is likely in the form of hot spot. Namely, the highest

concentration of NO is in the core of one hot spot. Once activated, those hot spots comprising NOS or thiol peptides generate NO at discrete compartmentalized areas.

Thus, we herein propose a new model - hot spots of nitric oxide - to analyze changes in patterns of NO production in astrocyte endfeet by counting up the total number and mean of hot spots intensity. Examined through surface plots of astrocyte endfeet, we decided to define the size of one ROI as 1.03 μm × 1.33 μm (or 5 × 6 pixels), which is large enough to overlay the entire dimension of one hot spot of NO. All data are based on the values obtained from inner core of hot spots where contains the highest fluorescent intensity of DAF-FM.

Data analysis.

For all experiments, images were recorded by Olympus confocal software (FV10-ASW Ver. 03.01) and ROIs were randomly selected. Fluorescent intensity of DAF-FM and surface plots of astrocytic endfoot were obtained by ImageJ software. All statistical tests were carried out using GraphPad Prism 6.0. Data were presented as mean ± S.E.M. Two groups comparisons were analyzed by two-tailed Student's *t*-test. Multi-comparisons were appropriately subjected to one-way or two-way ANOVA followed by Bonferroni post-hoc tests as indicated. Statistical significance was considered as if $p < 0.05$.

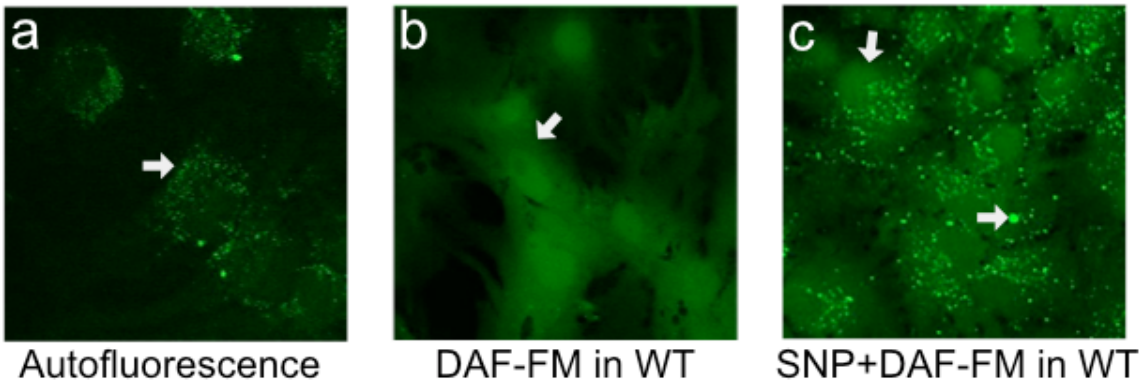

Figure 2-1 The validation of the technique indicating nitric oxide in living astrocytes

Examples of fluorescent images showing *i*) autofluorescence (a, white arrow) in wild-type (WT) astrocyte cultures without applying DAF-FM (a NO marker), *ii*) fluorescence of DAF-FM (b, white arrow), and *iii*) increased DAF-FM fluorescence (c) when applying SNP (a NO donor), using single photon microscopy (400X). White arrows indicate cytosolic NO and new NO produced by SNP.

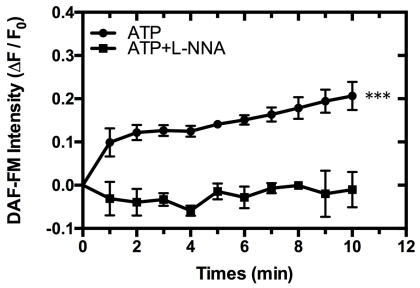

Figure 2-2 ATP stimulates NO production in cortical astrocyte cultures

Time courses of DAF-FM intensity in purified WT astrocyte cultures during 10-min perfusion with ATP (100 μM, n=59 cells for ATP treatment from 3 WT pups). ***$p < 0.001$, two-way ANOVA with Bonferroni post-hoc test. The three curves showed a significant enhancement of DAF-FM intensities upon applications of neurotransmitters. Meanwhile, the responses were eliminated by pretreatment with a non-selective NOS inhibitor, L-NNA (100 μM, 15 min).

CHAPTER 3

Cholinergic stimulation elicits eNOS-dependent release of nitric oxide in astrocytes

Introduction

Astrocytes are the most abundant cells in the brain and play diverse roles including tripartite synapses and regulation of CBF. One messenger that could potentially be involved in the regulation of both synaptic activity and CBF is nitric oxide (NO). However, the mechanism by which NO can be produced in astrocytes remains unknown. Since Ca^{2+}-dependent eNOS in endothelial cells can be activated by cholinergic stimulation and the ensuing Ca^{2+} increase, we emitted the hypothesis that a similar mechanism may exist in astrocytes in proximity to cholinergic neurons. In cortical astrocytic cultures and acute brain slices from C57BL/6, $eNOS^{-/-}$ and $nNOS^{-/-}$ mice, respectively, NO production was evaluated using DAF-FM diacetate under confocal microscopy.

Results

ACh induces eNOS-dependent NO production in astrocyte cultures

Previous studies found that ACh trigger intracellular Ca^{2+} elevation via muscarinic and/or nicotinic acetylcholine receptors (mAChR/nAChR) in the heart (Massion et al., 2003) and brain (Dajas-Bailador and Wonnacott, 2004), resulting in activation of Ca^{2+}-dependent eNOS (Feron et al., 1997; Massion et al., 2003; Krieg et al., 2005). Indeed, it was found that cytosolic Ca^{2+} activates Akt, which in turn, raises eNOS activity and induces formation of microdomain of mAChR-eNOS complex (Danson et al., 2005; Krieg et al., 2005). Thus, in our purified cortical astrocyte cultures, NO production was evaluated by assessing DAF-FM intensity (Figure 3-1, n = 3 pups, 68 cells for WT, 82 cells for $nNOS^{-/-}$ and 73 cells for $eNOS^{-/-}$). Increased NO production (21.8 %) was evoked during 10-min perfusion with ACh (10 μM) in wild type (WT) group (Figure 3-1B, n=3; $***p < 0.001$), a small but reliable elevation (11.8 %) was displayed in $nNOS^{-/-}$ group (Figure 3-1B, n=3; $*p < 0.05$; two-way ANOVA with Bonferroni post-hoc test), while no increase was observed in $eNOS^{-/-}$ astrocytes. Nevertheless, NO production in response to ACh was blocked by 15-min pre-treatment with L-NNA (100 μM), indicating that this response is NOS-dependent (Figure 3-1B). Notably, NO intensity was not enhanced in $eNOS^{-/-}$ group, but over 20 % increases occurred in WT group and approximately 10 % increases occurred in $nNOS^{-/-}$ group (Figure 3-1B). Taken together, our data suggested that ACh-induced

NO production in cortical astrocyte cultures mainly relies on eNOS signalling, which is in accordance with findings in cardiac myocytes (Feron et al., 1997).

eNOS in cortical astrocytes is predominantly around neurons

Immunoperoxidase labeling of NOS in sensory-motor cortex confirmed the expression of both eNOS and nNOS in astrocytes under physiological conditions (Figure 3-2A, data of nNOS are not shown). To demonstrate the specificity of antibodies, immunolabeling of eNOS and nNOS was tested on $eNOS^{-/-}$ and $nNOS^{-/-}$ mice respectively. Expressions of both eNOS and nNOS in astrocytes were first identified and quantified using electron microscopy within 96 profiles (Figure 3-2B, n=3 WT mice). 71 ± 5 % of eNOS was distributed in perineuronal processes, whereas 29 ± 5 % were in peri-vascular endfeet (Figure 3-2B, *t*-test, $***p < 0.001$). The data of eNOS distribution in astrocytes performed a preferential distribution in perineuronal processes.

Previous reports in cardiac myocytes found a functional coupling between release of ACh from parasympathetic input and postsynaptic activation of eNOS (Massion et al., 2005). The eNOS-dependent ACh evoked NO production in astrocyte cultures suggests a spatial proximity between cholinergic neurons and astrocytic eNOS. This spatial connection between cholinergic inputs and astrocytic eNOS was assessed by dual immunofluorescence staining in ChAT-eGFP mice, which express enhanced green fluorescent protein in choline acetyltransferase-containing neurons (Figure 3-3a, e, h). Indeed, images of dual staining showed that astrocytic eNOS express close to cholinergic neurons (Figure 3-3, e-h), in contrast to the vasculature (Figure 3-3, b-d). It is suggested a potential spatial coupling between astrocytic eNOS and cholinergic neurons. Collectively, these results support the hypothesis that eNOS is not only located in astrocytes but tend to be distributed spatially in the vicinity of cholinergic neurons rather than the vasculature. This distribution may have functional connection with cholinergic inputs.

eNOS colocalizes with caveolin-1 and -3 in cortical astrocytes

Plenty of studies implied that eNOS was compartmentalized within caveolae, via colocalization with caveolins, for instance, caveolin-1 (Cav-1) in endothelial cells and caveolin-3 (Cav-3) in cardiomyocytes (Feron et al., 1996; Xu et al., 1999; Paton. et al., 2002; Massion et al., 2004). In the brain, Cav-3 was identified in rat astrocytes (Ikezu et al., 1998), while Cav-1

is abundant in reactive astrocytes as well as in cerebral endothelial cells (Badaut et al., 2015). To verify whether eNOS in astrocytes colocalizes with Cav-1 or -3, triple immunostaining was performed on slices from mouse somatosensory cortex. Cav-1 and -3 were both found in astrocytes and colocalized with eNOS in the somatosensory cortex (Figure 3-4).

ACh influences changes in patterns of hot spots of NO in endfeet of perivascular astrocytes

To determine *ex vivo* impact of ACh on NO production in astrocytes, we bath applied ACh (10 μM) for 10 min upon acute brain slice preparations. Meanwhile, to analyze changes in localized NO intensity in response to ACh, we used an analysis model - hot spot similar to the one used for subcellular analysis of Ca^{2+} spikes (Frick A et al., 2001). Thus, a color scale was used and hot spots were illustrated with reddish peak in surface plot of astrocyte endfoot (Figure 3-5A). Changes in the total number and average intensity of these hot spots were obtained during 10-min superfusion with ACh (Figure 3-5). In *ex vivo* study (Figure 3-5B), astrocytic endfeet enwrapping parenchymal arterioles were selected as regions of interest (ROIs) in the somatosensory cortex (detailed information was described in methodology).

NO production increased in response to ACh. There was no significance on the total number of hot spots between WT (8.00 ± 1.53) and $nNOS^{-/-}$ (7.67 ± 1.20) /$eNOS^{-/-}$ (8.00 ± 2.00) groups (n=3 mice; Figure 3-6a). Meanwhile, NO intensity was reduced dramatically in $eNOS^{-/-}$ (11.5 %) and $nNOS^{-/-}$ (11.1 %), compared to WT group (22.0 %) (n=3 mice, $^{**}p < 0.01$, $^{***}p < 0.001$; one-way ANOVA with Bonferroni post hoc tests).

Since NO pools were already present in the preparation before ACh stimulation, they were eliminated by N-ethylmaleimide (NEM, 200 μM, pre-treated for 10 min), a thiol pool remover. There was no significant difference in the number of hot spots between WT and $nNOS^{-/-}$ groups (Figure 3-6b, n=3 mice, 4.67 ± 0.33 vs. 4.67 ± 0.33), while in $eNOS^{-/-}$, no new hot spot was induced in response to ACh (Figure 3-6b). To further test the output of NOS and nitrosothiol pool, we analyzed the response strength of each hot spot in astrocytic endfoot. Again, there was undetectable NO production upon ACh stimulation in $eNOS^{-/-}$ while both WT and $nNOS^{-/-}$ groups produced NO at similar level, 0.198 ± 0.033 vs. 0.185 ± 0.040 ($\Delta F/F_0$).

Discussion

Our present work focuses on ACh-induced NO release from astrocytes in an eNOS-dependent manner. By means of one and two-photon confocal microscopy as well as electron microscopy, our novel findings suggest: (*i*) superfusion with ACh raised NO levels in isolated astrocytes *in vitro* and in brain slices *ex vivo* via eNOS-mediated signalling; (*ii*) eNOS docks within astrocytic processes around cholinergic neurons rather than the vasculature; (*iii*) astrocytic eNOS was localized within caveolae containing Cav-1 and -3; (*iv*) upon ACh stimulation, both cytosolic nitrosothiol pool and astrocytic eNOS contributed to an increase in endfoot NO intensity.

eNOS distribution in astrocytes

In accord with our electron microscopy data and immunostaining images, perineuronal astrocytes expressed higher density of eNOS compared to perivascular astrocytic endfeet. The proximity of astrocytic eNOS with cholinergic neurons is coherent with the model of cholinergic volume transmission. In the cortex, ACh diffuses mainly through volume-transmission model, instead of synaptic transmission pathway (for a review (Hirase et al., 2014)), since cholinergic neurons display few dendritic spines and branches in cerebral cortex (Umbriaco et al., 1995). Thus, within approachable distance, cholinergic neuron-released ACh has a potential to induce an increase in eNOS activity in adjacent astrocytes. Similarly, eNOS in cardiomyocytes is activated by ACh through M2 receptors. In these cells M2 receptors are translocated to eNOS/Cav-3 and form the mAChR-eNOS complex essential for regulation of Ca^{2+} influx in caveolae ((Feron et al., 1997) ((Paton. et al., 2002), for a review). This dynamic translocation of mAChR into caveolae indicates that cholinergic stimulation is functionally coupled to eNOS and its localization.

Caveolae microdomains in NO production

In astrocytes, eNOS colocalizes with Cav-1 and -3. This is supported by previous data which clearly illustrated that astrocytic eNOS colocalizes with Cav-1 and -3 in rat brain slice (Badaut et al., 2015). The association between eNOS and Cav-1 and -3 is well known in cardiomyocytes (Feron et al., 1996; García-Cardeña et al., 1996; Massion et al., 2004). Although

predominant in endothelial cells, Cav-1 is also present in astrocytes (Cameron et al., 1997), whereas brain Cav-3 has been largely described in astrocytes (Virgintino et al., 2002; Shin et al., 2005). Caveolae compartmentation of eNOS plays a paradoxical role both inhibiting basal eNOS activity by the enzyme (Feron et al., 1998) or ensuring the efficient activation of the enzyme upon agonist stimulation (Feron et al., 1997; Feron et al., 1999).

With regard to the colocalization between eNOS and Cav-1, it should be noted that it is possible that the Cav-1 colocalized with eNOS is from the vasculature instead of astrocytic endfoot, since Cav-1 is the predominant isoform expressed in endothelial cells. However, our advanced single photon confocal and specific antibodies could markedly reduce this possibility.

Associations between S-nitrosothiol pool and NO

In addition to NOS, S-nitrosothiols possibly act as a form of NO storage and transport. S-nitrosylation is an important post-translational modulation of proteins and plays key roles in the control of protein functions and related signalling cascades (Kumar et al., 2017). Depletion of the S-nitrosothiol pools with NEM demonstrated the importance of eNOS in the ACh-dependent NO production. With regard to S-nitrosothiol pool, a prior study pointed out that ACh induced NO released from S-nitrosothiol pool in a Ca^{2+}-dependent manner (Chvanov M et al., 2006).

Potential sources of artifacts

In brain slices superfused with ACh, and changes in NO were obtained from perivascular astrocytic endfoot. In this case, it is possible that neurons were activated by ACh and released active factors such as glutamate and ATP, which in turn triggered perivascular astrocytes and resulted in an increase in NO. Additionally, stimulated astrocytes can, in turn, release gliotransmitters (e.g. glutamate, D-serine) to have effects on surrounding astrocytic compartments. However, a significant increase in NO was observed in WT and $nNOS^{-/-}$ astrocyte cultures but not $eNOS^{-/-}$ cultures, implying that *in vitro* astrocytes have the capacity to produce NO in response to ACh. Moreover, ACh did not induce new NO production in $eNOS^{-/-}$ astrocytic endfoot when S-nitrosothiols were depleted, suggesting that this NO pool is the consequence of eNOS probably from neighboring endothelial cells. Last but not least, to try to suppress active factors released from neurons and astrocytes themselves, tetrodotoxin and inhibitors like SNARE inhibitors (e.g. botulinum toxins), are both required during *ex vivo*

experiments. Tetrodotoxin is specific to inhibit voltage-gated Na^+ channels to deplete action potential, while SNARE inhibitors can prevent intracellular vesicle fusion and exocytosis.

In summary, the present study pointed out that astrocytes express eNOS, and characterized anatomical and pharmacological facets of astrocytic eNOS. Spatially, eNOS colocalizes with caveolin-1 and -3, and is mainly localized within perineuronal astrocytes. Pharmacologically, cholinergic stimulation specifically induces an increase in NO production in an eNOS-dependent manner. Besides, we found that S-nitrosothiols, a storage of intracellular NO, could release NO upon ACh stimulation. Therefore, our findings provide a novel understanding of astrocyte-derived NO, which may play key roles in enhancement of cortical plasticity and, by extension, multiple pathological processes, such as Alzheimer's disease.

Figures

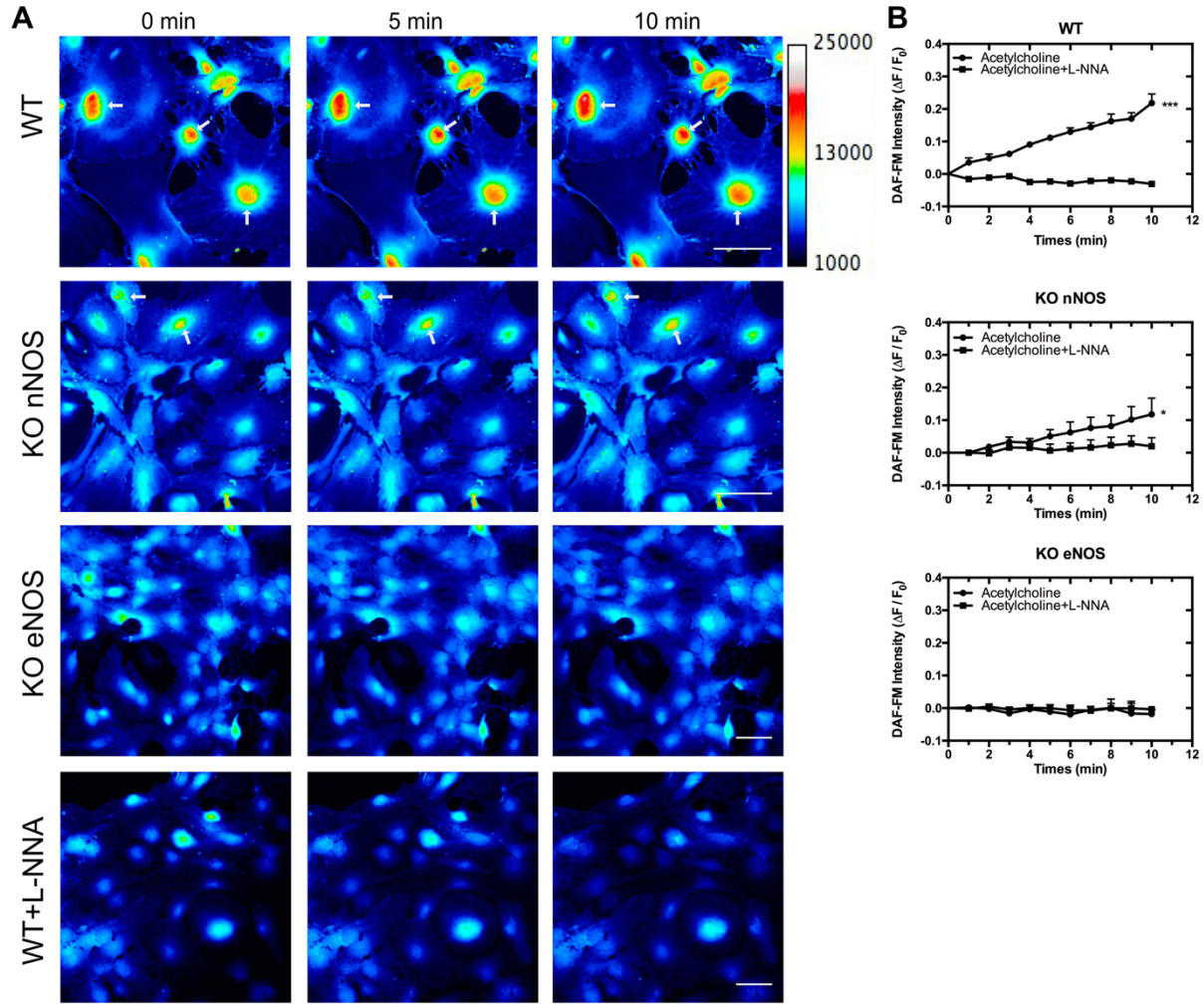

Figure 3-1 ACh stimulates an eNOS-dependent NO production in cortical astrocyte cultures

A. Examples of pseudocolor images shows that intensity of DAF-FM was increased in WT and $nNOS^{-/-}$ astrocytes (white arrows) after 5 and 10 min perfusion with 10 μM ACh, whereas the increase was attenuated in $eNOS^{-/-}$ astrocytes. Meanwhile, pretreatment with 100 μM L-NNA (NOS inhibitor) in WT astrocytes inhibited the response to ACh as well. Scale bar = 50 μm. *B*. Time courses of changes in DAF-FM intensity upon perfusion with 10 μM ACh in WT (n=3; ***$p < 0.001$), KO nNOS groups (n=3; *$p < 0.05$; two-way ANOVA with Bonferroni post-hoc test) and KO eNOS. Error bars indicate mean ± S.E.M.

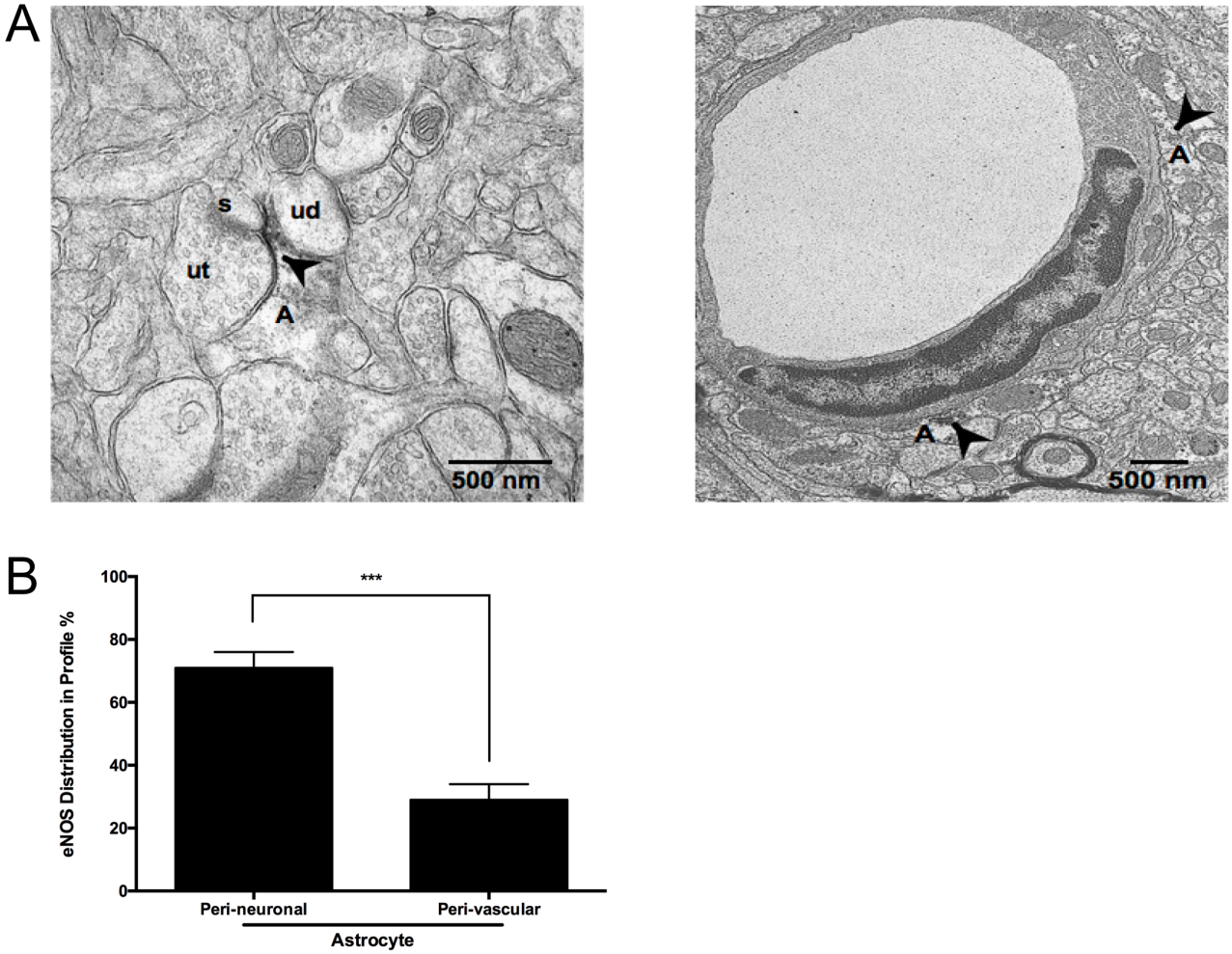

Figure 3-2 Astrocytic eNOS in WT mice exists alongside neurons rather than cerebral vasculature

A. Electron microscopic images of astrocytes in mouse sensory-motor cortex. eNOS labeled by immunoperoxidase (black arrows), located within peri-neuronal (left) and peri-vascular (right) astrocytic processes (A) which are near unlabeled axon terminals (ut), spines (s) and unlabeled dendrites (ud). Scale bar = 500 nm. *B*. Bar graph shows eNOS is abundantly expressed in astrocytes, and the distribution of eNOS is higher in peri-neuronal than in peri-vascular astrocytic processes. Data were obtained from 6 vibratome sections (n=3 WT mice; ***$p < 0.001$; *t*-test). Error bars indicate mean ± S.E.M.

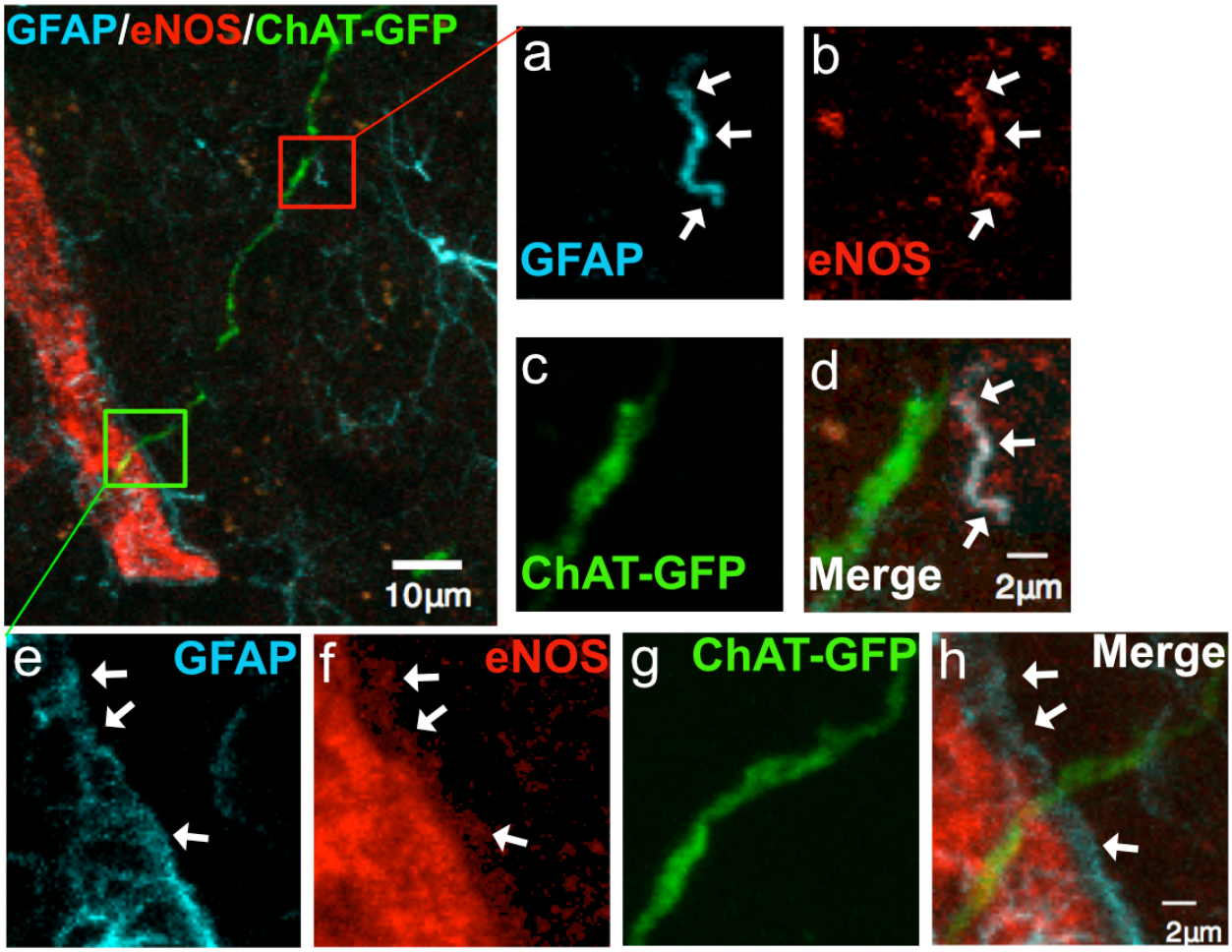

Figure 3-3 Spatial connection between astrocytic eNOS and cholinergic neurons

Dual immunostaining of ChAT-eGFP mouse brain (a) suggested that astrocytic eNOS were prone to be located within astrocytic processes in the vicinity of areas of cholinergic neurons (e-h) but not that of vessels (b-d). Higher magnification images of region 1 (green) and region 2 (red) showed that the more astrocytes were close to cholinergic neurons (e-h), higher intensities of eNOS were expressed, but this phenomenon was not observed at the areas of vessels (e-g). Astrocytes (cyan) were labeled by GFAP antibody conjugated with Cy3 (c, f), eNOS (red) were detected by Alexa Fluor 488 anti-mouse for total eNOS (d, g), cholinergic neurons (green) were identified by transgenic green fluorescent protein (GFP) (h). White arrows indicate dual colocalization of eNOS and GFAP. Scale bar = 20 μm (a), 10 μm (b-h).

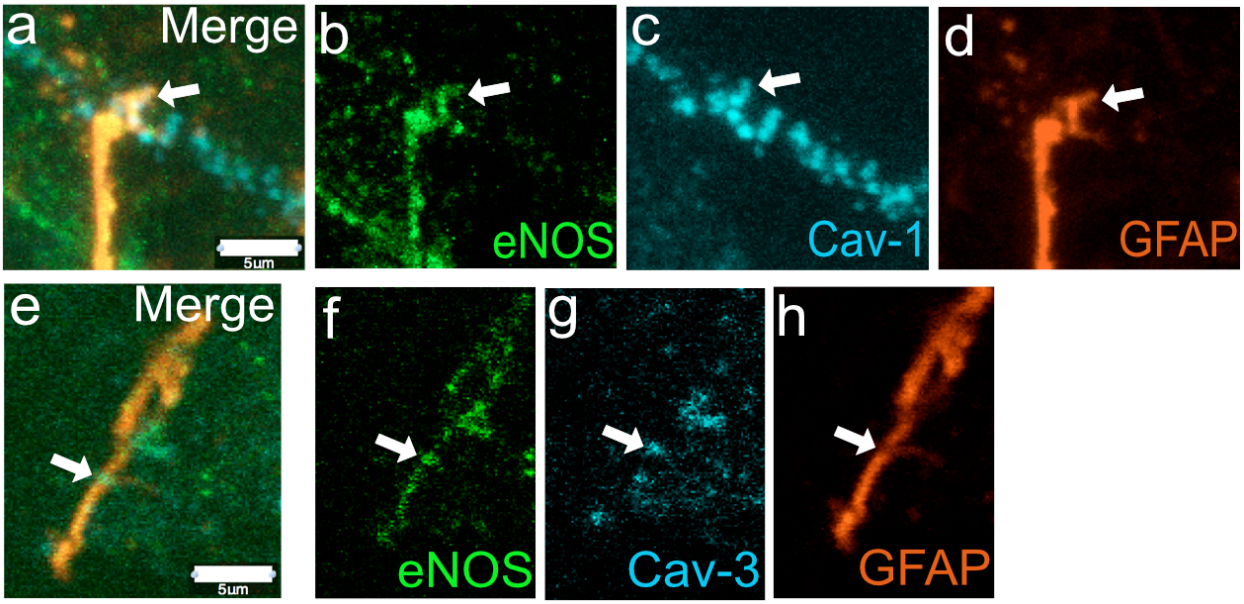

Figure 3-4 Colocalization of astrocytic eNOS and caveolin-1/caveolin-3 of somatosensory cortex

Immunofluorescence detection was carried out using Alexa Fluor 488 anti-mouse for total eNOS (green), Cy3 anti-mouse for GFAP (orange) and Alexa Fluor 647 anti-rabbit for Cav-1 (a-e) (cyan) and Cav-3 (f-j) (cyan). Scale bar=20 μm (a, f). Higher magnification images of the square areas (red) are shown on the right (b-e, g-j). Arrows (white) indicate triple colocalization. Triple staining (e) for eNOS (b), Cav-1 (c) and GFAP (d) represents colocalization of astrocytic eNOS and Cav-1 in one endfoot. The other triple staining (j) for eNOS (g), Cav-3 (h) and GFAP (i) represents colocalization of astrocytic eNOS and Cav-3 in one astrocytic process. Scale bar=5 μm (b-e, g-j).

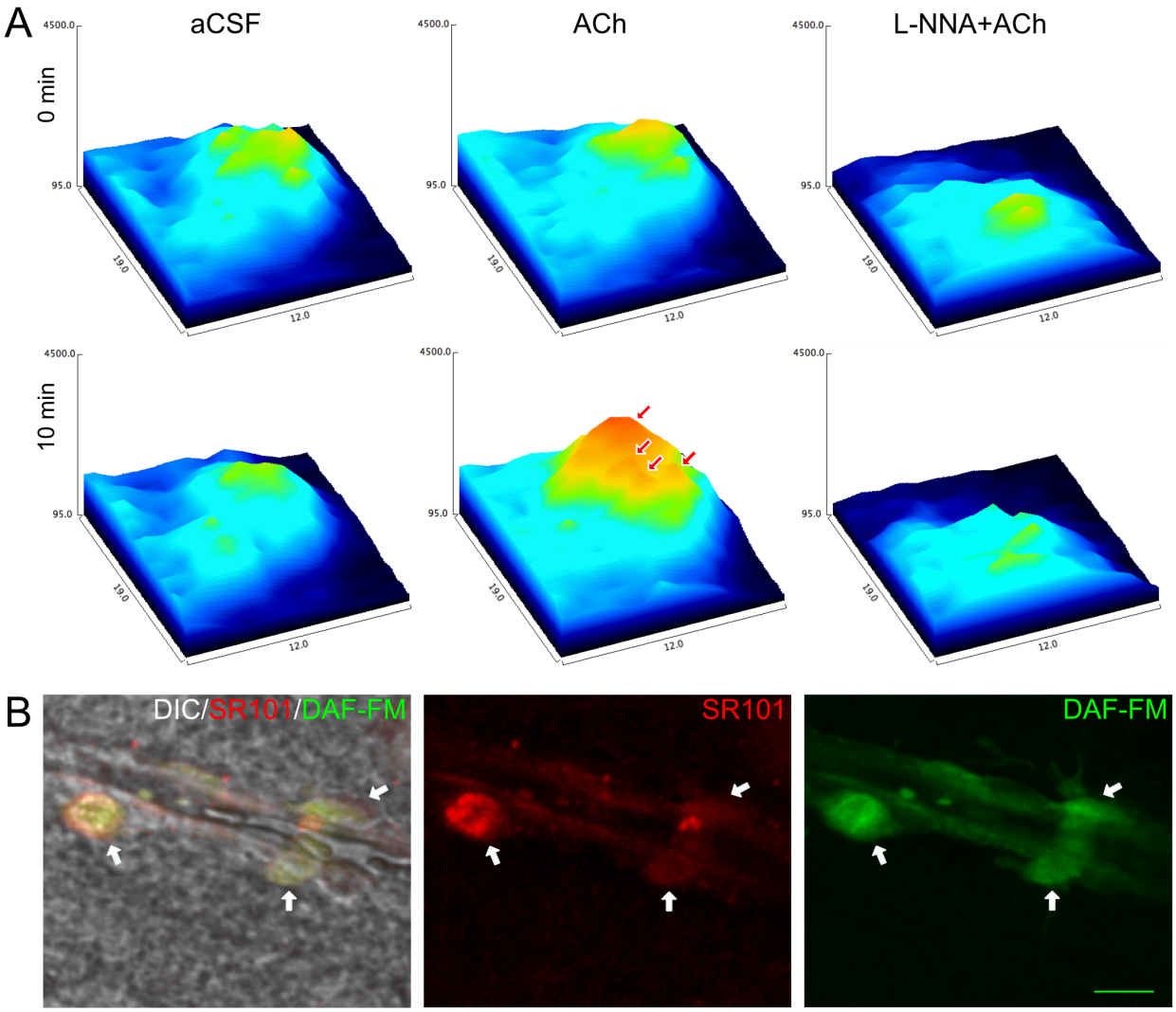

Figure 3-5 Identification of hot spots in astrocytic endfoot *ex vivo*

A. Examples of surface plots in one astrocyte endfoot with 3D pseudocolor graphs illustrating changes in DAF-FM intensity. The x and y coordinates on surface plots represent pixels of the surface plot. The height and the color indicate pixel intensity. Hot spot is defined as each reddish peak. Intensity of hot spots (red arrows) was enhanced in response to 10-min ACh (10 μM) stimulation but was attenuated by pretreatment with L-NNA (b). The data also indicated that intensity was rarely changed by perfusion with aCSF (c). *B*. Example of images show one arteriole in an acute brain slice loaded with SR101 (red, an astrocyte marker) and DAF-FM (green), under the differential interference contrast (DIC) and fluorescent imaging. After merged, the images show that regions preferentially loaded with DAF-FM and analyzed were perivascular astrocytic endfeet (white arrows). Scale bar = 10 μm.

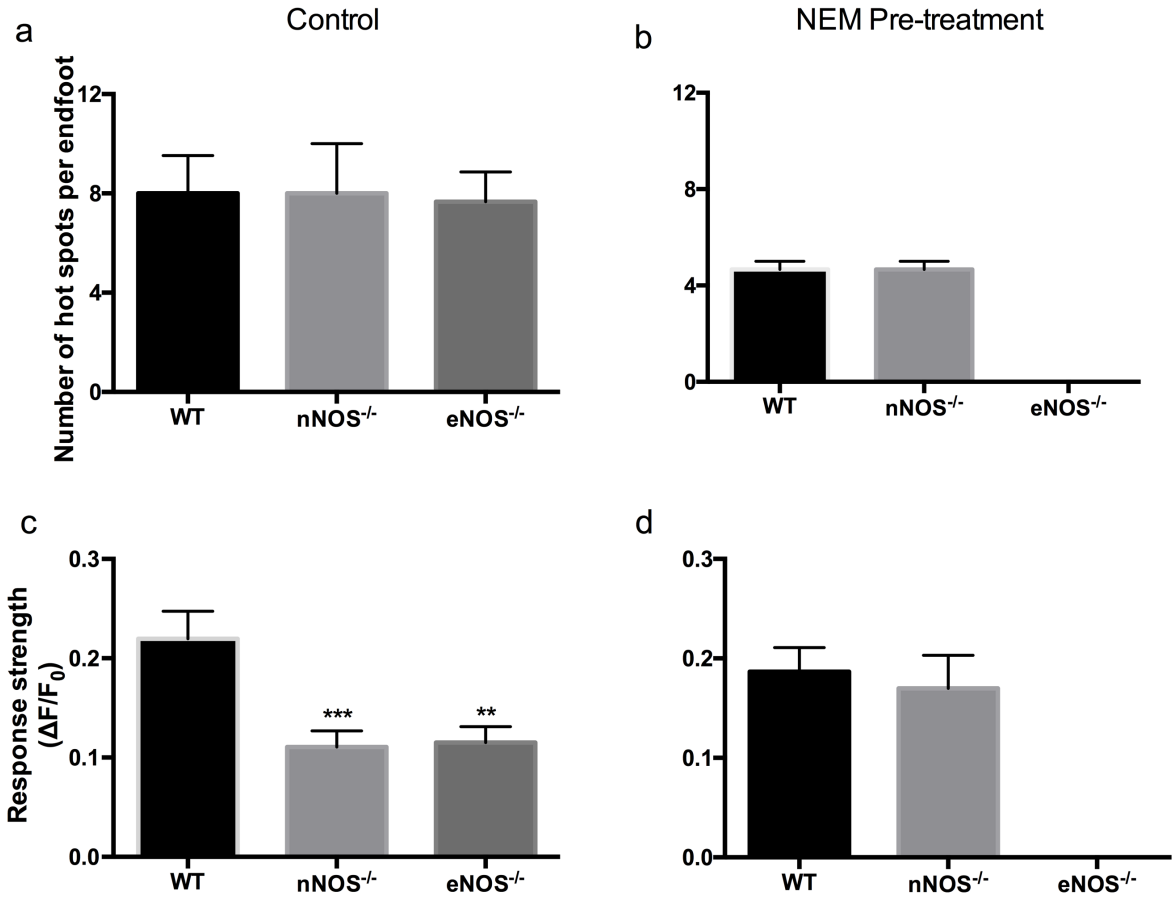

Figure 3-6 Determination of hot spots coming from eNOS, nNOS and S-nitrosothiol pool in astrocytic endfoot

After 10-min ACh superfusion, endfeet did not display any difference on the total number of hot spots between WT, and $eNOS^{-/-}$ and $nNOS^{-/-}$ groups (a). Nonetheless, the amplitude of the response to ACh in WT endfeet was significantly stronger than for KO eNOS and KO nNOS groups (**$p < 0.01$ vs. WT group, ***$p < 0.001$ vs. WT group; one-way ANOVA with Bonferroni post hoc tests) (c). In the presence of NEM (a thiol pool remover, 200 μM), however, ACh did not induce new hot spots in KO eNOS endfeet. No significant difference was found between WT and KO nNOS groups in neither the total number (b) nor response strength (d) of hot spots.

CHAPTER 4

nNOS-produced nitric oxide in astrocytes requires ryanodine receptor activity

Introduction

In the brain, astrocytes play a key role for the support of neuronal metabolism and maintenance of extracellular glutamate homeostasis. Glutamate is the most abundant neurotransmitter in the brain. Thus, to sense dynamic neuronal activity, astrocytes express considerable glutamatergic receptors, including NMDA receptors, AMPA/KA receptors, group I mGluRs and group II mGluRs (Porter and McCarthy, 1995; Silva et al., 1999). Once activated, these glutamatergic receptors regulate astrocytic Ca^{2+} dynamic and activate corresponding signalling pathways. One of the potential signaling pathway is the one of the nitric oxide synthase (NOS). In astrocytes, the presence of either eNOS and nNOS have been demonstrated (Gabbott and Bacon, 1996; Wiencken and Casagrande, 1999; Iwase et al., 2000; Adachi et al., 2010). However, the mechanisms by which constitutive NOS are activated in astrocytes under physiological conditions remain unknown. Both constitutive NOS requires the Ca^{2+}-calmodulin complex to be activated suggesting that any mechanism that increases intracellular Ca^{2+} concentrations may potentially activate one of the constitutive NOS. Interestingly, eNOS and nNOS had been associated to different cellular localizations suggesting that each NOS is associated to a specific pathway. Because of the well-known association between glutamatergic receptors (Christopherson et al., 1999; Ouardouz et al., 2009) and nNOS in neurons and the importance of this enzyme in synaptic signaling events, the objective of the present study is to determine the association between glutamatergic stimulation and astrocytic NO production from nNOS.

Results

We previously demonstrated that both eNOS and nNOS are expressed in astrocytes and glutamate induces an increase in NO intensity in astrocyte cultures by measures of DAF-FM (NO probe) intensity (Figure 4-2A). We consequently hypothesized that each NOS is activated by a different pathway in different compartment of the astrocytes

Subcellular distributions of nNOS in astrocytes and neurons of the sensorimotor cortex of WT mice

To assess the ultrastructural distribution of nNOS, immunogold labeling of nNOS was performed on sensorimotor cortex of WT mouse. The specificity of the nNOS antiserum in brain

slice was verified in nNOS$^{-/-}$ mice (data not shown). Analysis of electron microscopy images showed a high level of nNOS in perineuronal astrocytes (56 ± 9 % profiles) compared to neurons and perivascular astrocytes (Figure 4-1C, 32 ± 11 % and 12 ± 4 % profiles, ***p<0.001, One-way ANOVA with Bonferroni post hoc test). The results were obtained from the sensorimotor cortex from 3 mice where 168 profiles were collected and calculated (Figure 4-1).

Furthermore, a quantitative analysis of nNOS density in different subcellular compartments (average number of gold particles/cell or compartment, n=3 WT mice, Figure 4-1D) presented that in either astrocytes or neurons, the highest density of nNOS were found in the cytosol. Cytosolic nNOS particles/profile in perineuronal astrocytes constitute 29.0 ± 4.6 (n=14 profiles); in neurons, 42.0 ± 7.0 in the soma (n=17 profiles), while 7.6 ± 1.4 localized in the dendrites (n= 10 profiles). Then, the second highest density of nNOS was in the nucleus, 13.0 ± 8.0 particles/profile in the nucleus of perineuronal astrocytes (n=4 profiles), whereas 9.5 ± 3.0 were in the nucleus of neurons (n=13 profiles). Only few nNOS particles were seen in the plasma membrane (Figure 4-1D). 1.6 ± 0.4 nNOS particles/profile in the membrane of perineuronal astrocytes (n=5 profiles). In neurons, 0.8 ± 0.4 nNOS particles/profile were observed in the membrane of the soma (n=9 profiles), and 1.0 ± 0.0 were in the membrane of dendrites (n= 4 profiles). Pre-vascular astrocytes showed the lowest distribution (12.0 ± 4.0 nNOS particles/profiles) and densities (9.6 ± 3.4, n=7 profiles) of nNOS. This large distribution of nNOS in astrocytes may have potential role in cellular communication and maintain physiological functions in the brain.

nNOS-dependent NO production is triggered by *t*-ACPD in *in vitro* and *ex vivo* astrocytes

We determined the effect of distinct glutamatergic receptors activation such as mGluRs, NMDA and AMPA receptors on NO levels. The specific group I/II mGluRs agonist, *t*-ACPD, was bath-applied as were glutamate (Figure 4-2A) and its analogues NMDA (shown in next chapter) and AMPA (Figure 4-2B) to selectively activate NMDA and AMPA receptors. Activation of these receptors all induced an increase in astrocytic NO. To determine the specificity of each constitutive NOS for each receptor, changes in astrocytic NO was assessed for 10 minutes in cortical astrocyte cultures of WT, eNOS$^{-/-}$ and nNOS$^{-/-}$ mice. The treatment of *t*-ACPD (100 μM) for 10 minutes did not alter NO levels specifically in nNOS$^{-/-}$ astrocyte cultures (n=81 cells in 3 pups), whereas a significant increase in NO was observed in WT

(13.9 %) and eNOS$^{-/-}$ (12.8 %) groups (Figure 4-3A, n=60 cells for 3 WT pups, n=66 cells for 3 eNOS$^{-/-}$ pups; *$p < 0.05$, ***$p < 0.001$). Pre-treatment with L-NNA (L-N-Nitro-arginine), a non-selective NOS inhibitor, eliminated *t*-ACPD-induced NO elevation, in agreement with a NOS role in producing NO. Next, to examine the responses of astrocytes to *t*-ACPD within the neurovascular unit, astrocytes of the somatosensory cortex were chosen as *ex vivo* study subjects (detailed information was stated in methodology), due to endfeet-derived NO potentially has effect on vascular response. In accordance with *in vitro* data, superfusion of brain slices with t-ACPD (100 μM) elevated NO levels in WT (12.4 %) (n=6 mice, **$p < 0.01$) and eNOS$^{-/-}$ mice (9.0 %) (n=3 mice, *$p < 0.05$). However, the NO increases were absent in nNOS$^{-/-}$ mice (Figure 4-3A, n=3 mice).

Our prior *ex vivo* study suggested a compartmentalization of eNOS-produced NO. We thus postulated that a similar pattern may exist in nNOS-produced NO. Analysis of NO hot spots was performed in cortical astrocytes. As indicated in image of Figure 4-3B, one yellow/reddish peak is deemed as one NO hot spot. X/Y axis displays scale of the surface of astrocytic endfoot, while Z-axis indicates NO intensity. Meanwhile, the size of our regions of interest shown in Figure 4-3C (a black rectangle) is approximately 5×6 pixels. In accordance with data on isolated astrocytes (Figure 4-3A), the total number of hot spots and mean intensity of hot spots were all significantly reduced in astrocytes from nNOS$^{-/-}$ mice (Figure 4-3B, n=3 mice per group, *$p<0.05$), whereas eNOS$^{-/-}$ mice presented insignificant difference from WT group. These results revealed that in response to *t*-ACPD, nNOS compartmentally produced NO in astrocytes.

To further demonstrate that the NO response is dependent on nNOS, the nNOS inhibitor NPLA (10 μM) prevented the NO production in response to *t*-ACPD (Figure 4-3D, **$p<0.01$ from *t*-ACPD group) similarly to the L-NNA-treated group (*$p<0.05$ from *t*-ACPD group). However, the eNOS inhibitor L-NIO (10 μM) did not attenuate the NO increase. Jointly, these results suggest that *t*-ACPD exclusively stimulated nNOS-produced NO in a compartmentalization manner.

nNOS colocalizes with RyR2 and RyR3 in perineuronal and perivascular astrocytes

mGluRs are known to induce Ca^{2+} release from the ER. In addition, since data revealed by electron microscopy showed the highest density of nNOS in the cytosol and that nNOS in

cardiomyocytes is tightly associated with RyRs (Matyash et al., 2001; Liu and Huang, 2008), we performed immunofluorescence staining of RyRs and nNOS in cortical astrocytes. Despite subtypes 2 and 3 of RyRs have been found to be expressed in astrocytes (Matyash et al., 2001; Kesherwani and Agrawal, 2012; Kaja et al., 2015), the distribution of RyRs in cortical astrocytes remains unknown. Analysis of the immunofluorescent images revealed that RyR2 (Figure 4-4, A-B) as well as RyR3 (Figure 4-4, C-D) are expressed in both perineuronal astrocytes (Figure 4A, 4C) and endfeet (Figure 4B, 4D). Moreover, nNOS was found to colocalized with RyR 2 and 3 (white arrows) in the somata and processes.

Activation of RyR facilitates nNOS activity and evokes an increase in endfoot NO

Since astrocytic nNOS has close anatomical connection with RyR2 and RyR3, we sought to test whether in astrocytic endfoot mobilization of ER Ca^{2+} is fundamental to raise the nNOS-dependent NO levels evoked by *t*-ACPD. *t*-ACPD-induced changes in NO was abolished by pre-treatment with BAPTA-AM (Ca^{2+} chelator, 50 μM, 40 min), which is in line with enzyme kinetics depending on Ca^{2+} (Figure 4-5A). Then ER receptors and enzymes responsible for ER Ca^{2+} regulation were inhibited by pre-treatment with different inhibitors, including CPA (SERCA inhibitor which decreases the ER Ca^{2+} pool, 30 μM, 20 min), Ry (which act as a RyR inhibitor at 100 μM, 20 min), X-C (xestospongin C, blocker of IP_3 receptor, 20 μM, 15 min, data are not shown) and 2-APB (blocker of IP_3 receptor, 100 μM, 25 min), respectively. NO production was attenuated in all conditions suggesting that elevation of intracellular NO relies on ER Ca^{2+} mobilization (Figure 4-5A, n=4 mice, ***p<0.001).

To further understand effects of ER receptors, we used ryanodine (Ry in 2 μM) to selectively activate RyRs (for a review in (Thomas and Williams, 2012)). Strikingly, activation of RyRs alone evoked an increase in endfoot NO (6.0 %, not significant vs. *t*-ACPD group) (Figure 4-5B). In the presence of *t*-ACPD, the increased response remained when 2-APB blocked IP_3Rs and Ry activated RyRs (6.3 %), whereas it was suppressed when either IP_3Rs or RyRs were blocked. Next, we investigated whether activation of RyRs induced nNOS-derived NO. In the presence of *t*-ACPD, pre-treatment of brain slices with NPLA (10 μM, 20 min) but not L-NIO (4.3 %) (10 μM, 20 min) abolished RyRs-mediated elevation of NO (Figure 4-5B, n = 5 mice, *p<0.05, **p<0.01). Data showed that only astrocytic nNOS was activated by *t*-ACPD. Collectively, our results suggested a potential signalling pathway to activate nNOS in astrocytic

endfeet (Figure 4-5C). That is, *t*-ACPD-induced activation of IP_3R triggers RyRs activity via Ca^{2+}-induced Ca^{2+} release, and then RyR-mediated Ca^{2+} efflux stimulates nNOS activity, resulting in an increase in endfeet NO levels.

Discussion

In the present study, we have demonstrated that, *i*) among glutamatergic receptor agonists, *t*-ACPD is the only one to specifically induce nNOS-dependent NO production in astrocytes; *ii*) subcellular localization of nNOS shows a colocalization with RyR2 and RyR3; *iii*) *t*-ACPD leads to activation of nNOS which depends on IP_3R/RyR-mediated Ca^{2+} mobilization. These anatomical and pharmacological evidences suggest a tight structural association between nNOS and RyRs in astrocytes specifically activated by metabotropic glutamate receptors.

Subcellular distribution of nNOS in perivascular astrocytes

Although, nNOS are classically associated to neurons, immunogold identification of nNOS in mice revealed a higher density of nNOS in astrocytes than in neurons. Interestingly, most of nNOS was found in the cytosol followed by nucleus and the plasma membrane, and this distribution was similar in neurons and astrocytes. These results are consistent with the findings that brain nNOS exists in particulate and soluble forms (Hecker et al., 1994) and that it is mainly distributed in the cytosol far from membranes in a patch-like form (Rothe et al., 1998). Nuclear localization of nNOS has also been previously observed in cultured astrocytes of rats (Yuan et al., 2004). The subcellular localization of nNOS in the cell may contribute to its diverse functions.

NO production induced by glutamatergic activation

In neurons, the association between glutamatergic receptors and nNOS is well recognized (Christopherson et al., 1999; Ouardouz et al., 2009). Using specific glutamatergic receptor agonists in conjunction with $eNOS^{-/-}$ and $nNOS^{-/-}$ mice, we demonstrated for the first time that the selective group I/II metabotropic receptor agonist, *t*-ACPD, specifically induces nNOS-dependent NO production. *t*-ACPD is known to trigger a rise in intracellular Ca^{2+} concentration through inositol 1,4,5-triphosphate (IP_3Rs) and ryanodine receptors (RyRs) in the ER (Straub et

al., 2006; Panatier and Robitaille, 2016). In cardiomyocytes, nNOS associates with molecules that regulate Ca^{2+} at the ER level, including SERCA (Burkard et al., 2007) and RyR (Jian et al., 2014).

Functional link between IP_3Rs, RyRs and nNOS in astrocytes

All subtypes of RyR are expressed in the brain, which include RyR1, RyR2 and RyR3 (Kushnir et al., 2010). We found that both RyR2 and RyR3 are expressed in cortical astrocytes in agreement with previous studies (Matyash et al., 2001; Kesherwani and Agrawal, 2012). We then tested the functional link between IP_3Rs and RyRs with nNOS during *t*-ACPD stimulation using 2-APB and ryanodine. 2-APB acts as a blocker of both IP_3Rs and TRP channels (Bootman et al., 2002; Drumm et al., 2015). It is well established that ryanodine activates the RyRs at <10 μM, while it irreversibly inhibits channel opening at higher concentrations >100 μM (Chiarella et al., 2004; Thomas and Williams, 2012). Interestingly, both IP_3Rs and RyRs inhibition prevented NO increase in response to *t*-ACPD, while RyRs activation in the absence of *t*-ACPD increased NO production. These results suggest that activation of nNOS requires both IP_3Rs and RyRs activity. RyRs activation was probably evoked by Ca^{2+} crosstalk between IP_3Rs and RyRs via an underlying mechanism termed Ca^{2+}-induced Ca^{2+} release.

In addition to regulation of Ca^{2+} flux, RyRs are considered as redox sensors in cells. Their proximity with nNOS provides a potential mechanism by which RyRs regulate cytosolic redox processes by means of regulation of NO production.

Potential sources of artifacts

During the superfusion of brain slice, *t*-ACPD may also activate neuronal mGluRs, leading to the release of factors such as glutamate. It is general proposed that *t*-ACPD activates astrocytic mGluR5 and induces an increase in Ca^{2+} via activation of PLC, which produces IP_3 in the cytosol (for a review (Panatier and Robitaille, 2016)). However, the fact that the results present similar profiles in isolated astrocytes compared to brain slices strongly suggest an astrocytic specific stimulation of mGluRs. Nonetheless, emerging findings revealed low levels of mGluR5 expression in physiological adult astrocytes (Sun et al., 2013; Kim et al., 2016). It is possible that mGluR5 distributes in astrocytes in a polarized manner due to mGluRs are deemed to sense extracellular glutamate levels (Lavialle et al., 2011). Further immuno-

fluorescent staining need to be done to demonstrate mGluR5 distribution especially on astrocytes. However, effect of other group I/II mGluRs such as mGluR3 cannot be excluded in the study. Thus, it is necessary to apply the mGluR3 inhibitor (LY341495) or antagonists such as (S)-α-ethylglutamic acid and β-NAAG. The interest of using *t*-ACPD in the current study is to study the nNOS specific pathway in response to a glutamatergic agonist. A further study may focus on the subtype of mGluRs evoked by *t*-ACPD. Furthermore, t-ACPD-activated astrocytes also were able to produce and release gliotransmitters (e.g. glutamate). In that cases, further studies need to repeat and abolish neuronal action potential (by tetrodotoxin) as well as exocytosis (by botulinum toxins) before starting the stimulation.

In conclusion, the results of this study show that cortical astrocytes express nNOS. Perfusion with *t*-ACPD specifically induces nNOS-dependent NO production in astrocytes. Subcellularly, astrocytic nNOS colocalizes with RyR2 and RyR3. Pharmacologically, *t*-ACPD triggers IP3Rs activity, which stimulate RyRs and thus resulting in nNOS-produced NO production. The finding of this novel IP_3R/RyR/nNOS signalling in astrocytes may provide means for better understanding of NVC.

Figures

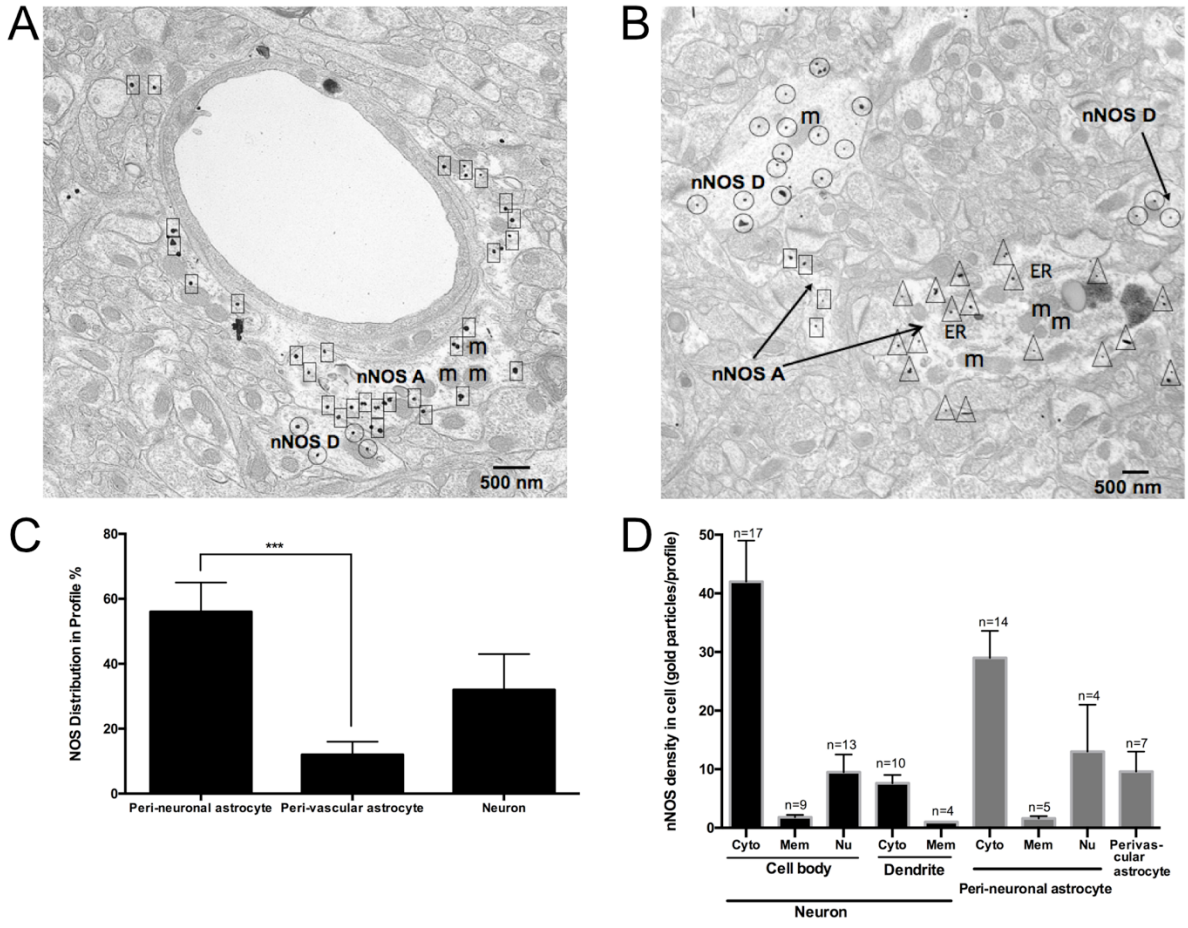

Figure 4-1 Subcellular distribution of nNOS in astrocytes and neurons of the sensorimotor cortex

Electron micrographs showing nNOS immunogold labeling (*A*-*B*, black dots) in dendrites (encircled, nNOS D), astrocytic processes (squares, nNOS A) and perineuronal astrocytic soma (triangles, nNOS A) in sensorimotor cortex of WT mice. m: mitochondria; ER: endoplasmic reticulum. *C*, Distributions of nNOS immunolabeling in perineuronal astrocytes, perivascular astrocytes and neurons (n=168 profiles, 3 WT mice), ***$p<0.001$, One-way ANOVA with Bonferroni post-hoc test. *D*, Densities of nNOS immunolabeling in neuronal and perineuronal astrocyte compartments as well as perivascular astrocytes (average number of gold particles/cell or compartment, 3 WT mice). Cyto: cytosol, Mem: membrane, Nu: nucleus. Scale bar = 500 nm. Data are shown as mean ± S.E.M.

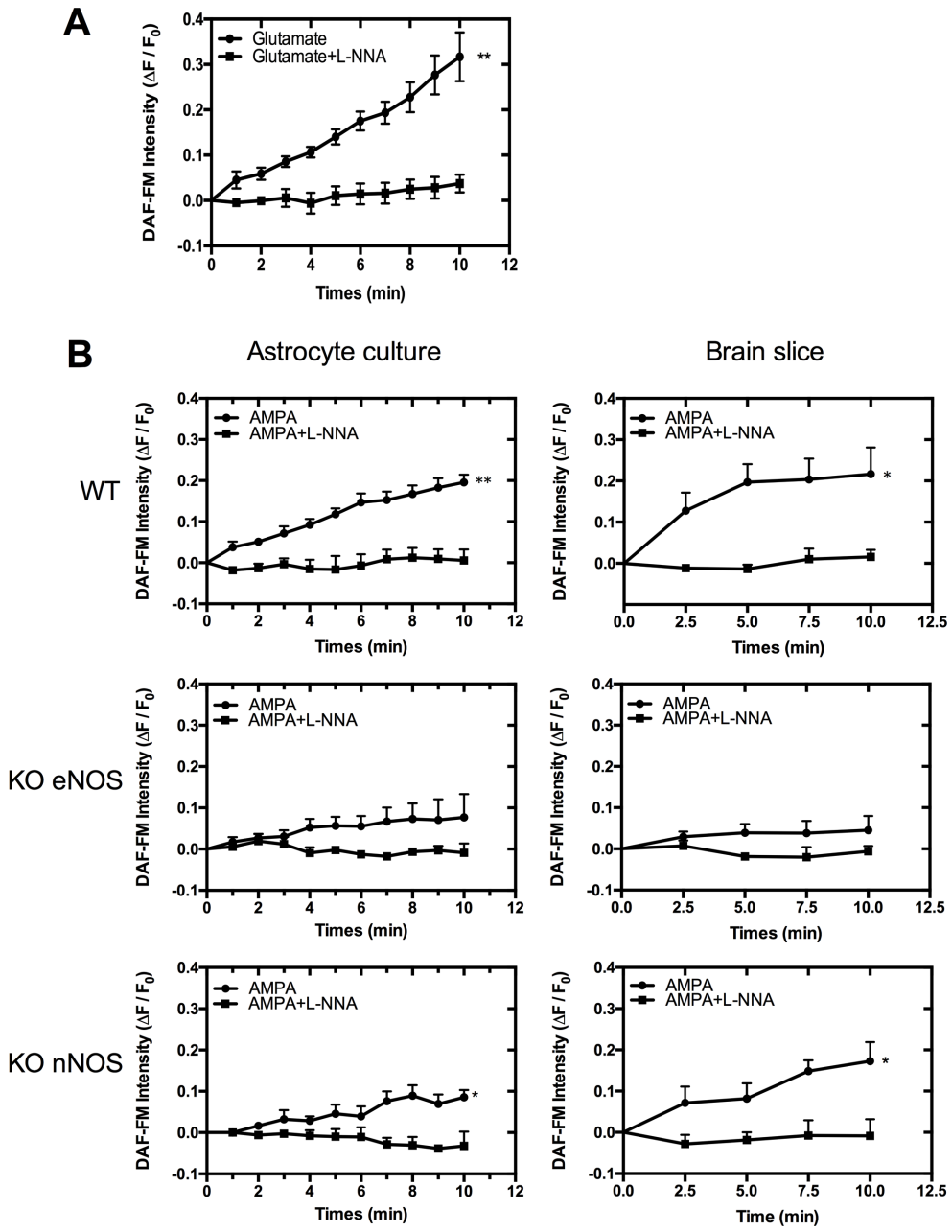

Figure 4-2 Glutamate and its analogue induced NO formation in cortical astrocytes

A. Time courses of DAF-FM intensity in purified WT astrocyte cultures during 10-min perfusion with glutamate (100 μM, n=67 cells from 3 WT pups). $^{**}p < 0.05$, two-way ANOVA with Bonferroni post-hoc test. *B*. Time courses of changes in DAF-FM intensity after superfusion with 30 μM AMPA in WT, eNOS$^{-/-}$ and nNOS$^{-/-}$ astrocyte cultures and perivascular astrocytic endfeet in brain slices, respectively (n=3 pups/adult mice; $^{*}p < 0.05$, $^{**}p < 0.01$; two-way ANOVA with Bonferroni post-hoc test). The increased response was prevented by pre-treatment with L-NNA (a non-selective NOS inhibitor, 100 μM, 15 min). Error bars indicate mean ± S.E.M.

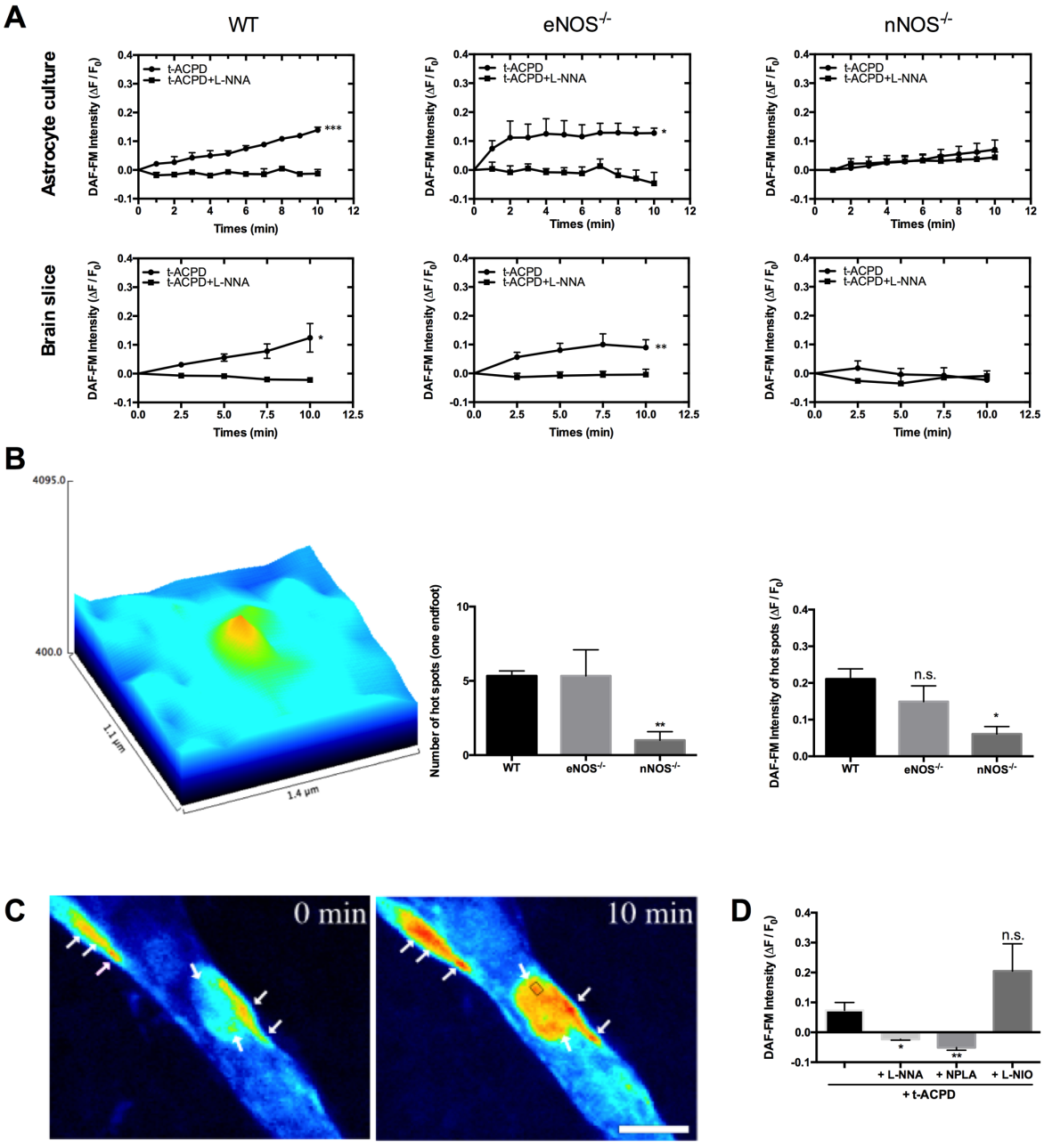

Figure 4-3 Increased NO production in astrocytes elicited by t-ACPD in both purified cultures and acute brain slices

Figure 4-3. *A*, Time courses of DAF-FM (NO marker) intensities in purified astrocyte cultures and perivascular astrocytic endfeet in brain slices respectively, during 10-min perfusion with *t*-ACPD (100 μM) in WT (n=60 cells from 3 pups, n=6 mice), eNOS$^{-/-}$ (n=66 cells from 3 pups, n=3 mice) and nNOS$^{-/-}$ mice. Excluding nNOS$^{-/-}$ mice (n=81 cells from 3 pups, n=3 mice); *p < 0.05, **p < 0.01, ***p < 0.001, two-way ANOVA with Bonferroni post-hoc test. In a different group, increased DAF-FM intensity was prevented after pretreatment with the non-selective NOS inhibitor, L-NNA (100 μM, 15 min). *B*, Summary data showing changes in hot spots intensity for astrocytic NO from WT, eNOS$^{-/-}$ and nNOS$^{-/-}$ mice (n=3 mice for eNOS$^{-/-}$ and nNOS$^{-/-}$, n=6 mice for WT), during 10-min *ex vivo* imaging. An example of surface plot in astrocytic endfoot (left) showing one hot spot (reddish peak). X and Y axis display scales of the surface, while Z-axis and pseudocolor indicate NO intensity. In response to *t*-ACPD, both the number and the average intensity of hot spots in astrocytic endfeet were notably reduced in nNOS$^{-/-}$ but not in eNOS$^{-/-}$ mice (*p<0.05, one-way ANOVA with Bonferroni post-hoc test). Reductions are also observed but not significantly in eNOS$^{-/-}$ mice, suggesting that activation of endfoot nNOS caused increased NO. *C*, Pseudocolor images of astrocytic endfeet enwrapping parenchymal arteriole *ex vivo*. Increased NO (white arrows) was induced in different areas of endfeet. A black rectangle in left image showed the size of one hot spot, which is 5×6 pixels. Scale bar = 10 μm. *D*, *t*-ACPD induced an increase in endfoot NO intensity was blocked by the pretreatment with L-NNA (100 μM, 15 min) or the selective nNOS inhibitor, NPLA (10 μM, 20 min). But NO intensity did not change in the presence of the eNOS inhibitor, L-NIO (10 μM, 20 min). *p<0.05, **p<0.01, n.s., not significant vs t-ACPD group, one-way ANOVA with Bonferroni post-hoc test. Data are shown as mean ± S.E.M.

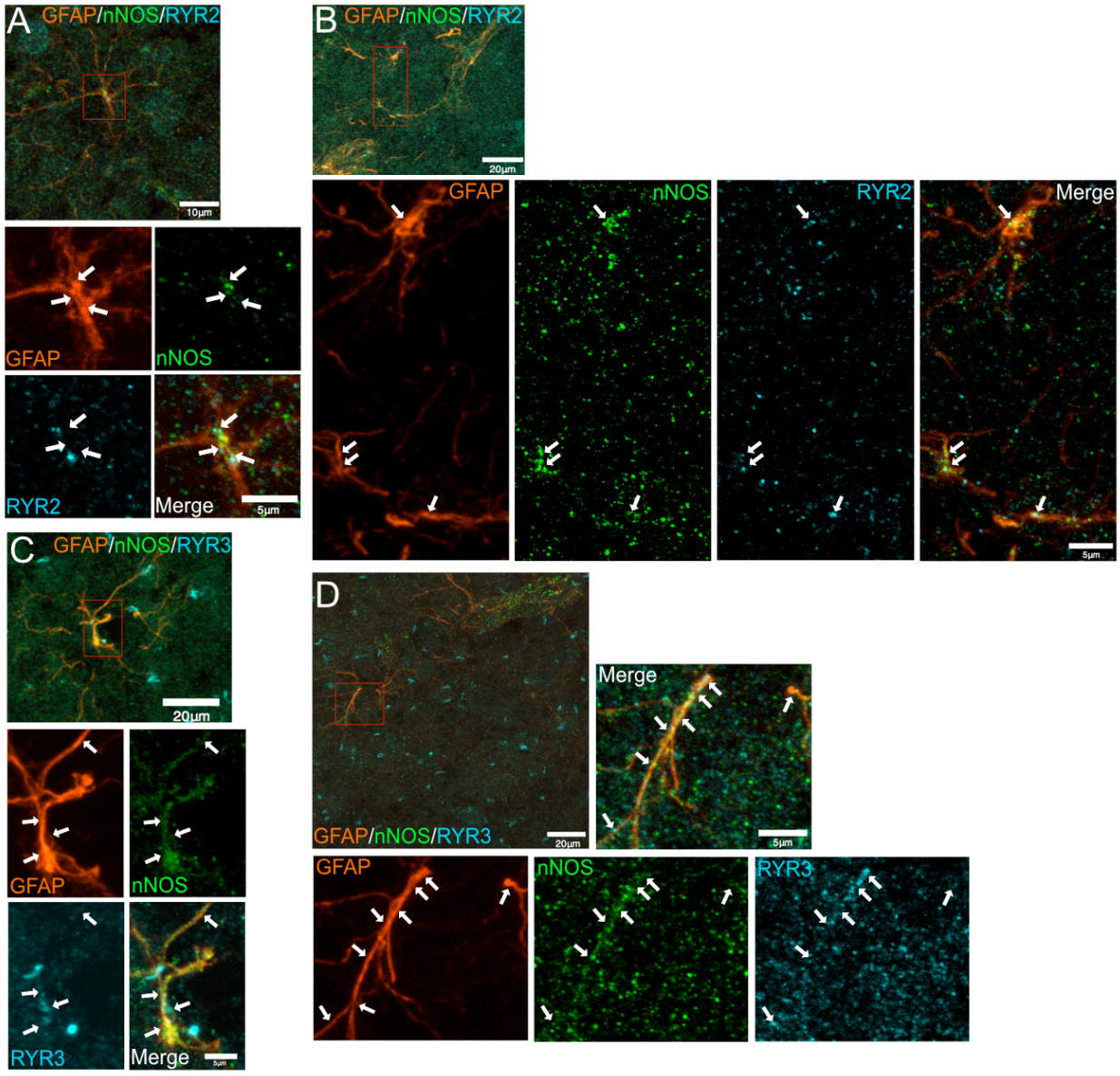

Figure 4-4 Colocalization between nNOS and RyR2 and 3 in astrocytes of the somatosensory cortex

Data of triple immunostaining depict that nNOS (green) not only colocalizes (white arrows) with RyR2 (cyan) in perineuronal (*A*) and perivascular astrocytes (*B*), but also colocalizes (white arrows) with RyR3 (cyan) in perineuronal (*C*) and perivascular astrocytes (*D*). GFAP (orange) is a marker of astrocyte. scale bar = 10 μm for *A*; scale bar = 20 μm for *B*, *C*, *D*; scale bar = 5 μm for higher magnification images.

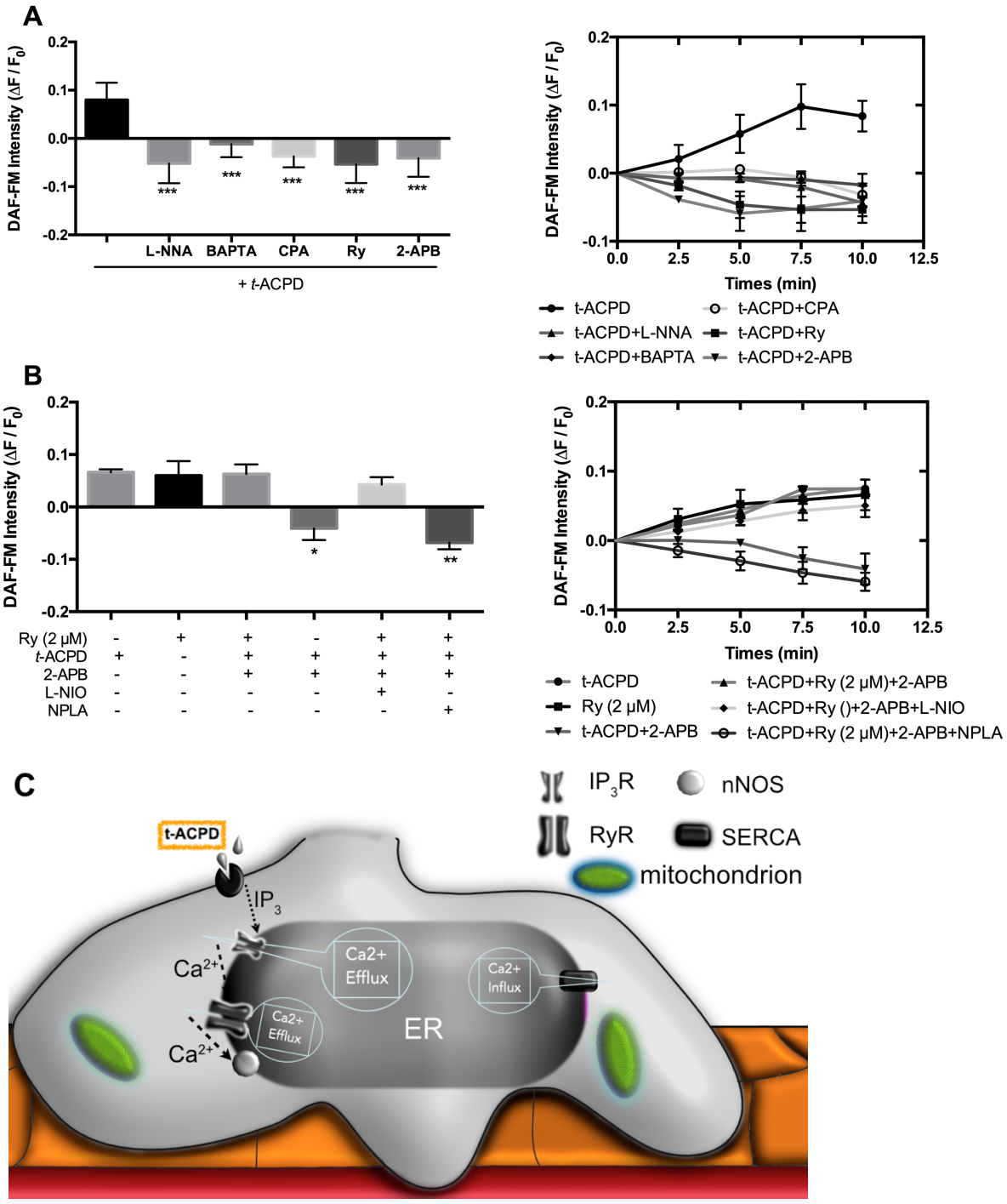

Figure 4-5 RyRs activation promotes nNOS activity and leads to an increase in NO

Figure 4-5. *A*, *t*-ACPD-induced (100 μM, 10 min) increase in NO was blocked by pre-treatment with L-NNA (NOS blocker, 100 μM, 15 min), BAPTA (Ca^{2+} chelator, 50 μM, 40 min), CPA (SERCA inhibitor, 30 μM, 20 min), ryanodine (Ry, a RyR inhibitor in 100 μM, 20 min), or 2-APB (IP_3R blocker, 100 μM, 15 min). n=4 WT mice, ***p<0.001 vs. *t*-ACPD group, one-way ANOVA with Bonferroni post-hoc test. *B*, Changes in NO intensity in response to *t*-ACPD (100 μM) in the presence of Ry in 2 μM (agonist of RyR), 10 μM L-NIO (20 min pretreatment, an eNOS inhibitor), NPLA (10 μM, 20 min pretreatment, a nNOS inhibitor). n=5 mice, *p<0.05, **p<0.01, n.s., not significant, one-way ANOVA with Bonferroni post-hoc test. Data are shown as mean ± S.E.M. *C*, A schematic diagram showing *t*-ACPD-elicited stimulation of IP_3Rs triggers RyRs via Ca^{2+}-induced Ca^{2+} release, which further activates adjacent nNOS in the ER, leading to an increase in endfoot NO.

CHAPTER 5

Associations between NMDA receptor and constitutive NOS in astrocytes

Introduction

Neuronal NMDA receptor (NMDAR) is an iGluR, mediating postsynaptic signal transmission. The intracellular domain of NMDAR via scaffolding PSD protein is functionally tethered to various kinases and enzymes, especially nNOS capable of producing NO in response to NMDAR activation. It has been discovered that the second PDZ motif of PSD-95 connects carboxyl terminus of NR2B subunit to a PDZ motif of N-terminal domain of nNOS, leading to the formation of the NMDAR/PSD-95/nNOS signalling cassette (Brenman et al., 1996b; Sattler et al., 1999). Investigations on astrocytic NMDAR have led to the discovery of multiple features that differ from neuronal NMDAR. First, NMDA receptors located in cortical astrocytes show a weak sensitivity to Mg^{2+}. Second, all subunits forming functional NMDA receptors have been identified in adult human astrocytes (Lee et al., 2010), but most astrocytic NMDA receptors in the cortex display low expression of NR2B and high densities of NR2C and NR2D, presenting a fairly low permeability to Ca^{2+}. Third, the classic co-agonists of NMDA receptor, glycine and D-serine, cannot potentiate the activation of NMDA receptors in cortical astrocytes (Palygin et al., 2011).

The primary function of astrocytic NMDA receptor is to induce an increase in intracellular Ca^{2+} via its ion channel, leading to the release of gliotransmitters such as glutamate and ATP. Notably, astrocytic NMDAR also displays metabotropic-like signalling, resulting in stimulation of NMDAR-coupled kinases and phosphatases as well as release of Ca^{2+} from ER (Marmiroli and Cavaletti, 2012; Jimenez-Blasco et al., 2015; Montes de Oca Balderas and Aguilera, 2015). We previously demonstrated that cortical astrocytes express eNOS and nNOS. However, the relationships between astrocytic NMDAR and constitutive NOS (eNOS and nNOS) had never been studied. We sought to identify the source of NO produced by activation of astrocytic NMDAR, and the anatomical relationship between NMDAR and constitutive NOS.

Results

NMDA induces NO increase through both eNOS and nNOS in astrocytes

In the presence of NMDA, intracellular NO intensity increased in cultured WT astrocytes (17.8 %) (Figure 5-1A). To understand the source of NO production induced by NMDA, we applied NMDA (40 μM) for 10 min to stimulate astrocyte cultures and astrocytic endfeet of WT,

eNOS$^{-/-}$ and nNOS$^{-/-}$ mice (n=3 pups/adult mice, *p < 0.05, **p < 0.01, ***p < 0.001), respectively (Figure 5-1A). Increased DAF-FM fluorescent intensity was significantly detected in both *in vitro* (16.8 % for eNOS$^{-/-}$ and 8.8 % for nNOS$^{-/-}$) and *ex vivo* preparations (16.9 % for WT, 11.2 % for eNOS$^{-/-}$, 12.3 % for nNOS$^{-/-}$), but was abolished by pre-treatment with the non-selective NOS inhibitor, L-NNA (100 μM, 15 min). NO production was lower in eNOS$^{-/-}$ and nNOS$^{-/-}$ mice compared to their control. Then NO production was further analysed by counting the number of hot spots and their maximal intensity (Figure 5-1B). Compared to WT mice, the total number and mean intensity of endfoot hot spots were both reduced significantly in eNOS$^{-/-}$ and nNOS$^{-/-}$ mice (*p<0.05, **p<0.01, one-way ANOVA with Bonferroni post-hoc test). Altogether, those data indicated that both eNOS- and nNOS contribute to the increase in intracellular NO evoked by NMDA.

Astrocytic NMDA receptor is functional coupled to nNOS via NR2B/PSD-95 complex

Neuronal NR2B subunit binds to PSD-95, a scaffolding protein tethering intracellular complexes, such as the NR2B/PSD-95/nNOS complex, which produces neuronal NO upon NMDAR activation (Sattler et al., 1999). To determine whether this complex is existed and functions in astrocytes, immunofluorescent labeling for NR2B, nNOS and GFAP was applied on brain slice preparations. As indicated in Figure 5-2A (white arrow), astrocytic NR2B colocalized with nNOS. Next, we used a peptide Tat to uncouple NR2B from PSD-95/nNOS proteins. The scrambled peptide S-Tat served as control. In Tat-treated group, NO production was significant lower (4.2 %) after 10-min exposure with NMDA (40 μM, n=3 mice, *p<0.05), compared to the scrambled S-Tat (10.0 %) (Figure 5-2B, not significant vs. 11.6 % of treatment with NMDA only). To investigate whether the NO increase is dependent on the NR2B subunit, slices were pretreated with Ro25-6981 (25 min). In the presence of Ro25-6981 (3 μM), the increase in NO induced by NMDA (40 μM) was attenuated (3.5 %) (n=3 mice, *p<0.05, **p<0.01). Collectively, our data suggest that NR2B-containing NMDAR was anatomically and functional coupled to nNOS via PSD-95 protein.

NR2B-containing NMDA receptor is compartmentalized within caveolae comprising both caveolin-1 and -3

Previous investigations in neurons showed that caveolin-1 (Cav-1) was essential for NMDAR-mediated signal transduction (Head et al., 2008). Surprisingly, our triple staining images in astrocytes revealed that NR2B-NMDARs colocalizes with Cav-1 and -3.

Discussion

Neuronal NMDAR-nNOS signalling has been investigated under both physiological and pathological conditions. However, little is known about the relationships between astrocytic NMDAR and eNOS/nNOS. Our findings provide several clues about astrocytic NMDAR: *i*) activation of NMDAR potentially induces both eNOS- and nNOS-derived NO production in astrocytes; *ii*) NR2B, a NMDAR subunit, is functionally coupled to nNOS in astrocytes via PSD-95 protein; *iii*) the NR2B subunit colocalized with caveolae membrane containing either Cav-1 or -3.

NO sources upon NMDA activation

Based on our results (Figure 5-1), an increase in NO was observed in $eNOS^{-/-}$ and $nNOS^{-/-}$. It indicates that both eNOS and nNOS are involved in NO production in response to NMDA. NMDA-nNOS pathway has been extensively demonstrated in many cell types such as neurons and kidney cells (Sattler et al., 1999; Tian et al., 2008). The NMDA-eNOS association had been shown in brain-derived endothelial cell, pyramidal neurons and A549 lung cancer cells (Kano et al., 1998; Scott et al., 2007; Li et al., 2011; LeMaistre et al., 2012). Those prior findings are consistent with our observations in astrocytes and suggest that these observations do not correspond to compensatory effects of the knockout.

NR2B/nNOS signalling in astrocytes

Seven subunits of NMDA receptor has been identified, including NR1, NR2A, NR2B, NR2C, NR2D, NR3A and NR3B. It is noteworthy that neuronal NR2B subunit is known to be linked to NO production via the PSD-95/nNOS complex. Our anatomical results showed low expression of astrocytic NR2B in the somatosensory cortex (Figure 5-2A and Figure 5-3),

relative to what had been demonstrated in neurons of the prefrontal cortex (Hu et al., 2010). Indeed, the transcription level of NR2B mRNA in astrocytes is much lower than other subunits, and only a small subpopulation of NMDARs in astrocytes is inhibited by selective NR2B antagonist (Lalo et al., 2006; Montes de Oca Balderas and Aguilera, 2015).

Like neurons, our study found that astrocytes express functional NR2B/PSD-95/nNOS complex (Sattler et al., 1999). In the presence of the specific NMDA-NR2B antagonist, Ro25-6981, less NO was produced in response to NMDA (Figure 5-2B). This pointed out the importance of NR2B in NMDA-induced NO production in astrocytes. In addition, the reduction of NO production by the Tat peptide suggest that nNOS is attached to the NR2B subunit through the PSD-95 protein. However, on the basis of the staining data (Figure 5-2A), not all nNOS were colocalized with NR2B. Indeed, our previous studies (Figure 4-3) showed colocalization between RyRs and nNOS in the astrocytic ER. Therefore, the immunostaining data indicated that astrocytic nNOS was localized in both plasma and the ER membranes.

NMDA/caveolin colocalization in astrocytes

Caveolae, 50–100 nm vesicular invaginations of the cell plasma membrane, have emerged as the site of the important events at the plasma membrane such as vesicular trafficking as well as signal transduction (Frank et al., 2001). We demonstrated that the colocalization between Cav-1 or -3 with NR2B in astrocytes of the somatosensory cortex. Neurons express Cav-1 and -3. Recent study of neuronal caveolins revealed that Cav-1 colocalizes with NMDAR to facilitate of Src and ERK1/2 phosphorylation in response to NMDA, hence contributing to NMDAR-mediated signalling (Head et al., 2008). The PSD-95 PDZ domains facilitate interactions between nNOS and the NMDA receptor, leading to S-nitrosylation of the NR1 and NR2A subunits of the NMDA receptor.

Furthermore, elevated NO partook in modulation of target proteins via S-nitrosylation (Wynia-Smith and Smith, 2017). This result, combined with the recent findings, suggest that the post-translational modulation of NMDAR-mediated signalling may occur and involve in two underlying mechanisms: Cav-1-assisted phosphorylation and NO-mediated S-nitrosylation.

Our prior findings detected that astrocytic eNOS colocalizes with Cav-1 and -3. Future studies are required to determine the possibility that NMDA-eNOS association may occur within these caveolin membrane domains.

NMDA-eNOS signaling in astrocytes

Although *ex vivo* preparations were stimulated by bath-application of NMDA, the NO increase in astrocytes could be potentially induced by factors such as ACh released from NMDA-activated neurons (Buchholzer and Klein, 2002) or gliotransmitters secreted from NMDA-activated astrocytes. Nonetheless, significant NO increases were observed in our purified astrocyte cultures (approximately 98 %), which rarely contained cell types other than astrocytes. Still, to obtain accurate data, eliminating action potential and preventing neurotransmitter exocytosis are necessary for a deeper understanding of the mechanisms. For instance, using tetrodotoxin and SNARE inhibitors such as tetanus toxin can achieve our goal.

In conclusion, the current study revealed that *i*) NR2B, a NMDAR subunit, colocalizes with caveolin -1 and -3 in the astrocytic membrane; *ii*) NR2B also colocalizes with astrocytic nNOS; *iii*) NMDA induces an increase in NO production in astrocytes by activation of both eNOS and nNOS; *iv*) astrocytes express functional complex of NR2B/PSD-95/nNOS. Such findings add more knowledge regarding the astrocytic NMDA receptor-mediated functions, which may help to better understand NMDA receptor-induced neuroprotection and toxicity under pathological conditions.

Figures

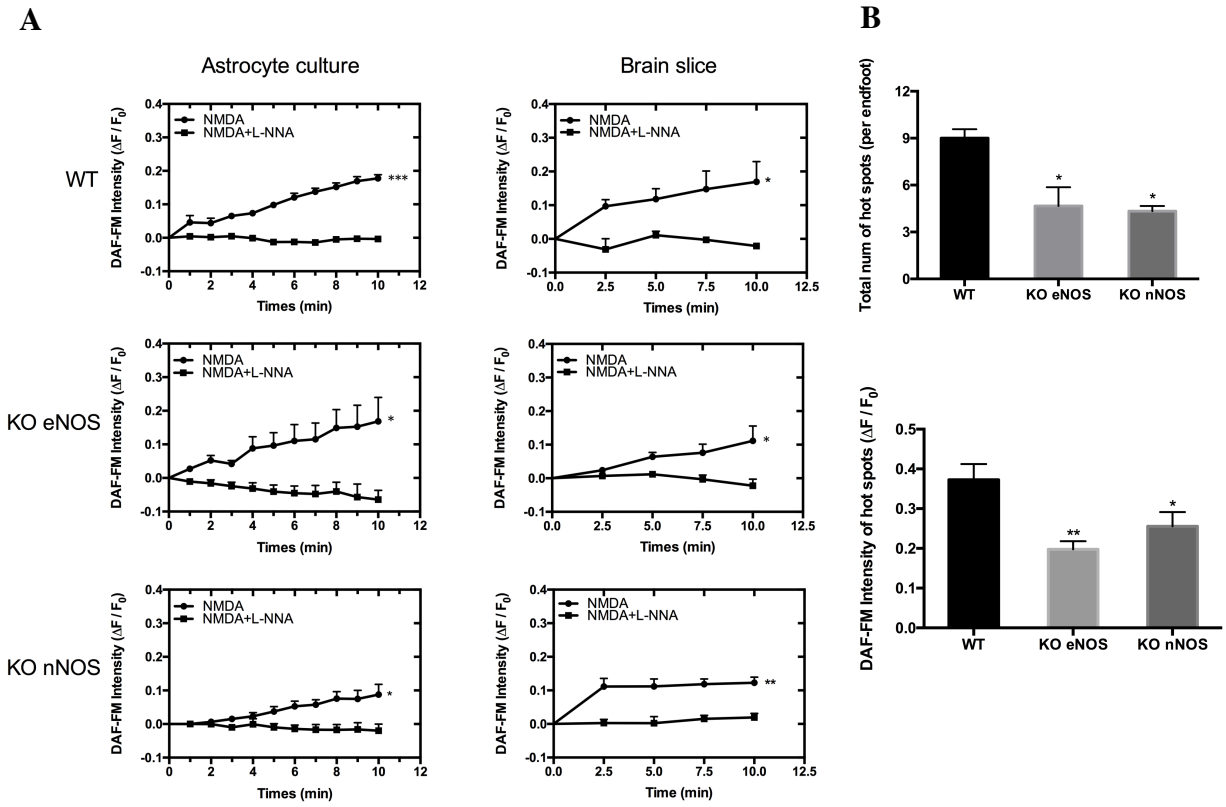

Figure 5-1 NMDA induced both eNOS and nNOS-dependent NO formation in cortical astrocytes

A. Time courses of changes in DAF-FM intensity after superfusion with 40 μM NMDA in WT, eNOS$^{-/-}$ and nNOS$^{-/-}$ astrocyte cultures and perivascular astrocytic endfeet in brain slices, respectively (n=3 pups/adult mice; *$p < 0.05$, **$p < 0.01$, ***$p < 0.001$; two-way ANOVA with Bonferroni post-hoc test). The increased response was prevented by pre-treatment with L-NNA (a non-selective NOS inhibitor, 100 μM, 15 min). Error bars indicate mean ± S.E.M. *B*. Summary of *ex vivo* data showing changes in the number and intensity of NO hot spots in astrocytic endfeet from WT, KO eNOS and KO nNOS mice (n=3 mice per group) respectively. In response to 10-min NMDA, patterns of hot spots including the total number and response strength were evidently reduced in perivascular astrocytic endfeet of knockout groups, compared with the WT group (*p<0.05, **p<0.01, one-way ANOVA with Bonferroni post-hoc test). The *in vitro* and *ex vivo* data of astrocytes suggest the activation of both eNOS and nNOS in response to NMDA.

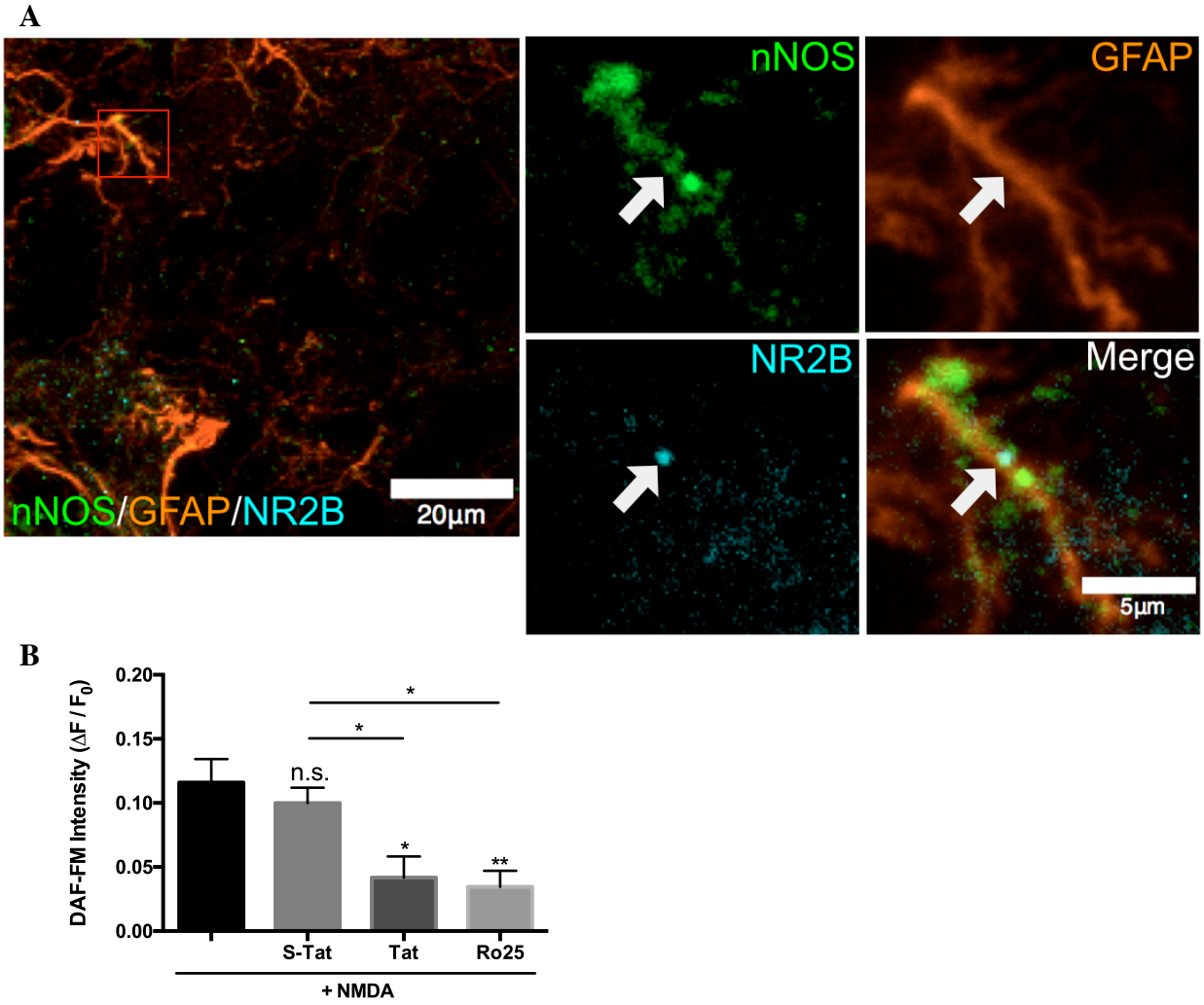

Figure 5-2 Colocalization of nNOS, NR2B and astrocytes in the somatosensory cortex

A. Images depict the colocalization (white arrows indicated) between nNOS (green) and NR2B (cyan, a NMDA receptor subunit) in astrocytes (orange, GFAP). scale bar = 20 µm for the left image; scale bar = 5 µm for higher magnification images. *B*. NMDA-induced (40 µM) increase in endfoot NO was attenuated by the NR2B-NMDA specific antagonist Ro25-6981 (25 min pretreatment with 3 µM,) or by breaking the linkage between NR2B and PSD-95/nNOS complex using the Tat a peptide (20 µM, 30 min pretreatment). The elevated response was unaffected by the control scrambled Tat (S-Tat, 20 µM, 30 min pretreatment) which has no effects on the PDZ-linking domain between NR2B and PSD-95/nNOS. n=3 mice; n.s., not significant, *p<0.05, **p<0.01, one-way ANOVA with Bonferroni post-hoc test.

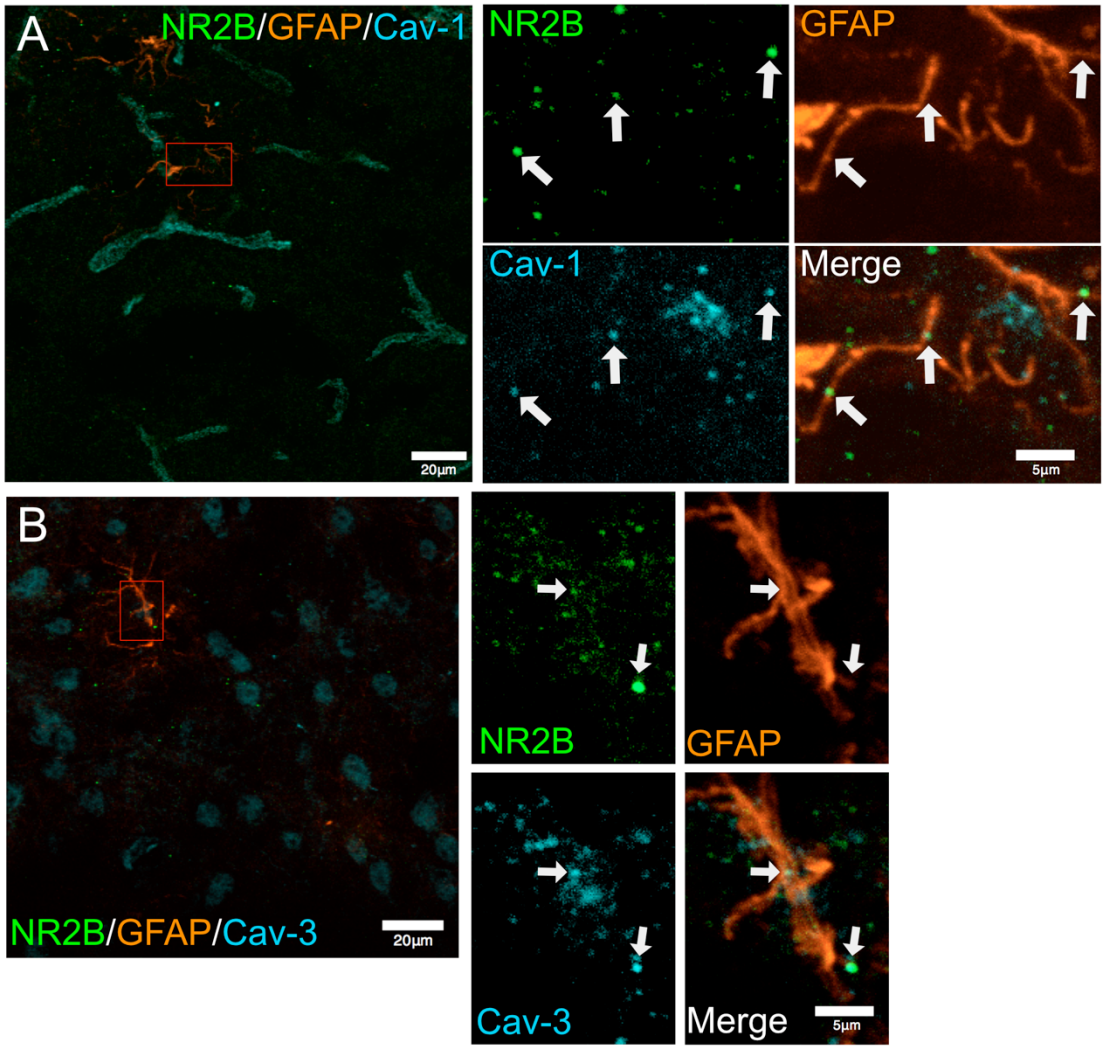

Figure 5-3 Colocalization of NR2B, caveolins and astrocytes in the somatosensory cortex

White arrows represent the colocalization between NR2B (green, a NMDA receptor subunit) and Caveolin (Cav)-1 or -3 (Cav-1 for *A* or Cav-3 for *B*, cyan) in astrocytes (orange, GFAP). scale bar = 20 μm for *A* and *B*; scale bar = 5 μm for higher magnification images.

CHAPTER 6

GENERAL DISCUSSION and PERSPECTIVES

To our knowledge, this is the first evidence that the two constitutive NOSs (eNOS and nNOS) co-exist in mouse cortical astrocytes and contribute to NO production in response to multiple neurotransmitters, including acetylcholine and distinct glutamate analogues. General associations between our results are further discussed in this section.

NO production monitoring

DAF-FM is a sensitive NO indicator for living cells and can detect NO at concentrations as low as 3 nM (Kojima et al., 1999). The fluorescence signal of DAF-FM is very low. Once reacted with NO, a covalent and stable DAF-FM/NO complex is formed and releases fluorescence at 515 nm wavelength for a quite long period. The fluorescent intensity begins to reduce at about 98 %, 63 % and 28 % after 1, 2 and 3 hours, respectively (Kojima et al., 1999). In addition, the laser seems to induce a certain level of photobleaching since there is a slight continuous decrease of fluorescence all along DAF-FM monitoring as demonstrated in our results. To prevent significant fluorescence quenching, each brain slice was excited less than 30 minutes under the confocal microscopy during the experiment. Theoretically, once attached to DAF-FM, NO could not perform biological functions so that we could not study NO biological effects while monitoring its production with this dye. However, the aim of our study is to evaluate the physiological capability of astrocytes to produce NO in response to distinct stimuli. Considering the properties that it cannot induce neurotoxic and does not react with reactive oxidative species, DAF-FM is an appropriate NO indicator in our studies compared to other fluorescent NO-indicators such as rhodamine fluorophore (for a review in (Sharma, 2012)).

Responses of astrocyte cultures

Purified astrocyte cultures were obtained from cortical layers of postnatal day 0 to day 3 mouse pups. Cultured astrocytes are immature cells, which may express receptors differently than in mature cells. This feature may blur identification of certain receptors in adult preparations. For example, mGluR5 expression decreases with age and turns to be undetectable in adult mice, while mGluR3 displays a stable expression in astrocytes at all developmental periods (Sun et al., 2013). Furthermore, unlike astrocyte *in situ*, isolated astrocyte does not live in the *in situ* environment and loses cellular polarization as well as original phenotype. Indeed, previous investigation observed changes in RNA transcription between *in vitro* and *in vivo*

models (Richey et al., 1987). However, response of pure *in vitro* preparations can exclude interference from other cell types such as neurons.

Analysis model of NO - hot spot

NO is a gaseous signal and diffuses rapidly and radially into surrounding areas of low NO concentrations. In astrocytes, it is likely that eNOS and nNOS exhibit compartmentalized expression in astrocytes. Therefore, NO production was analyzed in the form of hot spot. To be specific, the highest concentration of NO is in the core of one hot spot probably at the level of NOS localization. Thus, once activated, NOS generate NO in compartmentalized areas. Then, changes in hot spots were recorded and analyzed on the basis as $\Delta F/F_0 = (F_n - F_0) / F_0$, where F_n is the fluorescence intensity at frame n and F_0 is the baseline of DAF-FM intensity. Two parameters of hot spot were further calculated, the total number of new hot spots and mean intensity of those hot spots. Collectively, this analysis model ensures two aspects of our investigation: *i*) NO is exclusively generated inside astrocyte, and *ii*) compartmentalized production of NO.

The involvement of S-nitrosothiol pools in the NO production

S-nitrosothiol pools formed through NO-protein interaction are considered as intracellular NO storages, which can redistribute and release NO. SH-groups of cysteine residues are feasible to be either reversibly S-nitrosylated into SNO-groups or irreversibly oxidized and form disulfide bonds. To conduct the S-nitrosylation, only ionisable cysteines and cysteines in hydrophobic microenvironment are able to react with NO, S-nitrosoglutathione (GSNO) and N_2O_3, etc.

Up to date, nearly 100 proteins are identified as S-nitrosylation targets. Here I describe four important proteins that have previously been demonstrated to be important targets. *i*) NF-κB, which is predominantly activated under oxidative stress situations. Experimental studies revealed that NO targets its p50 subunit and cysteine 62 (Matthews et al., 1992; Hayashi et al., 1993). *ii*) Hypoxia-inducible factors (HIF), NO inhibits its activation in the early stage of hypoxia (Sogawa et al., 1998). *iii*) RyRs, NO regulates its channel activity via poly-S-nitrosylation (Xu et al., 1998). That is, low concentration of NO activates RyRs, while high level suppresses RyRs activity. This regulatory mechanism implies a tight NO-Ca^{2+} crosstalk in the

cell, since we found that RyRs are associated to specific activation of astrocytic nNOS. *iv*) eNOS and nNOS, which produce NO locally regulates themselves (Erwin et al., 2005; Erwin et al., 2006). Importantly, prior investigations discovered that subcellular compartmentalization is a key feature of S-nitrosylation. Certain proteins physically interact with eNOS or nNOS, such as mitochondrial procaspase-3 (Matsumoto et al., 2003), since local regulation of these compartmentalized proteins requires a high concentration of NO. Indeed, scientific studies found that eNOS-derived NO locally S-nitrosylates proteins at the Golgi apparatus, the site for post translational modulation (Iwakiri et al., 2006).

Under pathological conditions, iNOS-induced S-nitrosylation displays unlimited subcellular localization due to the high amount of NO produced by iNOS (Nathan and Shiloh, 2000). In addition, glutathione (GSH) is the most abundant thiols in the cell. It should be noted that GSNO formation consumes reduced GSH, resulting in redox-dependent signalling pathway and inducing nitrosative stress (Calabrese et al., 2003). Changes in oxidant/antioxidant balance is further associated with the neuropathological processes, such as Alzheimer's disease and stroke.

In the present studies, a NO increase in response to Ach in $eNOS^{-/-}$ mice was observed in brain slices but not in isolated astrocytes. However, the NO increase observed in brain slices was abolished when *ex vivo* preparations were pretreated with the thiol pool remover NEM. The data of hot spots indicate that these NO hot spots were released from S-nitrosothiols. These results suggest that NO coming from other cell types can participate in forming S-nitrosothiol pools in astrocytes. Though cellular thiol pools in vivo are quite few, most of them are large molecular mass (M_r > 5000), the NO released from which can bind to GSH and hence form GSNO (Liu et al., 2001). Chvanov et al. showed that approximately 3 μM thiol pools belong to the small molecular weight S-nitrosothiols, which are denitrosylated in response to ACh stimulation (Chvanov M et al., 2006). This reaction relies on calpain protein and is modulated by Ca^{2+} (Chvanov M et al., 2006). These findings suggest that fine regulation of NO production is executed at several levels and contributes to physiological and pathological processes.

The presence of cholinergic receptors in astrocytes

Immunological investigations have identified both mAChRs and nAChRs in protoplasmic astrocytes of the cerebral cortex *in situ*. Though endothelial cells (M2 and 5) and VSMCs (M1,

2, 3, and 5) express mAChRs (Elhusseiny et al., 1999), it is found that human astrocytes express all subgroups of mAChRs, M1 - 5 mAChRs (Elhusseiny et al., 1999; Shelton and McCarthy, 2000). Moreover, the expression of α7-containing nAChRs is extensively distributed in astrocytes, where it is involved in synaptic transmission (Pirttimaki et al., 2013). Altogether, this suggests that ACh is capable to activate both mAChRs and nAChRs in astrocytes and hence leading to an increase in NO. A further study is required to investigate which subtype of cholinergic receptor predominantly participates in this response.

mGluRs expression in astrocytes

Emerging studies has previously demonstrated that astrocytes express numerous mGluR5 in either immature or reactive status (Sun et al., 2013; Kim et al., 2016), while adult astrocytes express abundant mGluR3 and few mGluR2 and 5 (Sun et al., 2013; Wang et al., 2016; Copeland et al., 2017). mGluR4 and 8 were found on the reactive astrocytes localized around sclerosis lesions (Geurts et al., 2005). Therefore, it seems that the other mGluRs, including mGluR1, 4, 6, 7 and 8, are absent in mouse astrocytes under physiological states (Ferraguti et al., 2001; Sun et al., 2013).

Unlike mGluR5, which is functionally linked to PLC activity, leading to an increase in IP_3 and IP_3R-mediated Ca^{2+} efflux, activation of group II and III mGluRs decreases AC activity, which further inhibits downstream voltage-dependent Ca^{2+} channels and reduces NOS activity in astrocytes (Durand et al., 2010; Marmiroli and Cavaletti, 2012). Besides, activation of mGluR2 and mGluR3 decreases release of glutamate (Moghaddam and Adams, 1998). In our studies, *t*-ACPD, an agonist of group I and II mGluRs, was found to trigger a rise in NO in astrocytes. Furthermore, our results on isolated astrocytes strongly suggest that only astrocytic mGluR5 has the capacity for activating constitutive NOS and inducing NO production in response to *t*-ACPD stimulation. Though mGluR5 expression is fairly low in adult astrocytes, previous studies have not detected the subcellular distribution of mGluR5, which may display a polarized distribution at perivascular endfeet similar to AQP4, either (Cruz et al., 2013) or at the terminus of perineuronal processes (Ricci et al., 2009). A specific immunofluorescent staining of different astrocytic mGluRs in adult brain slices is necessary, especially in perivascular endfeet and close to synapses.

iGluRs-induced NO production

Superfusion with NMDA induced an increase in astrocyte NO from both eNOS and nNOS. Likewise, in the presence of AMPA, an increase in NO was observed in $eNOS^{-/-}$ and $nNOS^{-/-}$ astrocytes. These data imply that activation of iGluRs (NMDA or AMPA receptors) could elicit both eNOS- and nNOS-dependent NO in astrocytes. In fact, activation of iGluRs increases intracellular Ca^{2+} concentration, which could further activate Ca^{2+}-dependent constitutive NOS (eNOS and nNOS). In the present work, we found that astrocytic NMDA receptor was functionally associated with nNOS and eNOS. This could be attributed to either an increase in intracellular Ca^{2+} or a metabotropic-like effect. Indeed, previous studies found that astrocytic NMDA receptor functioned in a Ca^{2+} flux-independent manner via multiple proteins such as nNOS coupled to the NMDA receptor intracellular domain (Montes de Oca Balderas and Aguilera, 2015).

A similar underlying mechanism may exist for AMPA receptor, which contains PDZ domains interacting with kinases (e.g. CaMKII, PKC and PKA) and has the capacity to elevate of intracellular Ca^{2+} level (for a review in (Henley and Wilkinson, 2013)). Thus, exposure to AMPA activates nNOS and contributes to the formation of reactive nitrogen species (RNS) in neurons (Joshi et al., 2015). Increased NO, in turn, can upregulate AMPA receptor subunits by either NO-induced S-nitrosylation or NO/cGMP signalling pathway (Huang et al., 2005). In addition, phosphorylation of nNOS at the S1412 regulates AMPA receptor trafficking via NO (Rameau et al., 2007). However, suppression of AMPA receptors was found to lead to upregulation of nNOS expression (Baader and Schilling, 1996). These regulatory mechanisms indicate a bidirectional coupling between AMPA receptor and nNOS and may provide a basis of understanding roles of astrocytic eNOS/nNOS upon AMPA stimulation.

NO effects on Ca^{2+} signalling

All agonist that triggered NO production in the present studies have the capacity to induce an increase in intracellular Ca^{2+}. Thus, a rise in NO could serve to prolong Ca^{2+} signalling effects via cGMP- and RyR-mediated pathways (Willmott et al., 2000). NO can also upregulate the release of ATP and glutamate from astrocytes and neurons (McNaught and Brown, 1998; Bal-Price et al., 2002). Thus, NO-mediated release of ATP and glutamate can, in turn, induce and

amplify the Ca^{2+} increases in astrocytes and neighboring cells, such as neurons, VSMCs and endothelial cells, which express purinergic and glutamatergic receptors (Krizbai et al., 1998; Eltzschig et al., 2006; Taurin et al., 2008). This leads to a potential NO generation and a long lasting Ca^{2+} response to mGluRs activation (Pasti et al., 1995). Altogether, these results indicate the existence of crosstalk between Ca^{2+} and NO in these cells, and suggest that a mechanism by which local neuronal activity synchronizes and controls ambient microenvironment in the brain. It is noteworthy that in astrocytes NO is able to mediate cytokine-enhanced release of glutamate and inhibit glutamate uptake, contributing to the considerably extracellular glutamate levels and neuronal death (Ida et al., 2008).

The role of NO in NVC

Many research groups that have specifically inhibited eNOS and nNOS to assess the roles in the NVC response to NO found that NO acts as a vasodilator probably derived from endothelial cells and neurons, respectively (Ignarro et al., 1987; Rungta and Charpak, 2016). Indeed, Mishra et al. concluded that arteriole vasodilation in the cortex is likely mediated by neuron-derived NO, which may affect diverse targets such as membrane channels and signalling pathways (Mishra et al., 2016). However, little is known about the capacity of astrocytic endfeet to produce NO and the role of astrocyte-derived NO in NVC. To bridge this biological gap, we conducted experiments in isolated and *ex vivo* astrocytes. Our study showed that astrocytes produce NO upon distinct cholinergic and glutamatergic stimulations.

This present work sheds a new light on the map of CBF regulation and enriches theoretical basis of NVC. In response to neuronal activity, astrocyte-derived NO is a potential signalling molecule involving in CBF regulation in the brain. NO contributions to vasodilation targets multiple proteins. Diffused NO activates soluble GC and results in an increase in cGMP, which further attenuates contraction of VSMCs through a cGMP-dependent pathway (Lau et al., 1998; Bolz et al., 2003). NO also decreases CYP 4A ω-hydroxylase activity to suppress generation of the vascular constrictor 20-HETE (Sun et al., 1998; Oyekan et al., 1999; Mulligan and MacVicar, 2004). Furthermore, NO could S-nitrosylate protein cysteines by means of the post-translational modulation to enhance vasodilatory effect. Experimental evidence shows that both vascular K_{ATP} channels (Thomas and Victor, 1997) and RyRs reversibly interact with NO by S-

nitrosylation to attenuate vasoconstriction (Stoyanovsky et al., 1997; Xu et al., 1998). In addition to regulation of vasodilation, endothelium-derived NO affects astrocytic metabolism reversibly in the nanomolar concentration range by depleting intracellular glucose and producing lactate (Martín et al., 2017).

The interaction between NO and neurons

Neurons such as pyramidal neurons in the hippocampus can express not only nNOS but eNOS, (O'dell et al., 1994; Tricoire and Vitalis, 2012). Endogenous NO play crucial roles in modulation of neuronal plasticity mainly through two pathways, one is dependent on cGMP-mediated cascades such as modulation of ion channels (Erdemli and Krnjević, 1995; Zulazmi et al., 2017) and neuronal receptors (Cabrera-Pastor et al., 2016); and the other is dependent on nitrosylation (Dejanovic and Schwarz, 2014) and RNS-induced (Banerjee et al., 2015) signalling pathways independently of cGMP, such as facilitation of axon pruning (Rabinovich et al., 2016).

In the early developing neurons, NO can regulate neuronal transcription by control of the CREB DNA binding (Riccio et al., 2006). Under physiological conditions, NO influences synaptic transmission and promotes synaptic plasticity. For instance, hippocampal long-term potentiation is modulated by NO/cGMP signalling via control of L-type voltage-gated Ca^{2+} channels opening (Pigott and Garthwaite, 2016). Besides, NO can regulate neuron-released neurotransmitters such as GABA (Tarasenko et al., 2014) and ACh (Prast et al., 1994). Notably, NO exhibits a biphasic effect on glutamate release. It can either facilitate the learning process via inducing glutamate release from hippocampal dentate gyrus neurons (Wang et al., 2014) or directly inhibit synaptic secretion of glutamate (Kamisaki et al., 1995). Considering that ACh and glutamate analogues induced an increase in astrocytic NO in our experiments, a tight interplay between astrocytes and neurons via complex coupling mechanisms most probably involve NO. However, NO acts as a neuronal stressor if high NO concentrations are available.

On the other hand, our electron microscopy data revealed that both astrocytic eNOS and nNOS display preferential distribution in astrocytic processes but not endfeet. Since astrocytic cNOS expression locates closer to areas of stimulation rather than areas of effect, it suggests three functional roles: *i*) astrocyte-derived NO may play more important roles in maintaining and modulating neuronal plasticity; *ii*) the fewer cNOS in endfeet is capable to produce enough

NO to participate in local CBF regulation; *iii*) higher densities of cNOS located in astrocytic processes can produce NO at high concentrations which may not only be available to have impacts on ambient neuronal compartments but also can reach to and have effects on neighboring vessels.

Taken together, these findings point out that NO is an important modulator of neuronal functions via cGMP-dependent and -independent pathways. Astrocyte-derived NO can further assist and contribute to a fine-tuned modulation of physiological and pathological processes in neurons.

Clinical application

NO is implicated in pathological processes, such as NMDAR-mediated toxicity, astrocyte death and convulsive action (Aarts et al., 2002; Durand et al., 2010; Javadian et al., 2016). Animal experimental studies discovered that NOS inhibitors such as L-NNA and 7-nitroindazole exhibit pro- and anticonvulsive properties in seizure models (Javadian et al., 2016). However, alternation of expression of the eNOS and nNOS proteins is inconsistent under pathological conditions. For example, the total level of eNOS in the frontal cortex of schizophrenia mice was found to be reduced, whereas no changes were found in nNOS protein expression (Liu et al., 2016). On the contrary, astrocytic eNOS was markedly upregulated in the brain of patients with sporadic AD (Lüth et al., 2001). These findings add complexity to the understanding of the roles of eNOS and nNOS in the brain, and also imply that both eNOS and nNOS may partake in different stages of pathological processes.

Knowing the presence of eNOS and nNOS in astrocytes and their interactions with glutamatergic receptors increases our awareness about many potential side effects of drugs acting on these pathways. For example, NA-1, a PSD-95 inhibitor under the Phase III clinical trial, perturbs the connection between neuronal NR2B and PSD-95/nNOS complex and reduces stroke damage (Cook et al., 2012). This novel drug acts as a neuroprotectant and is promising for treatment of acute ischemic stroke. In the present *ex vivo* study on astrocytic NMDAR, the PSD-95 inhibitor decreased NMDA-induced increase in endfoot NO. It would be interesting to understand the contribution of astrocytic nNOS in the effect of treatment with the PSD-95 inhibitor affects astrocytic-derived NO after stroke and the pathophysiological consequences.

Perspective

To extend our present works in this dissertation, the following investigations are planned in the future.

1) To understand the biological effects of astrocytic eNOS and nNOS separately, specific deletion or inhibition of astrocytic eNOS and/or nNOS is required, especially for the study of its contributions to NVC. Astrocytic specific deletion of caveolins or other NOS-associated proteins would also give further insight on the specific regulatory mechanisms of NO production.

2) To further demonstrate spatial coupling between astrocytic eNOS and cholinergic neurons, multiple types of neurons should be considered, such as dopamine neurons, glutamatergic neurons and GABAergic neurons. It would also be interesting to specifically activate cholinergic neurons and to study its biological effects (ex: vascular tone) while astrocytic eNOS is specifically inhibited or not. Moreover, we will identify and further activate astrocytic cholinergic receptors and transporters in astrocytes.

3) To better understand response of astrocyte-derived NO, neuronal-released active factors should be excluded using tetrodotoxin and SNARE inhibitors. This would eliminate action potentials and inhibit formation of vesicle containing factors (e.g. glutamate) respectively.

4) To further identify the anatomical and functional link between NMDA receptor and eNOS in astrocytes.

CHAPTER 7

GENERAL CONCLUSIONS

In this dissertation, we identified polarized subcellular distribution and colocalization of eNOS and nNOS in astrocytes, and demonstrated possible signalling pathway that evoke eNOS- and nNOS-dependent NO production. The following discoveries are concluded from the present work in detail:

1) Astrocytes *in situ* expressed eNOS and nNOS. Astrocytic processes contained higher density of both eNOS and nNOS in comparison to astrocytic endfeet.
2) eNOS expression in astrocytes was compartmentalized with caveolin-1 and -3. In astrocytes, eNOS-dependent NO was produced upon cholinergic stimulation.
3) The nNOS density was found to be less in the plasma membrane. Thus, a portion of nNOS was colocalized with RyR2 and RyR3, and another portion was colocalized with NMDAR in astrocytic plasma membrane via NR2B/PSD-95 complex.
4) *t*-ACPD evoked NO production which is entirely nNOS-dependent while other glutamatergic agonists were eliciting both eNOS and nNOS dependent NO production.
5) *t*-ACPD induced NO production from astrocytes is dependent on RyR-mediated Ca^{2+} influx signalling, which was possibly activated by IP3R-mediated Ca^{2+} via Ca^{2+}-induced Ca^{2+} release.
6) Astrocytic membrane nNOS was functionally coupled to the NR2B/PSD-95 complex. In addition, astrocytic NR2B was colocalized with caveolin-1 and caveolin-3, suggesting a potential link between NR2B-containing NMDAR and eNOS.

Therefore, our findings suggest that astrocytes produce eNOS- and nNOS-derived NO in response to cholinergic and glutamatergic stimulations. This increased endfoot NO may further have an impact on adjacent vascular response and contribute to neurovascular coupling.

REFERENCES

Aarts M, Liu Y, Liu L, Besshoh S, Arundine M, Gurd JM, Wang YT, Salter MW, Tymianski M (2002) Treatment of Ischemic Brain Damage by Perturbing NMDA Receptor–PSD-95 Protein Interactions. Science 298:846-851.

Achour SB, Pont-Lezica L, Béchade C, Pascual O (2010) Is astrocyte calcium signaling relevant for synaptic plasticity? Neuron glia biology 6:147-155.

Adachi M, Abe M, Sasaki T, Kato H, Kasahara J, Araki T (2010) Role of inducible or neuronal nitric oxide synthase in neurogenesis of the dentate gyrus in aged mice. Metabolic brain disease 25:419-424.

Agarwal A, Wu P-H, Hughes EG, Fukaya M, Tischfield MA, Langseth AJ, Wirtz D, Bergles DE (2017) Permeability Transition Pore Induces Microdomain Calcium Transients in Astrocyte Processes. Neuron 93:587-605.

Ahmed SM, Rzigalinski BA, Willoughby KA, Sitterding HA, Ellis EF (2000) Stretch-Induced Injury Alters Mitochondrial Membrane Potential and Cellular ATP in Cultured Astrocytes and Neurons. Journal of Neurochemistry 74:1951-1960.

Alloisio S, Cugnoli C, Ferroni S, Nobile M (2004) Differential modulation of ATP-induced calcium signalling by A1 and A2 adenosine receptors in cultured cortical astrocytes. British journal of pharmacology 141:935-942.

Amador FJ, Stathopulos PB, Enomoto M, Ikura M (2013) Ryanodine receptor calcium release channels: lessons from structure-function studies. FEBS J 280:5456-5470.

Antoni SD, Ranno E, Spatuzza M, Cavallaro S, Catania MV (2017) Endothelin-1 Induces Degeneration of Cultured Motor Neurons Through a Mechanism Mediated by Nitric Oxide and PI3K/Akt Pathway. Neurotox Res.

Aronica E, Gorter JA, Rozemuller AJ, Yankaya B, Troost D (2015) Activation of metabotropic glutamate receptor 3 enhances interleukin (IL)-1β-stimulated release of IL-6 in cultured human astrocytes. Neuroscience 130:927-933.

Aronica E, Van Vliet EA, Mayboroda OA, Troost D, Da Silva FHL, Gorter JA (2000) Upregulation of metabotropic glutamate receptor subtype mGluR3 and mGluR5 in reactive astrocytes in a rat model of mesial temporal lobe epilepsy. European Journal of Neuroscience 12:2333-2344.

Aronica E, Gorter JA, Ijlst‐Keizers H, Rozemuller AJ, Yankaya B, Leenstra S, Troost D (2003) Expression and functional role of mGluR3 and mGluR5 in human astrocytes and glioma cells: opposite regulation of glutamate transporter proteins. European Journal of Neuroscience 17:2106-2118.

Baader SL, Schilling K (1996) Glutamate Receptors Mediate Dynamic Regulation of Nitric Oxide Synthase Expression in Cerebellar Granule Cells. J Neurosci 16:1440-1449.

Babich LH, Shlykov SH, Kandaurova NV, Kosterin SA (2010) Transmembrane Ca2+ exchange in depolarized rat myometrium mitochondria. Ukrains' kyi biokhimichnyi zhurnal (1999) 83:56-62.

Babu YS, Sack JS, Greenhough TJ, Bugg CE, Means AR, Cook WJ (1985) Three-dimensional structure of calmodulin. Nature 315:37-40.

Badaut J, Ajao DO, Sorensen DW, Fukuda AM, Pellerin L (2015) Caveolin expression changes in the neurovascular unit after juvenile traumatic brain injury: signs of blood-brain barrier healing? Neuroscience 285:215-226.

Bal-Price A, Moneer Z, Brown GC (2002) Nitric Oxide Induces Rapid, Calcium- Dependent Release of Vesicular Glutamate and ATP From Cultured Rat Astrocytes. Glia 40:312-323.

Banerjee S, Melnyk SB, Krager KJ, Aykin-Burns N, Letzig LG, James LP, Hinson JA (2015) The neuronal nitric oxide synthase inhibitor NANT blocks acetaminophen toxicity and protein nitration in freshly isolated hepatocytes. Free Radical Biology and Medicine 89:750-757.

Barouch LA, Harrison RW, Skaf MW, Rosas GO (2002) Nitric oxide regulates the heart by spatial confinement of nitric oxide synthase isoforms. Nature 416:337.

Barry DS, Pakan JMP, McDermott KW (2014) Radial glial cells: key organisers in CNS development. The international journal of biochemistry & cell biology 46:76-79 %@ 1357-2725.

Bazargani N, Attwell D (2016) Astrocyte calcium signaling: the third wave. Nature neuroscience.

Bolz SS, Vogel L, Sollinger D, Derwand R, de Wit C, Loirand G, Pohl U (2003) Nitric oxide-induced decrease in calcium sensitivity of resistance arteries is attributable to activation of the myosin light chain phosphatase and antagonized by the RhoA/Rho kinase pathway. Circulation 107:3081-3087.

Bonder DE, McCarthy KD (2014) Astrocytic Gq-GPCR-Linked IP3R-Dependent Ca2 Signaling Does Not Mediate Neurovascular Coupling in Mouse Visual Cortex In Vivo. Journal of Neuroscience 34:13139-13150.

Bootman MD, Collins TJ, MacKenzie L, Roderick HL, Berridge MJ, Peppiatt CM (2002) 2-aminoethoxydiphenyl borate (2-APB) is a reliable blocker of store-operated Ca2+ entry but an inconsistent inhibitor of InsP3-induced Ca2+ release. The FASEB Journal 16:1145-1150.

Borea PA, Varani K, Vincenzi F, Baraldi PG, Tabrizi MA, Merighi S, Gessi S (2015) The A3 Adenosine Receptor: History and Perspectives. Pharmacological Reviews 67:74-102.

Bradley S, Challiss R (2011) Defining protein kinase/phosphatase isoenzymic regulation of mGlu5 receptor‐stimulated phospholipase C and Ca2+ responses in astrocytes. British journal of pharmacology 164:755-771.

Brancaccio M, Patton AP, Chesham JE, Maywood ES, Hastings MH (2017) Astrocytes Control Circadian Timekeeping in the Suprachiasmatic Nucleus via Glutamatergic Signaling. Neuron 93:1420-1435.

Brenman JE, Christopherson KS, Craven SE, McGee AW, Bredt DS (1996a) Cloning and characterization of postsynaptic density 93, a nitric oxide synthase interacting protein. Journal of Neuroscience 16:7407-7415.

Brenman JE, Xia H, Chao DS, Black SM, Bredt DS (1997) Regulation of Neuronal Nitric Oxide Synthase through Alternative Transcripts. Developmental Neuroscience 19:224-231.

Brenman JE, Chao DS, Gee SH, McGee AW, Craven SE, Santillano DR, Wu Z, Huang F, Xia H, Peters MF (1996b) Interaction of nitric oxide synthase with the postsynaptic density protein PSD-95 and α1-syntrophin mediated by PDZ domains. Cell 84:757-767.
Brophy CM, Whiteley EG, Lamb S, Beall A (1997) Cellular mechanisms of cyclic nucleotide-induced vasorelaxation. Journal of Vascular Surgery 25:390-397.
Brown AM, Ransom BR (2007) Astrocyte glycogen and brain energy metabolism. Glia 55:1263-1271 %@ 1098-1136.
Buchholzer M-L, Klein J (2002) NMDA-induced acetylcholine release in mouse striatum: role of NO synthase isoforms. Journal of Neurochemistry 82:1558-1560.
Buizza L, Cenini G, Lanni C, Ferrari-Toninelli G, Prandelli C, Govoni S, Buoso E, Racchi M, Barcikowska M, Styczynska M, Szybinska A, Butterfield DA, Memo M, Uberti D (2012) Conformational Altered p53 as an Early Marker of Oxidative Stress in Alzheimer's Disease. PloS one 7.
Bulotta S, Cerullo A, Barsacchi R, De Palma C, Rotiroti D, Clementi E, Borgese N (2006) Endothelial nitric oxide synthase is segregated from caveolin-1 and localizes to the leading edge of migrating cells. Experimental cell research 312:877-889.
Burda JE, Sofroniew MV (2014) Reactive gliosis and the multicellular response to CNS damage and disease. Neuron 81:229-248 %@ 0896-6273.
Burkard N, Rokita AG, Kaufmann SG, Hallhuber M, Wu R, Hu K, Hofmann U, Bonz A, Frantz S, Cartwright EJ (2007) Conditional neuronal nitric oxide synthase overexpression impairs myocardial contractility. Circulation research 100:e32-e44.
Burnley-Hall N, Willis G, Davis J, Rees DA, James PE (2017) Nitrite-derived nitric oxide reduces hypoxia-inducible factor 1a-mediated extracellular vesicle production by endothelial cells. Nitrc Oxide 63:1-12.
Bushong EA, Martone ME, Jones YZ, Ellisman MH (2002) Protoplasmic astrocytes in CA1 stratum radiatum occupy separate anatomical domains. Journal of Neuroscience 22:183-192.
Butts DA, Weng C, Jin J, Yeh C-I, Lesica NA, Alonso J-M, Stanley GB (2007) Temporal precision in the neural code and the timescales of natural vision. Nature 449:92-95.
Cabrera-Pastor A, Malaguarnera M, Taoro-Gonzalez L, Llansola M, Felipo V (2016) Extracellular cGMP Modulates Learning Biphasically by Modulating Glycine Receptors, CaMKII and Glutamate-Nitric Oxide-cGMP Pathway. Scientific Reports 6.
Calabrese V, Scapagnini G, Ravagna A, Bella R, Butterfield DA, Calvani M, Pennisi G, Stella AMG (2003) Disruption of Thiol Homeostasis and Nitrosative Stress in the Cerebrospinal Fluid of Patients with Active Multiple Sclerosis: Evidence for a Protective Role of Acetylcarnitine. Neurochemical research 28:1321-1328.
Cameron PL, Ruffin JW, Bollag R, Rasmussen H, Cameron RS (1997) Identification of caveolin and caveolin-related proteins in the brain. Journal of Neuroscience 17:9520-9535.
Chang PKY, Verbich D, McKinney RA (2012) AMPA receptors as drug targets in neurological disease–advantages, caveats, and future outlook. European Journal of Neuroscience 35:1908-1916.

Chen N, Sugihara H, Sharma J, Perea G, Petravicz J, Le C, Sur M (2012) Nucleus basalis-enabled stimulus-specific plasticity in the visual cortex is mediated by astrocytes. Proceedings of the National Academy of Sciences 109:E2832-E2841 %@ 0027-8424.

Chiarella P, Puglisi R, Sorrentino V, Boitani C, Stefanini M (2004) Ryanodine receptors are expressed and functionally active in mouse spermatogenic cells and their inhibition interferes with spermatogonial differentiation. Journal of Cell Science 117:4127-4134.

Chisari M, Scuderi A, Ciranna L, Volsi GL, Licata F, Sortino MA (2016) Purinergic P2Y1 Receptors Control Rapid Expression of Plasma Membrane Processes in Hippocampal Astrocytes. Mol Neurobiol.

Choi YK, Kim J-H, Lee D-K, Lee K-S, Won M-H, Jeoung D, Lee H, Ha K-S, Kwon Y-G, Kim Y-M (2016) Carbon monoxide potentiation of L-type Ca2+ channel activity increases HIF-1α-independent VEGF expression via an AMPKα/SIRT1-mediated PGC-1α/ERRα axis. Antioxidants & Redox Signaling %@ 1523-0864.

Christopherson KS, Hillier BJ, Lim WA, Bredt DS (1999) PSD-95 Assembles a Ternary Complex with theN-Methyl-D-aspartic Acid Receptor and a Bivalent Neuronal NO Synthase PDZ Domain. Journal of Biological Chemistry 274:27467-27473.

Chu LW, Ma ESK, Lam KKY, Chan MF, Lee DHS (2005) Increased Alpha 7 Nicotinic Acetylcholine Receptor Protein Levels in Alzheimer's Disease Patients. Dementia and Geriatric Cognitive Disorders 19:106-112.

Chvanov M, Gerasimenko OV, Petersen OH, Tepikin A (2006) Calcium-dependent release of NO from intracellular S-nitrosothiols. The EMBO Journal 25:3024-3032.

Ciccarelli R, D'Alimonte I, Ballerini P, D'Auro M, Nargi E, Buccella S, Di lorio P, Bruno V, Ferdinando N, Caciagli F (2007) Molecular Signalling Mediating the Protective Effect of A1 Adenosine and mGlu3 Metabotropic Glutamate Receptor Activation against Apoptosis by Oxygen/Glucose Deprivation in Cultured Astrocytes. Mol Pharmacol 71:1369-1380.

Clarke LE, Barres BA (2013) Emerging roles of astrocytes in neural circuit development. Nature Reviews Neuroscience 14:311-321 %@ 1471-1003X.

Cook DJ, Teves L, Tymianski M (2012) Treatment of stroke with a PSD-95 inhibitor in the gyrencephalic primate brain. Nature 483:213-217.

Copeland CS, Wall TM, Sims RE, Neale SA, Nisenbaum E, Parri HR, Salt TE (2017) Astrocytes modulate thalamic sensory processing via mGlu2 receptor activation. Neuropharmacology.

Crepel V, Mulle C (2015) Physiopathology of kainate receptors in epilepsy. Curr Opin Pharmacol 20:83-88.

Croft W, Dobson KL, Bellamy TC (2015) Plasticity of Neuron-Glial Transmission: Equipping Glia for Long-Term Integration of Network Activity. Neural Plasticity 2015.

Cruz NF, Ball KK, Froehner SC, Adams ME, Dienel GA (2013) Regional registration of [6-14C] glucose metabolism during brain activation of α-syntrophin knockout mice. Journal of neurochemistry 125:247-259.

Dajas-Bailador F, Wonnacott S (2004) Nicotinic acetylcholine receptors and the regulation of neuronal signalling. Trends in pharmacological sciences 25:317-324.

Daneman R, Prat A (2015) The blood–brain barrier. Cold Spring Harbor perspectives in biology 7:a020412 %@ 021943-020264.
Danson EJ, Choate JK, Paterson DJ (2005) Cardiac nitric oxide: emerging role for nNOS in regulating physiological function. Pharmacology & therapeutics 106:57-74.
Dedkova EN, Blatter LA (2009) Characteristics and function of cardiac mitochondrial nitric oxide synthase. The Journal of physiology 587:851-872.
Dejanovic B, Schwarz G (2014) Neuronal nitric oxide synthase-dependent S-nitrosylation of gephyrin regulates gephyrin clustering at GABAergic synapses. Journal of Neuroscience 34:7763-7768.
Dineley KT, Pandya AA, Yakel JL (2015) nicotinic ACh receptors as therapeutic targets in CNS disorders. Trends in Pharmacological Science 36:96-108.
Diniz LP, Almeida JC, Tortelli V, Lopes CV, Setti-Perdigão P, Stipursky J, Kahn SA, Romão LF, de Miranda J, Alves-Leon SV (2012) Astrocyte-induced synaptogenesis is mediated by transforming growth factor β signaling through modulation of D-serine levels in cerebral cortex neurons. Journal of Biological Chemistry 287:41432-41445 %@ 40021-49258.
Droste D, Seifert G, Seddar L, Jadtke O, Steinhauser C, Lohr C (2017) Ca2+-permeable AMPA receptors in mouse olfactory bulb astrocytes. Sci Rep 7:44817.
Drumm BT, Large RJ, Hollywood MA, Thornbury KD, Baker SA, Harvey BJ, McHale NG, Sergeant GP (2015) The role of Ca2+ influx in spontaneous Ca2+ wave propagation in interstitial cells of Cajal from the rabbit urethra. The Journal of physiology 593:3333-3350.
Dunn. K M, C H-ED, Liedtke WB, Nelson MT (2013) TRPV4 channels stimulate Ca2+-induced Ca2+ release in astrocytic endfeet and amplify neurovascular coupling responses. PNAS 110:6157-6162.
Dupont G, Lokenye EFL, Challiss RAJ (2011) A model for Ca 2+ oscillations stimulated by the type 5 metabotropic glutamate receptor: an unusual mechanism based on repetitive, reversible phosphorylation of the receptor. Biochimie 93:2132-2138 %@ 0300-9084.
Durand D, Caruso C, Carniglia L, Lasaga M (2010) Metabotropic glutamate receptor 3 activation prevents nitric oxide‐induced death in cultured rat astrocytes. Journal of neurochemistry 112:420-433.
Durand D, Carniglia L, Caruso C, Lasaga M (2011) Reduced cAMP, Akt activation and p65-c-Rel dimerization: mechanisms involved in the protective effects of mGluR3 agonists in cultured astrocytes. PloS one 6:e22235.
Dzamba D, Honsa P, Valny M, Kriska J, Valihrach L, Novosadova V, Kubista M, Anderova M (2015) Quantitative analysis of glutamate receptors in glial cells from the cortex of GFAP/EGFP mice following ischemia injury: Focus on NMDA receptors. Cell Mol Neurobiol 35:1187-1202.
Earley S, Heppner TJ, Nelson MT, Brayden JE (2005) TRPV4 Forms a Novel Ca2+ Signaling Complex With Ryanodine Receptors and BKCa Channels. Circ Res 97:1270-1279.
Elfering SL, Sarkela TM, Giulivi C (2002) Biochemistry of mitochondrial nitric-oxide synthase. Journal of Biological Chemistry 277:38079-38086.

Elhusseiny A, Cohen Z, Olivier A, Stanimirović DB, Hamel E (1999) Functional acetylcholine muscarinic receptor subtypes in human brain microcirculation: identification and cellular localization. Journal of Cerebral Blood Flow & Metabolism 19:794-802.

Eltzschig HK, Eckle T, Mager A, Küper N, Karcher C, Weissmüller T, Boengler K, Schulz R, Robson SC, Colgan SP (2006) ATP release from activated neutrophils occurs via connexin 43 and modulates adenosine-dependent endothelial cell function. Circulation Research 99:1100-1108.

Erdemli G, Krnjević K (1995) Nitric oxide tonically depresses a voltage-and Ca-dependent outward current in hippocampal slices. Neuroscience letters 201:57-60.

Erwin PA, Lin AJ, Golan DE, Michel T (2005) Receptor-regulated dynamic S-nitrosylation of endothelial nitric-oxide synthase in vascular endothelial cells. Journal of Biological Chemistry 280:19888-19894.

Erwin PA, Mitchell DA, Sartoretto J, Marletta MA, Michel T (2006) Subcellular targeting and differential S-nitrosylation of endothelial nitric-oxide synthase. Journal of Biological Chemistry 281:151-157.

Fasano C, Thibault D, Trudeau LE (2008) Culture of postnatal mesencephalic dopamine neurons on an astrocyte monolayer. Current protocols in neuroscience / editorial board, Jacqueline N Crawley [et al] Chapter 3:Unit 3 21.

Feoli AM, Leite MC, Tramontina AC, Tramontina F, Posser T, Rodrigues L, Swarowsky A, Quincozes-Santos A, Leal RB, Gottfried C (2008) Developmental changes in content of glial marker proteins in rats exposed to protein malnutrition. Brain research 1187:33-41.

Feron O, Han X, Kelly RA (1999) Muscarinic cholinergic signaling in cardiac myocytes: dynamic targeting of M2AChR to sarcolemmal caveolae and eNOS activation. Life sciences 64:471-477.

Feron O, Smith TW, Michel T, Kelly RA (1997) Dynamic targeting of the agonist-stimulated m2 muscarinic acetylcholine receptor to caveolae in cardiac myocytes. The Journal of Biological Chemistry 272:17744-17748.

Feron O, Belhassen L, Kobzik L, Smith TW, Kelly RA, Michel T (1996) Endothelial nitric oxide synthase targeting to caveolae specific interactions with caveolin isoforms in cardiac myocytes and endothelial cells. Journal of Biological Chemistry 271:22810-22814.

Feron O, Dessy C, Opel DJ, Arstall MA, Kelly RA, Michel T (1998) Modulation of the endothelial nitric-oxide synthase-caveolin interaction in cardiac myocytes Implications for the autonomic regulation of heart rate. Journal of Biological Chemistry 273:30249-30254.

Ferraguti F, Corti C, Valerio E, Mion S, Xuereb J (2001) Activated astrocytes in areas of kainate-induced neuronal injury upregulate the expression of the metabotropic glutamate receptors 2/3 and 5. Experimental brain research 137:1-11.

Figueroa XF, Lillo MA, Gaete PS, Riquelme MA, Saez JC (2013) Diffusion of nitric oxide across cell membranes of the vascular wall requires specific connexin-based channels. Neuropharmacology 75:471-478.

Foley J, Blutstein T, Lee SY, Erneux C, Halassa MM, Haydon P (2017) Astrocytic IP3/Ca2+ Signaling Modulates Theta Rhythm and REM Sleep. Frontiers in Neural Circuits 11.

Förster D, Reiser G (2016) Nucleotides protect rat brain astrocytes against hydrogen peroxide toxicity and induce antioxidant defense via P2Y receptors. Neurochem Int 94:57-66.
Frank PG, Galbiati F, Volonte D, Razani B, Cohen DE, Marcel YL, Lisanti MP (2001) Influence of caveolin-1 on cellular cholesterol efflux mediated by high-density lipoproteins. American Journal of Physiology-Cell Physiology 280:C1204-C1214.
Frick A, Zieglgansberger W, Dodt H (2001) Glutamate Receptors Form Hot Spots on Apical Dendrites of Neocortical Pyramidal Neurons. J Neurophysiol 86:1412-1421.
Gabbott P, Bacon S (1996) Localisation of NADPH diaphorase activity and NOS immunoreactivity in astroglia in normal adult rat brain. Brain research 714:135-144.
Gafni J, Munsch JA, Lam TH, Catlin MC, Costa LG, Molinski TF, Pessah IN (1997) Xestospongins: Potent Membrane Permeable Blockers of the Inositol 1,4,5-Trisphosphate Receptor. Neuron 19:723-733.
García-Cardeña G, Fan R, Stern DF, Liu J, Sessa WC (1996) Endothelial nitric oxide synthase is regulated by tyrosine phosphorylation and interacts with caveolin-1. Journal of Biological Chemistry 271:27237-27240.
Gebremedhin D, Zhang DX, Carver KA, Rau N, Rarick KR, Roman RJ, Harder DR (2016) Expression of CYP 4A ω-hydroxylase and formation of 20-hydroxyeicosatetreanoic acid (20-HETE) in cultured rat brain astrocytes. Prostaglandins and Other Lipid Mediators 124:16-26.
Geurts J, Wolswijk G, Bö L, Redeker S, Ramkema M, Troost D, Aronica E (2005) Expression patterns of Group III metabotropic glutamate receptors mGluR4 and mGluR8 in multiple sclerosis lesions. Journal of neuroimmunology 158:182-190.
Giaume C, Naus CC (2013) Connexins, gap junctions, and glia. Wiley Interdisciplinary Reviews: Membrane Transport and Signaling 2:133-142.
Girouard H, Bonev AD, Hannah RM, Meredith A, Aldrich RW, Nelson MT (2010) Astrocytic endfoot Ca2+ and BK channels determine both arteriolar dilation and constriction. Proceedings of the National Academy of Sciences of the United States of America 107:3811-3816.
Girouard H, Wang G, Gallo EF, Anrather J, Zhou P, Pickel VM, Iadecola C (2009) NMDA Receptor Activation Increases Free Radical Production through Nitric Oxide and NOX2. J Neurosci 29:2545-2552.
Gonzalez-Suarez AD, Nash AI, Garcia-Olivares J, Torres-Salazar D (2017) Emerging Evidence for a Direct Link between EAAT-Associated Anion Channels and Neurological Disorders. Journal of Neuroscience 37:241-243 %@ 0270-6474.
Granja MG, Braga LEG, Carpi-Santos R, de Araujo-Martins L, Nunes-Tavares N, Calaza KC, dos Santos AA, Giestal-de-Araujo E (2015) IL-4 Induces Cholinergic Differentiation of Retinal Cells In Vitro. Cell Mol Neurobiol 35:689-701.
Griffith CM, Xie M-X, Qiu W-Y, Sharp AA, Ma C, Pan A, Yan X-X, Patrylo PR (2016) Aberrant expression of the pore-forming K ATP channel subunit Kir6. 2 in hippocampal reactive astrocytes in the 3xTg-AD mouse model and human Alzheimer's disease. Neuroscience 336:81-101 %@ 0306-4522.
Guizzetti M, Moore NH, VanDeMark KL, Giordano G, Costa LG (2011) Muscarinic receptor-activated signal transduction pathways involved in the neuritogenic effect of

astrocytes in hippocampal neurons. European journal of pharmacology 659:102-107 %@ 0014-2999.
Haak LL, Heller HC, van den Pol AN (1997) Metabotropic Glutamate Receptor Activation Modulates Kainate and Serotonin Calcium Response in Astrocytes. J Neurosci 17:1825-1837.
Haglerød C, Hussain S, Nakamura Y, Xia J, Haug FM, Ottersen OP, Henley JM, Davanger S (2017) Presynaptic PICK1 facilitates trafficking of AMPA-receptors between active zone and synaptic vesicle pool. Neuroscience %@ 0306-4522.
Hansson E, Muyderman H, Leonova J, Allansson L, Sinclair J, Blomstrand F, Thorlin T, Nilsson M, Rönnbäck L (2000) Astroglia and glutamate in physiology and pathology: aspects on glutamate transport, glutamate-induced cell swelling and gap- junction communication. neurochemistry International 37:317-329.
Harris JJ, Jolivet R, Attwell D (2012) Synaptic energy use and supply. Neuron 75:762-777 %@ 0896-6273.
Hassanpoor H, Fallah A, Raza M (2014) Mechanisms of hippocampal astrocytes mediation of spatial memory and theta rhythm by gliotransmitters and growth factors. Cell Biology International 38:1355-1366.
Hatton GI, Parpura V (2004) Glial⇔ Neuronal Signaling: Springer Science & Business Media.
Hayashi T, Ueno Y, Okamoto T (1993) Oxidoreductive regulation of nuclear factor kappa B. Involvement of a cellular reducing catalyst thioredoxin. Journal of Biological Chemistry 268:11380-11388.
Head BP, Patel HH, Tsutsumi YM, Hu Y, Mejia T, Mora RC, Insel PA, Roth D, M, Drummond J, C, Patel P, M (2008) Caveolin-1 expression is essential for N-methyl-D- aspartate receptor-mediated Src and extracellular signal-regulated kinase 1/2 activation and protection of primary neurons from ischemic cell death. The FASEB Journal 22:828-840.
Hecker M, Mülsch A, Bassenge E, Förstermann U, Busse R (1994) Subcellular localization and characterization of nitric oxide synthase (s) in endothelial cells: physiological implications. Biochemical Journal 299:247-252.
Henley JM, Wilkinson KA (2013) AMPA receptor trafficking and the mechanisms underlying synaptic plasticity and cognitive aging. Dialogues in Clinical Neuroscience 15:11-27.
Herrera M, Hong NJ, Garvin JL (2006) Aquaporin-1 transports NO across cell membranes. Hypertension 48:157-164.
Hirase H, Iwai Y, Takata N, Shinohara Y, Mishima T (2014) Volume transmission signalling via astrocytes. Philos Trans R Soc Lond B Biol Sci 369:20130604.
Hirayama Y, Koizumi S (2017) Hypoxia-Independent Mechanisms of HIF-1α Expression in Astrocytes after Ischemic Preconditioning. Glia 65:523-530.
Hoft S, Griemsmann S, Seifert G, Steinhauser C (2014) Heterogeneity in expression of functional ionotropic glutamate and GABA receptors in astrocytes across brain regions: insights from the thalamus. Philos Trans R Soc Lond B Biol Sci 369:20130602.
Hu J, L, Liu G, Li Y, C, Gao WJ, Huang YQ (2010) Dopamine D1 receptor-mediated NMDA receptor insertion depends on Fyn but not Src kinase pathway in prefrontal cortical neurons. Molecular Brain 3.

Huang Y, Thathiah A (2015) Regulation of neuronal communication by G protein-coupled receptors. FEBS Lett 589:1607-1619.
Huang Y, Man H-Y, Sekine-Aizawa Y, Han Y, Juluri K, Luo H, Cheah J, Lowenstein C, Huganir RL, Snyder SH (2005) S-nitrosylation of N-ethylmaleimide sensitive factor mediates surface expression of AMPA receptors. Neuron 46:533-540.
Ida T, Hara M, Nakamura Y, Kozaki s, Tsunoda S, Ihara H (2008) Cytokine-induced enhancement of calcium-dependent glutamate release from astrocytes mediated by nitric oxide. Neuroscience letters 432:232-236.
Ignarro LJ, Buga GM, Wood KS, Byrns RE, Chaudhuri G (1987) Endothelium-derived relaxing factor produced and released from artery and vein is nitric oxide. Proceedings of the National Academy of Sciences 84:9265-9269.
Ikezu T, Ueda H, Trapp BD, Nishiyama K, Sha JF, Volonte D, Galbiati F, Byrd AL, Bassell G, Serizawa H (1998) Affinity-purification and characterization of caveolins from the brain: differential expression of caveolin-1,-2, and-3 in brain endothelial and astroglial cell types. Brain research 804:177-192.
Ito H, Hashimoto A, Matsumoto Y, Yao H, Miyakoda G (2010) Cilostazol, a phosphodiesterase inhibitor, attenuates photothrombotic focal ischemic brain injury in hypertensive rats. Journal of cerebral blood flow and metabolism : official journal of the International Society of Cerebral Blood Flow and Metabolism 30:343-351.
Iwakiri Y, Satoh A, Chartterjee S, Toomre DK, Chalouni CM, Fulton D, Groszmann RJ, Shah VH, Sessa WC (2006) Nitric oxide synthase generates nitric oxide locally to regulate compartmentalized protein S-nitrosylation and protein trafficking. PNAS 103:19777-19782.
Iwase K, Miyanaka K, Shimizu A, Nagasaki A, Gotoh T, Mori M, Takiguchi M (2000) Induction of endothelial nitric-oxide synthase in rat brain astrocytes by systemic lipopolysaccharide treatment. Journal of Biological Chemistry 275:11929-11933.
Jackson JG, Robinson MB (2015) Reciprocal Regulation of Mitochondrial Dynamics and Calcium Signaling in Astrocyte Processes. J Neurosci 35:15199-15213.
Javadian N, Rahimi N, Javadi-Paydar M, Doustimotlagh AH, Dehpour AR (2016) The modulatory effect of nitric oxide in pro-and anti-convulsive effects of vasopressin in PTZ-induced seizures threshold in mice. Epilepsy research 126:134-140.
Ji M, Miao Y, Dong L-D, Chen J, Mo X-F, Jiang S-X, Sun X-H, Yang X-L, Wang Z (2012) Group I mGluR-Mediated Inhibition of Kir Channels Contributes to Retinal Müller Cell Gliosis in a Rat Chronic Ocular Hypertension Model. The Journal of Neuroscience 32:12744-12755.
Jian Z, Han H, Zhang T, Puglisi J, Izu LT, Shaw JA, Onofiok E, Erickson JR, Chen Y-J, Horvath B (2014) Mechanochemotransduction during cardiomyocyte contraction is mediated by localized nitric oxide signaling. Science signaling 7:ra27.
Jimenez-Blasco D, Santofimia-Castano P, Gonzalez A, Almeida A, Bolanos JP (2015) Astrocyte NMDA receptors' activity sustains neuronal survival through a Cdk5-Nrf2 pathway. Cell Death Differ 22:1877-1889.

Johenning F, Theis A, Pannasch U, Rückl M, Rüdiger S, D S (2015) Ryanodine Receptor Activation Induces Long- Term Plasticity of Spine Calcium Dynamics. POLS Biology 13:e1002181.

Joshi DC, Tewari BP, Singh M, Joshi PG, B JN (2015) AMPA receptor activation causes preferential mitochondrial Ca2+ load and oxidative stress in motor neurons. Brain Research 1616:1-9.

Kai Y. Xu DLH, Ted M. Dawson, David S. Bredt, Lewis C. Becker (1999) Nitric oxide synthase in cardiac sarcoplasmic reticulum. Proceedings of the National Academy of Sciences of the United States of America 96:657-662.

Kaja S, Payne AJ, Patel KR, Naumchuk Y, Koulen P (2015) Differential subcellular Ca2+ signaling in a highly specialized subpopulation of astrocytes. Exp Neurol 265:59-68.

Kalashnyk O, Lykhmus O, Oliinyk O, Komisarenko S, Skok M (2014) α7 Nicotinic acetylcholine receptor-specific antibody stimulates interleukin-6 production in human astrocytes through p38-dependent pathway. international Immunopharmacology 23:475-479.

Kamatsuka Y, Fukagawa M, Furuta T, Ohishi A, Nishida K, Nagasawa K (2014) Astrocytes, but Not Neurons, Exhibit Constitutive Activation of P2X7 Receptors in Mouse Acute Cortical Slices under Non-stimulated Resting Conditions. Biol Pharm Bull 37:1958-1962.

Kamisaki Y, Wada K, Nakamoto K, Itoh T (1995) Nitric oxide inhibition of the depolarization-evoked glutamate release from synaptosomes of rat cerebellum. Neuroscience letters 194:5-8.

Kamynina AV, Holmström KM, Koroev DO, Volpina OM, Abramov AY (2013) Acetylcholine and antibodies against the acetylcholine receptor protect neurons and astrocytes against beta-amyloid toxicity. The international journal of biochemistry & cell biology 45:899-907 %@ 1357-2725.

Kandel ER, Schwartz JH, Jessell TM, Siegelbaum SA, Hudspeth AJ (2000) Principles of neural science: McGraw-hill New York.

Kano T, Shimizu-Sasamata M, Huang P, Moskowitz M, Lo E (1998) Effects of nitric oxide synthase gene knockout on neurotransmitter release in vivo. Neuroscience 86:695-699.

Kesherwani V, Agrawal SK (2012) Upregulation of RyR2 in hypoxic/reperfusion injury. J Neurotrauma 29:1255-1265.

Kim SS, Hayashi H, Ishikawa T, Shibata K, Shigetomi E, Shinozaki Y, Inada H, Roh SE, Kim SJ, Lee G, Bae H, Moorhouse AJ, Mikoshiba K, Fukazawa Y, Koizumi S, Nabekura J (2016) Cortical astrocytes rewire somatosensory cortical circuits for peripheral neuropathic pain. J Clin Invest 126.

Kim W, Kim SK, Nabekura J (2017) Functional and structural plasticity in the primary somatosensory cortex associated with chronic pain. Journal of Neurochemistry.

Kleinbongard P, Schulz R, Rassaf T, Lauer T, Dejam A, Jax T, Kumara I, Gharini P, Kabanova S, Özüyaman B (2006) Red blood cells express a functional endothelial nitric oxide synthase. Blood 107:2943-2951.

Kojima H, Urano Y, Kikuchi K, Higuchi T, Hirata Y, Nagano T (1999) Fluorescent Indicators for Imaging Nitric Oxide Production. Angew Chem Int Ed 38:3209-3212.

Konietzko U, Müller CM (1994) Astrocytic dye coupling in rat hippocampus: topography, developmental onset, and modulation by protein kinase C. Hippocampus 4:297-306.
Kovacs GG, Zsembery A, Anderson SJ, Komlosi P, gillespie GY, Bell PD, Benos DJ, Fuller CM (2005) Changes in intracellular Ca2 and pH in response to thapsigargin in human glioblastoma cells and normal astrocytes. AM J Physiol Cell Physiol 289:C361-371.
Krieg T, Philipp S, Cui L, Dostmann WR, Downey JM, Cohen MV (2005) Peptide blockers of PKG inhibit ROS generation by acetylcholine and bradykinin in cardiomyocytes but fail to block protection in the whole heart. American journal of physiology Heart and circulatory physiology 288:H1976-1981.
Krizbai IA, Deli MA, Pestenácz A, Siklós L, Szabó CA, András I, Joó F (1998) Expression of glutamate receptors on cultured cerebral endothelial cells. Journal of neuroscience research 54:814-819.
Kumar R, Jangir DK, Garima V, Shekhar S, Hanpude P, Kumar S, Kumari R, Singh N, Bhavesh NS, Jana NR, Maiti TK (2017) S-nitrosylation of UCHL1 induces its structural instability and promotes α-synuclein aggregation. Sci Rep 7.
Kushnir A, Betzenhauser M, Marks AR (2010) Ryanodine Receptor Studies Using Genetically Engineered Mice. FEBS Lett 584:1956-1965.
Lalo U, Pankratov Y, Kirchhoff F, North RA, Verkhratsky A (2006) NMDA Receptors Mediate Neuron-to-Glia Signaling in Mouse Cortical Astrocytes. The Journal of Neuroscience 26:2673-2683.
Larpthaveesarp A, Ferriero DM, Gonzalez FF (2015) Growth factors for the treatment of ischemic brain injury (growth factor treatment). Brain sciences 5:165-177.
Lau KS, Grange RW, Chang W-J, Kamm KE, Sarelius I, Stull JT (1998) Skeletal muscle contractions stimulate cGMP formation and attenuate vascular smooth muscle myosin phosphorylation via nitric oxide. FASEB Letters 431:71-74.
Lavialle M, Aumann G, Anlauf E, Pröls F, Arpin M, Derouiche A (2011) Structural plasticity of perisynaptic astrocyte processes involves ezrin and metabotropic glutamate receptors. PNAS 108:12915-12919.
Lee JH, Lee J, Choi KY, Hepp R, Lee J-Y, Lim MK, Chatani-Hinze M, Roche PA, Kim DG, Ahn YS (2008) Calmodulin dynamically regulates the trafficking of the metabotropic glutamate receptor mGluR5. Proceedings of the National Academy of Sciences 105:12575-12580.
Lee M-C, Ting KK, Adams S, Brew BJ, Chung R, Guillemin GJ (2010) Characterisation of the Expression of NMDA Receptors in Human Astrocytes. PloS one 5:e14123.
Lee MR, Li L, Kitazawa T (1997) Cyclic GMP Causes Ca2+ Desensitization in Vascular Smooth Muscle by Activating the Myosin Light Chain Phosphatase. J Biol Chem 272:5063-5068.
LeMaistre JL, Sanders SA, Stobart MJ, Lu L, Knox JD, Anderson HD, Anderson CM (2012) Coactivation of NMDA receptors by glutamate and D-serine induces dilation of isolated middle cerebral arteries. Journal of Cerebral Blood Flow & Metabolism 32:537-547.
Lewis JE, Ebling FJP (2017) Tanycytes as regulators of seasonal cycles in neuroendocrine function. Frontiers in Neurology 8:79 %@ 1664-2295.

Li L, Shen L, She H, Yue S, Feng D, Luo Z (2011) Nitric oxide-induced activation of NF–κB-mediated NMDA-induced CTP: phosphocholine cytidylyltransferase alpha expression inhibition in A549 cells. Cell biology and toxicology 27:41-47.
Li N, Sul JY, Haydon PG (2003) A calcium-induced calcium influx factor, nitric oxide, modulates the refilling of calcium stores in astrocytes. Journal of Neuroscience 23:10302-10310.
Li NZ, Sul JY, Haydon P (2003) A Calcium-Induced Calcium Influx Factor, Nitric Oxide, Modulates the Refilling of Calcium Stores in Astrocytes. J Neurosci 23:10302-10310.
Liu L, Hausladen A, Zeng M, Que L, Heitman J, Stamler JS (2001) A metabolic enzyme for ƒ-nitrosothiol conserved from bacteria to humans. Nature 410:490-494.
Liu P, Jing Y, Collie ND, Dean B, Bilkey DK, Zhang H (2016) Altered brain arginine metabolism in schizophrenia. Transl Psychiatry 6:e871.
Liu VWT, Huang PL (2008) Cardiovascular roles of nitric oxide: A review of insights from nitric oxide synthase gene disrupted mice. Cardiovascular research 77:19-29.
Liu X, Zhang Z, Guo W, Burnstock G, He C, Xiang Z (2013) The superficial glia limitans of mouse and monkey brain and spinal cord. The Anatomical Record 296:995-1007.
Lüth HJ, Holzer M, Gärtner U, Staufenbiel M, Arendt T (2001) Expression of endothelial and inducible NOS-isoforms is increased in Alzheimer's disease, in APP23 transgenic mice and after experimental brain lesion in rat: evidence for an induction by amyloid pathology. Brain Research 913:57-67.
MacVicar BA, Newman EA (2015) Astrocyte regulation of blood flow in the brain. Cold Spring Harb Perspect Biol 7.
Magistretti PJ, Allaman I (2015) A cellular perspective on brain energy metabolism and functional imaging. Neuron 86:883-901.
Maneshi MM, Maki B, Gnanasambandam R, Belin S, Popescu GK, Sachs F, Hua SZ (2017) Mechanical stress activates NMDA receptors in the absence of agonists. Scientific Reports 7 %@ 2045-2322.
Márkus NM, Hasel P, Qiu J, Bell KFS, Heron S, Kind PC, Dando O, Simpson TI, Hardingham GE (2016) Expression of mRNA encoding Mcu and other mitochondrial calcium regulatory genes depends on cell type, neuronal subtype, and Ca 2+ signaling. PloS one 11:e0148164 %@ 0141932-0146203.
Marmiroli P, Cavaletti G (2012) The Glutamatergic Neurotransmission in the Central Nervous System. Current Medicinal Chemistry 19:1269-1276.
Márquez-Rosado L, Solan JL, Dunn CA, Norris RP, Lampe PD (2012) Connexin43 phosphorylation in brain, cardiac, endothelial and epithelial tissues. Biochimica et Biophysica Acta (BBA)-Biomembranes 1818:1985-1992.
Martín A, S, Arce-Molina R, Galaz A, Pérez-Guerra G, Barros LF (2017) Nanomolar nitric oxide concentrations quickly and reversibly modulate astrocytic energy metabolism. Journal of Biological Chemistry 292:9432-9438.
Massion PB, Feron O, Dessy C, Balligand J-L (2003) Nitric oxide and cardiac function. Circulation research 93:388-398.

Massion PB, Pelat M, Belge C, Balligand JL (2005) Regulation of the mammalian heart function by nitric oxide. Comparative biochemistry and physiology Part A, Molecular & integrative physiology 142:144-150.
Massion PB, Dessy C, Desjardins F, Pelat M, Havaux X, Belge C, Moulin P, Guiot Y, Feron O, Janssens S, Balligand J-L (2004) Cardiomyocyte-Restricted Overexpression of Endothelial Nitric Oxide Synthase (NOS3) Attenuates -Adrenergic Stimulation and Reinforces Vagal Inhibition of Cardiac Contraction. Circulation 110:2666-2672.
Matos M, Shen H-Y, Augusto E, Wang Y, Wei CJ, Wang YT, Agostinho P, Boison D, Cunha RA, Chen J-F (2015) Deletion of adenosine A 2A receptors from astrocytes disrupts glutamate homeostasis leading to psychomotor and cognitive impairment: relevance to schizophrenia. Biological psychiatry 78:763-774 %@ 0006-3223.
Matschke V, Theiss C, Hollmann M, Schulze-Bahr E, Lang F, Seebohm G, Strutz-Seebohm N (2015) NDRG2 phosphorylation provides negative feedback for SGK1-dependent regulation of a kainate receptor in astrocytes. Front Cell Neurosci 9:387.
Matsumoto A, Comatas KE, Liu L, Stamler JS (2003) Screening for nitric oxide-dependent protein-protein interactions. Science 301:657-661.
Matthews JR, Wakasugi N, Virelizier J-L, Yodoi J, Hay RT (1992) Thiordoxin regulates the DNA binding activity of NF-χB by reduction of a disulphid bond involving cysteine 62. Nucleic acids research 20:3821-3830.
Matyash M, Matyash V, Nolte C, Sorrentino V, Kettenmann H (2001) Requrement of functional ryanodine receptor type 3 for astrocyte migration. The FASEB Journal.
McNaught KSP, Brown GC (1998) Nitric oxide causes glutamate release from brain synaptosomes. Journal of neurochemistry 70:1541-1546.
Meffert MK, Premack BA, Schulman H (1994) Nitric oxide stimulates Ca2+-independent synaptic vesicle release. Neuron 12:1235-1244.
Mishra A, Reynolds JP, Chen Y, Gourine AV, Rusakov DA, Attwell D (2016) Astrocytes mediate neurovascular signaling to capillary pericytes but not to arterioles. Nature neuroscience 19:1619-1627.
Moghaddam B, Adams BW (1998) Reversal of phencyclidine effects by a group II metabotropic glutamate receptor agonist in rats. Science 281:1349-1352.
Montes de Oca Balderas P, Aguilera P (2015) A Metabotropic-Like Flux-Independent NMDA Receptor Regulates Ca2+ Exit from Endoplasmic Reticulum and Mitochondrial Membrane Potential in Cultured Astrocytes. PloS one 10:e0126314.
Morales-Ruiz M, Jimenez W, Perez-Sala D, Ros J, Leivas A, Lamas S, Rivera F, Arroyo V (1996) Increased nitric oxide synthase expression in arterial vessels of cirrhotic rats with ascites. Hepatology 24:1481-1486.
Morita M, Kudo Y (2010) Growth Factors Upregulate Astrocyte [Ca2+]i Oscillation by Increasing SERCA2b Expression. Glia 58:1988-1995.
Mulligan SJ, MacVicar BA (2004) Calcium transients in astrocyte endfeet cause cerebrovascular constrictions. Nature 431:195-199.
Murohara T, Kugiyama K, Yasue H (1996) Interactions of Nitrovasodilators, Atrial Natriuretic Peptide and Endothelium-Derived Nitric Oxide. Journal of Vascular Research 33:78-85.

Murphy-Royal C, Dupuis JP, Varela JA, Panatier A, Pinson B, Baufreton J, Groc L, Oliet SHR (2015) Surface diffusion of astrocytic glutamate transporters shapes synaptic transmission. Nature neuroscience 18:219-226 %@ 1097-6256.

Nakata S, Tsutsui M, Shimokawa H, Yamashita T, Tanimoto A, Tasaki H, Ozumi K, Sabanai K, Morishita T, Suda O (2007) Statin treatment upregulates vascular neuronal nitric oxide synthase through Akt/NF-κB pathway. Arteriosclerosis, thrombosis, and vascular biology 27:92-98.

Namin SM, Nofallah S, Joshi MS, Kavallieratos K, Tsoukias NM (2003) Kinetic analysis of DAF-FM activation by NO: Toward calibration of a NO-sensitive fluorescent dye. Nitrc Oxide 28:39-46.

Nathan C, Shiloh MU (2000) Reactive oxygen and nitrogen intermediates in the relationship between mammalian hosts and microbial pathogens. Proceedings of the National Academy of Sciences 97:8841-8848.

Niswender CM, Conn PJ (2010) Metabotropic glutamate receptors: physiology, pharmacology, and disease. Annual review of pharmacology and toxicology 50:295-322 %@ 0362-1642.

Norenberg MD (1979) Distribution of glutamine synthetase in the rat central nervous system. Journal of Histochemistry & Cytochemistry 27:756-762.

O'dell TJ, Huang PL, Dawson TM, Dinerman JL, Snyder SH, Kandel ER, Fishman MC (1994) Endothelial NOS and the blockade of LTP by NOS inhibitors in mice lacking neuronal NOS. Science 265:542-547.

Obara-Michlewska M, Ruszkiewicz J, Zielinska M, Verkhratsky A, Albrecht J (2015) Astroglial NMDA receptors inhibit expression of Kir4.1 channels in glutamate-overexposed astrocytes in vitro and in the brain of rats with acute liver failure. Neurochem Int 88:20-25.

Ogura T, Yokoyama T, Fujisawa H, Kurashima Y, Esumi H (1993) Structural diversity of neuronal nitric oxide synthase mRNA in the nervous system. Biochemical and biophysical research communications 193:1014-1022.

Olsen ML, Khakh BS, Skatchkov SN, Zhou M, Lee CJ, Rouach N (2015) New Insights on Astrocyte Ion Channels: Critical for Homeostasis and Neuron-Glia Signaling. J Neurosci 35:13827-13835.

Ouardouz M, Coderre E, Basak A, Chen A, Zamponi GW, Hameed S, Rehak R, Yin X, Trapp BD, Stys PK (2009) Glutamate receptors on myelinated spinal cord axons: I. GluR6 kainate receptors. Annals of neurology 65:151-159.

Oyekan AO, Youseff T, Fulton D, Quilley J, McGiff JC (1999) Renal cytochrome P450 omega-hydroxylase and epoxygenase activity are differentially modified by nitric oxide and sodium chloride. J Clin Invest 104:1131-1137.

Palygin O, Lalo U, Pankratov Y (2011) Distinct pharmacological and functional properties of NMDA receptors in mouse cortical astrocytes. British journal of pharmacology 163:1755-1766 %@ 1476-5381.

Pan H, Chou Y, Sun SH (2015) P2X7R-Mediated Ca21-Independent D-Serine Release via Pannexin-1 of the P2X7R-Pannexin-1 Complex in Astrocytes. Glia 63:877-893.

Panatier A, Robitaille R (2016) Astrocytic mGluR5 and the tripartite synapse. Neuroscience 323:29-34.
Pandey V, Chuang CC, Lewis AM, Aley PK, Brailoiu E, Dun NJ, Churchill GC, Patel S (2009) Recruitment of NAADP-sensitive acidic Ca2+ stores by glutamate. Biochem J 422:503-512.
Parnis J, Montana V, Delgado-Martinez I, Matyash V, Parpura V, Kettenmann H, Sekler I, Nolte C (2013) Mitochondrial Exchanger NCLX Plays a Major Role in the Intracellular Ca2+ Signaling, Gliotransmission, and Proliferation of Astrocytes. J Neurosci 33:7206-7219.
Pasti L, Pozzan T, Carmignoto G (1995) Long-lasting changes of calcium oscillations in astrocytes A new form of glutamate-mediated plasticity. Journal of Biological Chemistry 270:15203-15210.
Pasti L, Volterra A, Pozzan T, Carmignoto G (1997) Intracellular calcium oscillations in astrocytes: a highly plastic, bidirectional form of communication between neurons and astrocytes in situ. Journal of Neuroscience 17:7817-7830 %@ 0270-6474.
Paton. JFR, Kasparov. S, Paterson. DJ (2002) Nitric oxide and autonomic control of heart rate: a question of specificity. TRENDS in Neuroscience 25:626-631.
Paxinos G, Franklin KBJX (2004) The mouse brain in stereotaxic coordinates: Gulf Professional Publishing.
Perea G, Araque A (2005) Properties of synaptically evoked astrocyte calcium signal reveal synaptic information processing by astrocytes. Journal of Neuroscience 25:2192-2203 %@ 0270-6474.
Petravicz J, Boyt KM, McCarthy KD (2014) Astrocyte IP3R2-dependent Ca2+ signaling is not a major modulator of neuronal pathways governing behavior. Frontiers in Behavioral Neuroscience 8.
Piazza M, Futrega K, Spratt DE, Dieckmann T, Guillemette JG (2012) Structure and dynamics of calmodulin (CaM) bound to nitric oxide synthase peptides: effects of a phosphomimetic CaM mutation. Biochemistry 51:3651-3661.
Pigott BM, Garthwaite J (2016) Nitric Oxide Is Required for L-Type Ca2+ Channel-Dependent Long-Term Potentiation in the Hippocampus. Frontiers in Synaptic Neuroscience 8.
Pirttimaki TM, Codadu NK, Awni A, Pratik P, Nagel DA, Hill EJ, Dineley KT, Parri HR (2013) α7 Nicotinic receptor-mediated astrocytic gliotransmitter release: Aβ effects in a preclinical Alzheimer's mouse model. PloS one 8:e81828.
Porter JT, McCarthy KD (1995) GFAP-positive hippocampal astrocytes in situ respond to glutamatergic neuroligands with increases in [Ca2+] i. Glia 13:101-112.
Prast H, Fischer H, Grass K, Philippu A (1994) Nitric oxide is a modulator of acetylcholine and glutamate release in the ventral striatum. Monitoring molecules in neuroscience:261-262.
Rabinovich D, Yaniv SP, Alyagor I, Schuldiner O (2016) Nitric oxide as a switching mechanism between axon degeneration and regrowth during developmental remodeling. Cell 164:170-182.
Radomski M, Palmer R, Moncada S (1987) Endogenous nitric oxide inhibits human platelet adhesion to vascular endothelium. The Lancet 330:1057-1058.

Raju K, Doulias PT, Evans P, Krizman EN, Jackson JG, Horyn O, Daikhin Y, Nissim I, Yudkoff M, Itzhak N, sharp KA, Robinson MB, Ischiropoulos H (2016) Regulation of brain glutamate metabolism by nitric oxide and S- nitrosylation. Sci Signal 8.

Rameau GA, Tukey DS, Garcin-Hosfield ED, Titcombe RF, Misra C, Khatri L, Getzoff ED, Ziff EB (2007) Biphasic Coupling of Neuronal Nitric Oxide Synthase Phosphorylation to the NMDA Receptor Regulates AMPA Receptor Trafficking and Neuronal Cell Death. J Neurosci 27:3445-3455.

Ratovitski EA, Bao C, Quick RA, McMillan A, Kozlovsky C, Lowenstein CJ (1999) An inducible nitric-oxide synthase (NOS)-associated protein inhibits NOS dimerization and activity. Journal of Biological Chemistry 274:30250-30257.

Redwine JM, Evans CF (2002) Markers of central nervous system glia and neurons in vivo during normal and pathological conditions. In: Protective and Pathological Immune Responses in the CNS, pp 119-140: Springer.

Revathikumar P, Bergqvist F, Gopalakrishnan S, Korotkova M, Jakobsson P, Lampa J, Le Maître E (2016) Immunomodulatory effects of nicotine on interleukin 1β activated human astrocytes and the role of cyclooxygenase 2 in the underlying mechanism. Journal of Neuroinflammation 13:256-268.

Ricci G, Volpi L, Pasquali L, Petrozzi L, Siciliano G (2009) Astrocyte–neuron interactions in neurological disorders. Journal of biological physics 35:317-336.

Riccio A, Alvania RS, Lonze BE, Ramanan N, Kim T, Huang Y, Dawson TM, Snyder SH, Ginty DD (2006) A nitric oxide signaling pathway controls CREB-mediated gene expression in neurons. Mol Cell 21:283-294.

Richey B, Cayley D, Mossing M, Kolka C, Anderson CF, Farrar TC, Record MT (1987) Variability of the intracellular ionic environment of Escherichia coli. Differences between in vitro and in vivo effects of ion concentrations on protein-DNA interactions and gene expression. Journal of Biological Chemistry 262:7157-7164.

Rothe F, Canzler U, Wolf G (1998) Subcellular localization of the neuronal isoform of nitric oxide synthase in the rat brain: a critical evaluation. Neuroscience 83:259-269.

Rungta R, Bernier L-P, Dissing-Olesen L, Groten CJ, LeDue JM, Ko R, Drissler S, MacVicar BA (2016) Ca2+ Transients in Astrocyte Fine Processes Occur Via Ca2+ Influx in the Adult Mouse Hippocampus. Glia 64:2903-2913.

Rungta RL, Charpak S (2016) Astrocyte endfeet march to the beat of different vessels. Nature neuroscience 19:1539-1541.

Sakuragi S, Niwa F, Oda Y, Mikoshiba K, Bannai H (2017) Astroglial Ca2+ signaling is generated by the coordination of IP3R and store-operated Ca2+ channels. Biochemical and Biophysical Research Communications 486:879-885.

Sattler R, Xiong Z, Lu WY, Hafner M, MacDonald JF, Tymianski M (1999) Specific Coupling of NMDA Receptor Activation to Nitric Oxide Neurotoxicity by PSD-95 Protein. Science 284:1845-1849.

Schools GP, Zhou M, Kimelberg HK (2006) Development of gap junctions in hippocampal astrocytes: evidence that whole cell electrophysiological phenotype is an intrinsic property of the individual cell. Journal of neurophysiology 96:1383-1392.

Schousboe A, Scafidi S, Bak LK, Waagepetersen HS, McKenna MC (2014) Glutamate metabolism in the brain focusing on astrocytes. Adv Neurobiol 11:13-30.
Scott G, Bowman S, Smith T, Flower Ra, Bolton C (2007) Glutamate-stimulated peroxynitrite production in a brain-derived endothelial cell line is dependent on N-methyl-D-aspartate (NMDA) receptor activation. Biochemical pharmacology 73:228-236.
Seifert G, Henneberger C, Steinhäuser C (2016) Diversity of astrocyte potassium channels: An update. Brain Research Bulletin %@ 0361-9230.
Selaković V, Balind SR, Radenović L, Prolić Z, Janać B (2013) Age-Dependent Effects of ELF-MF on Oxidative Stress in the Brain of Mongolian Gerbils. Cell Biochem Biophys 66:513-521.
Sharma R (2012) Inhibition of Nitric Oxide Synthase Gene Expression: In Vivo Imaging Approaches of Nitric Oxide with Multimodal Imaging: INTECH Open Access Publisher.
Shelton MK, McCarthy KD (2000) Hippocampal Astrocytes Exhibit Ca2+-Elevating Muscarinic Cholinergic and Histaminergic Receptors In Situ. Journal of neurochemistry 74:555-563.
Shen JX, Yakel JL (2012) Functional alpha7 nicotinic ACh receptors on astrocytes in rat hippocampal CA1 slices. J Mol Neurosci 48:14-21.
Sherwood MW, Arizono M, Hisatsune C, Bannai H, Ebisui E, Sherwood JL, Panatier A, Oliet SHR, Mikoshiba K (2017) Astrocytic IP3Rs: Contribution to Ca2+ Signalling and Hippocampal LTP. Glia 65:502-513.
Shigetomi E, Patel S, Khakh BS (2016) Probing the Complexities of Astrocyte Calcium Signaling. Trends in Cell Biology 26:300-312.
Shigetomi E, Kracun S, Sofroniew MV, Khakh BS (2010) A genetically targeted optical sensor to monitor calcium signals in astrocyte processes. Nature neuroscience 13:759-766 %@ 1097-6256.
Shigetomi E, Bushong EA, Haustein MD, Tong X, Jackson-Weaver O, Kracun S, Xu J, Sofroniew MV, Ellisman MH, Khakh BS (2013) Imaging calcium microdomains within entire astrocyte territories and endfeet with GCaMPs expressed using adeno-associated viruses. The Journal of General Physiology 141:633-647.
Shin T, Kim H, Jin J-k, Moon C, Ahn M, Tanuma N, Matsumoto Y (2005) Expression of caveolin-1,-2, and-3 in the spinal cords of Lewis rats with experimental autoimmune encephalomyelitis. Journal of neuroimmunology 165:11-20.
Silva G, Theriault E, Mills L, Pennefather P, Feeney C (1999) Group I and II metabotropic glutamate receptor expression in cultured rat spinal cord astrocytes. Neuroscience letters 263:117-120.
Silvagno F, Xia H, Bredt DS (1996) Neuronal nitric-oxide synthase-, an alternatively spliced isoform expressed in differentiated skeletal muscle. Journal of Biological Chemistry 271:11204-11208.
Smith BC, Underbakke ES, Kulp DW, Schief WR, Marletta MA (2013) Nitric oxide synthase domain interfaces regulate electron transfer and calmodulin activation. Proceedings of the National Academy of Sciences of the United States of America 110:E3577-3586.
Sofroniew MV, Vinters HV (2010) Astrocytes: biology and pathology. Acta neuropathologica 119:7-35 %@ 0001-6322.

Sogawa K, Numayama-Tsuruta K, Ema M, Abe M, Abe H, Fujii-Kuriyama Y (1998) Inhibition of hypoxia-inducible factor 1 activity by nitric oxide donors in hypoxia. Proceedings of the National Academy of Sciences 95:7368-7373.

Srinivasan R, Huang BS, Venugopal S, Johnston AD, Chai H, Zeng H, Golshani P, Khakh BS (2015) Ca2+ signaling in astrocytes from Ip3r2−/− mice in brain slices and during startle responses in vivo. Nature neuroscience 18:708-717.

Stamler JS, Simon DI, Osborne JA, Mullins ME, Jaraki O, Michel T, Singel DJ, Loscalzo J (1992) S-nitrosylation of proteins with nitric oxide: synthesis and characterization of biologically active compounds. Proceedings of the National Academy of Sciences 89:444-448.

Stavermann M, Meuth P, Doengi M, Thyssena A, Deitmer JW, Lohr C (2015) Calcium-induced calcium release and gap junctions mediate large-scale calcium waves in olfactory ensheathing cells in situ. Cell Calcium 58:215-225.

Stobart JL, Ferrari KD, Barrett MJP, Stobart MJ, Looser ZJ, Saab AS, B W (2016) Long-term In Vivo Calcium Imaging of Astrocytes Reveals Distinct Cellular Compartment Responses to Sensory Stimulation. cerebral Cortex:1-15.

Stoyanovsky D, Murphy T, Anno PR, Kim Y, M, Salama G (1997) Nitric oxide activates skeletal and cardiac ryanodine receptors. Cell Calcium 21:19-29.

Straub SV, Bonev AD, Wilkerson MK, Nelson MT (2006) Dynamic Inositol Trisphosphate-mediated Calcium Signals within Astrocytic Endfeet Underlie Vasodilation of Cerebral Arterioles. The Journal of General Physiology 128:659-669.

Sugihara H, Chen N, Sur M (2016) Cell-specific modulation of plasticity and cortical state by cholinergic inputs to the visual cortex. Journal of Physiology 110:37-43.

Suhs KW, Gudi V, Eckermann N, Fairless R, Pul R, Skripuletz T, Stangel M (2016) Cytokine regulation by modulation of the NMDA receptor on astrocytes. Neuroscience letters 629:227-233.

Sun C-W, Alonso-Galicia M, Taheri MR, Falck JR, Harder DR, Roman RJ (1998) Nitric oxide-20–hydroxyeicosatetraenoic acid interaction in the regulation of K+ channel activity and vascular tone in renal arterioles. Circulation Research 83:1069-1079.

Sun W, McConnell E, Pare J-f, Xu Q, Chen M, Peng W, Lovatt D, Han X, Smith Y, Nedergaard M (2013) Glutamate-Dependent Neuroglial Calcium Signaling Differs Between Young and Adult Brain. Science 339:197-200.

Suzuki S, Koshimizu H, Adachi N, Matsuoka H, Fushimi S, Ono J, Ohta KI, Miki T (2017) Functional interaction between BDNF and mGluR II in vitro: BDNF down-regulated mGluR II gene expression and an mGluR II agonist enhanced BDNF-induced BDNF gene expression in rat cerebral cortical neurons. Peptides 89:42-49.

Takarada T, Nakamichi N, Kawagoe H, Ogura M, Fukumori R, Nakazato R, Fujikawa K, Kou M, Yoneda Y (2012) Possible neuroprotective property of nicotinic acetylcholine receptors in association with predominant upregulation of glial cell line‐derived neurotrophic factor in astrocytes. Journal of neuroscience research 90:2074-2085 %@ 1097-4547.

Takata N, Mishima T, Hisatsune C, Nagai T, Ebisui E, Mikoshiba K, Hirase H (2011) Astrocyte calcium signaling transforms cholinergic modulation to cortical plasticity in vivo. J Neurosci 31:18155-18165.
Takeuchi A, Kim B, Matsuoka S (2015) The destiny of Ca(2+) released by mitochondria. J Physiol Sci 65:11-24.
Talukder MAH, Fujiki T, Morikawa K, Motoishi M, Kubota H, Morishita T, Tsutsui M, Takeshita A, Shimokawa H (2004) Up-regulated neuronal nitric oxide synthase compensates coronary flow response to bradykinin in endothelial nitric oxide synthase-deficient mice. Journal of cardiovascular pharmacology 44:437-445.
TANG XC, Kalivas PW (2003) Bidirectional modulation of cystine/glutamate exchanger activity in cultured cortical astrocytes. Annals of the New York Academy of Sciences 1003:472-475.
Tarasenko A, Krupko O, Himmelreich N (2014) New insights into molecular mechanism (s) underlying the presynaptic action of nitric oxide on GABA release. Biochimica et Biophysica Acta (BBA)-General Subjects 1840:1923-1932.
Taurin S, Sandbo N, Yau DM, Sethakorn N, Dulin NO (2008) Phosphorylation of β-catenin by PKA promotes ATP-induced proliferation of vascular smooth muscle cells. American Journal of Physiology-Cell Physiology 294:C1169-C1174.
Terunuma M, Haydon PG, Pangalos M, N, Moss SJ (2015) Purinergic receptor activation facilitates astrocytic GABAB receptor calcium signalling. Neuropharmacology 88:74-81.
Thomas GD, Victor RG (1997) Nitric oxide mediates contraction-induced attenuation of sympathetic vasoconstriction in rat skeletal muscle. The Journal of physiology 506:817-826.
Thomas NL, Williams AJ (2012) Pharmacology of ryanodine receptors and Ca2+-induced Ca2+ release. WIREs Membr Transp signal 1:383-397.
Tian J, Kim SF, Hester L, Snyder SH (2008) S-nitrosylation/activation of COX-2 mediates NMDA neurotoxicity. Proceedings of the National Academy of Sciences 105:10537-10540.
Toda N, Ayajiki K, Okamura T (2009) Cerebral blood flow regulation by nitric oxide: recent advances. Pharmacol Rev 61:62-97.
Tricoire L, Vitalis T (2012) Neuronal nitric oxide synthase expressing neurons: a journey from birth to neuronal circuits. Frontiers in Neural Circuits 6.
Uematsu K, Heiman M, Zelenina M, Padovan J, Chait BT, Aperia A, Nishi A, Greengard P (2015) Protein kinase A directly phosphorylates metabotropic glutamate receptor 5 to modulate its function. Journal of neurochemistry 132:677-686.
Umbriaco D, Garcia S, Beaulieu C, Descarries L (1995) Relational features of acetylcholine, noradrenaline, serotonin and GABA axon terminals in the stratum radiatum of adult rat hippocampus (CA1). Hippocampus 5:605-620.
Vargas JR, Takahashi DK, Thomson KE, Wilcox KS (2013) The expression of kainate receptor subunits in hippocampal astrocytes after experimentally induced status epilepticus. Journal of Neuropathology & Experimental Neurology 72:919-932 %@ 0022-3069.
Vasile F, Dossi E, Rouach N (2017) Human astrocytes: structure and functions in the healthy brain. Brain Structure and Function:1-13 %@ 1863-2653.

Venema VJ, Ju H, Zou R, Venema RC (1997) Interaction of neuronal nitric-oxide synthase with caveolin-3 in skeletal muscle Identification of a novel caveolin scaffolding/inhibitory domain. Journal of Biological Chemistry 272:28187-28190.
Vergouts M, Doyen PJ, Peeters M, Opsomer R, Michiels T, Hermans E (2017) PKC epsilon-dependent calcium oscillations associated with metabotropic glutamate receptor 5 prevent agonist-mediated receptor desensitization in astrocytes. Journal of Neurochemistry 141:387-399.
Verkhratsky A, Steinhäuser C (2000) Ion channels in glial cells. Brain Research Reviews 32:380-412.
Verkhratsky A, Butt AM (2007) Glial neurobiology: John Wiley & Sons.
Verkhratsky A, Burnstock G (2014) Purinergic and glutamatergic receptors on astroglia. Adv Neurobiol 11:55-79.
Verkhratsky A, Nedergaard M (2016) The homeostatic astroglia emerges from evolutionary specialization of neural cells. Phil Trans R Soc B 371:20150428 %@ 20150962-20158436.
Vienken H, Mabrouki N, Grabau K, Claas RF, Rudowski A, Schomel N, Pfeilschifter J, Lutjohann D, van Echten-Deckert G, Meyer Zu Heringdorf D (2017) Characterization of cholesterol homeostasis in sphingosine-1-phosphate lyase-deficient fibroblasts reveals a Niemann-Pick disease type C-like phenotype with enhanced lysosomal Ca2+ storage. Sci Rep 7:43575.
Vignoli B, Canossa M (2017) Glioactive ATP controls BDNF recycling in cortical astrocytes. Communicative & Integrative Biology 10:e1277296.
Virgintino D, Robertson D, Errede M, Benagiano V, Tauer U, Roncali L, Bertossi M (2002) Expression of caveolin-1 in human brain microvessels. Neuroscience 115:145-152.
Wang S, Pan D-X, Wang D, Wan P, Qiu D-L, Jin Q-H (2014) Nitric oxide facilitates active avoidance learning via enhancement of glutamate levels in the hippocampal dentate gyrus. Behavioural Brain Research 271:177-183.
Wang W, Kiyoshi CM, Du Y, Ma B, Alford CC, Chen H, Zhou M (2016) mGluR3 Activation Recruits Cytoplasmic TWIK-1 Channels to Membrane that Enhances Ammonium Uptake in Hippocampal Astrocytes. Mol Neurobiol 53:6169-6182.
Wang X, Lippi G, Carlson DM, Berg DK (2013) Activation of α7-containing nicotinic receptors on astrocytes triggers AMPA receptor recruitment to glutamatergic synapses. Journal of Neurochemistry 127:632-643.
Wang Y, Veremeyko T, Wong AHK, Fatimy RE, Wei Z, Cai W, Krichevsky AM (2017a) Downregulation of miR-132/212 impairs S-nitrosylation balance and induces tau phosphorylation in Alzheimer's disease. Neurobiology of Aging 51:156-166.
Wang YY, Sung CC, Chung KKK (2017b) Novel enhancement mechanism of tyrosine hydroxylase enzymatic activity by nitric oxide through S-nitrosylation. Sci Rep 7.
Watanabe M, Masaki K, Yamasaki R, Kawanokuchi J, Takeuchi H, Matsushita T, Suzumura A, Kira J-i (2016) Th1 cells downregulate connexin 43 gap junctions in astrocytes via microglial activation. Scientific Reports 6.
Weaver AK, Bomben VC, Sontheimer H (2006) Expression and function of calcium-activated potassium channels in human glioma cells. Glia 54:223-233 %@ 1098-1136.

Wiencken AE, Casagrande VA (1999) Endothelial Nitric Oxide Synthetase (eNOS) in Astrocytes: Another Source of Nitric Oxide in Neocortex. Glia 26:280-290.
Willmott NJ, Wong K, Strong AJ (2000) A Fundamental Role for the Nitric Oxide-G-Kinase Signaling Pathway in Mediating Intercellular Ca2+ Waves in Glia. J Neurosci 20:1767-1779.
Woehrling EK, Parri HR, Erin HY, Hill EJ, Maidment ID, Fox GC, Coleman MD (2015) A predictive in vitro model of the impact of drugs with anticholinergic properties on human neuronal and astrocytic systems. PloS one 10:e0118786 %@ 0111932-0116203.
Woo DH, Han K-S, Shim JW, Yoon B-E, Kim E, Bae JY, Oh S-J, Hwang EM, Marmorstein AD, Bae YC (2012) TREK-1 and Best1 channels mediate fast and slow glutamate release in astrocytes upon GPCR activation. Cell 151:25-40 %@ 0092-8674.
Wu J, Lee MR, Kim T, Johng S, Rohrback S, Kang N, Choi D (2011) Regulation of ethanol-sensitive EAAT2 expression through adenosine A1 receptor in astrocytes. Biochemical and Biophysical Research Communications 406:47-52.
Wu K-C, Kuo C-S, Chao C-C, Huang C-C, Tu Y-K, Chan P, Leung Y-M (2015) Role of voltage-gated K+ channels in regulating Ca2+ entry in rat cortical astrocytes. The Journal of Physiological Sciences 65:171-177.
Wynia-Smith SL, Smith BC (2017) Nitrosothiol formation and S-nitrosation signaling through nitric oxide synthases. Nitric Oxide 63:52-60.
Xu KY, Huso DL, Dawson TM, Bredt DS, Becker LC (1999) Nitric oxide synthase in cardiac sarcoplasmic reticulum. Proceedings of the National Academy of Sciences 96:657-662.
Xu L, Eu JP, Meissner G, Stamler JS (1998) Activation of the cardiac calcium release channel (ryanodine receptor) by poly-S-nitrosylation. Science 279:234-237.
Yan J, Zhang H, Yin Y, Li J, Tang Y, Purkayastha S, Li L, Cai D (2014) Obesity-and aging-induced excess of central transforming growth factor-[beta] potentiates diabetic development via an RNA stress response. Nature medicine 20:1001-1008 %@ 1078-8956.
Yao HH, Ding JH, Zhou F, Wang F, Hu LF, Sun T, Hu G (2005) Enhancement of glutamate uptake mediates the neuroprotection exerted by activating group II or III metabotropic glutamate receptors on astrocytes. Journal of neurochemistry 92:948-961.
Yao Y, Chen Z-L, Norris EH, Strickland S (2014) Astrocytic laminin regulates pericyte differentiation and maintains blood brain barrier integrity. Nature communications 5.
Young SZ, Platel J-C, Nielsen JV, Jensen N, Bordey A (2010) GABAA increases calcium in subventricular zone astrocyte-like cells through L-andT-type voltage-gated calcium channels. GABA signaling in health and disease %@ 2889190846.
Yu W, Zhu H, Wang Y, Li G, Wang L, Li H (2015) Reactive Transformation and Increased BDNF Signaling by Hippocampal Astrocytes in Response to MK-801. PloS one 10:e0145651.
Yu W-F, Guan Z-Z, Bogdanovic N, Nordberg A (2005) High selective expression of α7 nicotinic receptors on astrocytes in the brains of patients with sporadic Alzheimer's disease and patients carrying Swedish APP 670/671 mutation: a possible association with neuritic plaques. Experimental neurology 192:215-225 %@ 0014-4886.

Yuan Z, Liu B, Yuan L, Zhang Y, Dong X, Lu J (2004) Evidence of nuclear localization of neuronal nitric oxide synthase in cultured astrocytes of rats. Life sciences 74:3199-3209.

Zhu N, Wang K, Wei M, Lan Y, Chen Q, Wang Y (2016) Activation of glial α7 nAChR promotes neurogenesis by suppressing Aβ-mediated neuroin ammation in Alzheimer's disease. Int J Clin Exp Pathol 9:11014-11024.

Zulazmi NA, Gopalsamy B, Min JCS, Farouk AAO, Sulaiman MR, Bharatham BH, Perimal EK (2017) Zerumbone Alleviates Neuropathic Pain through the Involvement of l-Arginine-Nitric Oxide-cGMP-K+ ATP Channel Pathways in Chronic Constriction Injury in Mice Model. Molecules 22:555.